BASICITY AND CATALYTIC ACTIVITY OF POROUS MATERIALS BASED ON A (Si,Al)-N FRAMEWORK

A.I. Saugar[a], C. Márquez-Álvarez[a], I.J. Villar-Garcia[b], T. Welton[c], J. Pérez-Pariente[a,*]

[a] Instituto de Catálisis y Petroleoquímica, CSIC, C/Marie Curie 2, 28049-Cantoblanco, Spain. [b] Department of Materials, Imperial College London. [c] Department of Chemistry, Imperial College London, Exhibition Road, South Kensington SW7 2AZ, United Kingdom.

* Corresponding author: jperez@icp.csic.es

Abstract

Porous materials based on a framework containing T-N linkages, where T represents silicon or silicon and aluminium atoms, have been prepared by the ammonolysis at low temperature of the corresponding silicon and aluminium chlorides in an ionic liquid, both in the presence and in the absence of mineralizing agents such as pyrrolidine, ammonia and sodium amide. IR spectroscopy and XPS data are consistent with these materials having a framework based on T-NH-T groups (T = Si or Al), that contain also a large fraction of T-NH_2 terminal groups. Moreover, XPS evidences the presence of Si-NH-Al groups whenever aluminium is present in the solid. The basic strength of the materials has been determined by pyrrole adsorption, and it has been found that the average basic strength increases with the population of T-NH-T groups and with the aluminium content of the framework. However, this strength is lower than that of a calcined hydrotalcite (Al/(Al+Mg) = 0.33) taken as a reference. These materials are

active and very selective catalysts in the Michael addition reaction between chalcone [and malononitrile (pK_a 11), but turned to be inactive when diethylmalonate having a weaker acidity (pK_a 13.3) is used as donor.

Keywords: Silicon-aluminium imide; Porous materials; Heterogeneous base catalyst; Michael addition; Pyrrole adsorption.

1. Introduction

There is a wide interest towards microporous and mesoporous materials based on corner-sharing TO_4 (T = Si, Al) tetrahedral units, focused on their application in acid-catalyzed reactions. The catalytic properties of these materials are much dependent on the nature of the active centers and on their textural properties. In contrast to the extensive development of those solid acid catalysts, efforts to develop basic microporous and mesoporous materials are significantly lower, even though base-catalyzed reactions play an important role in a number of industrially relevant processes such as the production of fine chemicals.

Due to the lower electronegativity of nitrogen with respect to oxygen, materials based on a nitrogen-containing network would have higher basicity than their oxide counterparts. Silicon diimide, $Si(NH)_2$, which is an amorphous and reactive solid, is isoelectronic and isostructural with SiO_2. Thereby, as silicon dioxide allows the formation or porous solids based on corner-sharing SiO_4 tetrahedral units, silicon diimide would allow the formation of a network built by SiN_4 units.

In heterogeneous catalysis, materials should have a high surface area and pore volume in order to facilitate access of the reactant molecules to the active sites, which in a

silicon-nitrogen based compound would be =NH or even terminal Si-NH_2 groups. In this regard, a limited number of strategies have been developed with the goal of obtaining porous and high-surface area Si-N materials. Pyrolysis of polysilazanes and poly(organosilazanes) results in the formation of microporous silicon imidonitrides, being some of them active in the base-catalyzed Knoevenagel reaction [1-3].

Bradley and co-workers have reported the preparation of a silicon diimide gel containing a significant amount of dimethylamino groups by acid-catalyzed ammonolysis of tris(dimethylamino)silylamine ($[Si(NH_2)(NMe_2)_3]$ (TDSA)) [4]. Pyrolysis of the gel under flowing ammonia at 1000 ºC leads to mesoporous silicon imidonitride with high surface area (466 m^2/g) but with a low amount of Si-NH-Si catalytic active sites [5]. Recently gels prepared from TDSA were used to produce high surface area aerogels by supercritical drying of the gels with ammonia [6].

In the conventional procedures used to prepare silicon nitride ceramics, silicon halides, silicon tetrachloride usually, are reacted with ammonia in an organic solvent to produce the ammonium salt and amorphous silicon diimide, $Si(NH)_2$, which decomposes at higher temperatures to form Si_3N_4 [7] as well as nitridosilicates [8]. Kaskel and co-workers have synthesized high-surface-area mesoporous silicon imidonitride solids by heating the mixture of silicon diimide and ammonium halide in an ammonia flow [9-11].

Until now, the basicity and catalytic activity of the materials obtained from silicon diimide or organosilicon compounds has been hardly investigated as the amount of NH sites in these materials is significantly low, so they do not exhibit a high catalytic activity. With the aim of preparing materials of strong basicity, silicon imidonitride solid obtained from silicon diimide has been used as a support for alkali metals. Potassium-loaded high surface area silicon imidonitride materials were found to be

efficient base catalysts suitable for the side-chain alkylation of toluene [12] and for alkene isomerization reactions [11].

Aiming to increase the intrinsic basicity of these nitrides, aluminium has been incorporated into the Si-N framework. As aluminium atoms are less electronegative than silicon, the Al-N bonds are more polar than Si-N, so the basicity of the nitrogen atoms would be increased.

To generate porous silicon aluminium imide materials, a precursor containing aluminium and silicon ($(C_4H_8O)Al[NHSi(NMe_2)_3]_3$), was prepared was prepared by reacting tris(dimethylamino)silylamidolithium $(Me_2N)_3$-SiNHLi with aluminium trichloride in tetrahydrofuran [13]. The acid-catalyzed ammonolysis reaction of this precursor results in the formation of a silicon aluminium imide gel with a significant amount of dimethylamino groups. Pyrolysis of the gel at 1000 ºC under flowing ammonia leads to an amorphous mesoporous silicon aluminium nitride with a Si:Al molar ratio of 2.9:1 but with a low surface area (190 m^2/g) [14]. Although the heat treatment removes completely the residual dimethylamino groups, it also leads to condensation reactions between the Si-NH and Al-NH functional groups, reducing the amount of catalytic active sites in the material.

Kaskel et al. have synthesized the oxygen-free precursor $[EtAl(\mu\text{-}NHEt)(\mu\text{-}NEt)_2\text{-}Si(NHEt)]_2$, the crystal structure of which contains aluminium and silicon in tetrahedral coordination and bridging and terminal ethylamino groups [15]. When this compound is treated with supercritical ammonia at 150 ºC in a high-pressure autoclave, a xerogel imidonitride with a Al:Si ratio close to 1 and a surface area of 760 m^2/g is obtained [16]. This aluminium-containing silicon imidonitride shows a high catalytic activity in the Michael addition reaction between malononitrile and acrylonitrile, reaching a yield of 96 %. Nevertheless, an extensive study about the correlation between the basic

properties of these silicon aluminium imidonitrides and their catalytic activity has never been reported.

Most of the procedures previously reported to obtain imidonitrides from a silicon diimide or a silicon aluminium imide gel make use of an organic solvent whose main role in the preparation process is to absorb the heat produced by the highly exothermic ammonolysis reaction. In order to design a new synthesis pathway where the solvent would play an active role in the formation of the silicon diimide gel, a novel solvothermal pathway has been recently developed in our group to prepare porous silicon-nitrogen network-based materials from a silicon diimide-type gel obtained by the ammonolysis of silicon tetrachloride using an ionic liquid as solvent [17].

Several studies have demonstrated that some ionic liquids, which are organic salts with high chemical and thermal stability [18], can dissolve high amounts of gaseous ammonia reaching much higher solubilities than the organic solvents currently employed in the ammonolysis reaction [19, 20]. We have demonstrated in our previous report that when the silicon diimide precursor gel is subjected to a thermal treatment in the presence of ammonia dissolved in the ionic liquid, this basic compound can catalyze the condensation process of Si-N moieties improving the textural properties of the resulting silicon-nitrogen network-based materials.

Hydroxyl anions are commonly used to solubilize silicate species in the hydrothermal preparation of silica gels at high pH. In this regard, amide anion (NH_2^-), which is isoelectronic to OH^- anion, could act as a mineralizing agent in the preparation of Si-N based materials. The present paper, reports on the use of $NaNH_2$ as a mineralizing agent in the preparation of silicon-nitrogen based materials by our already reported synthesis technique and its effect in the chemical composition and the textural properties of the resulting materials. We also extend our preparation method to synthesize new porous

silicon-nitrogen based materials containing aluminium in their network, from a silicon aluminium imide gel obtained by the joint ammonolysis reaction of silicon tetrachloride and aluminium chloride using an ionic liquid as solvent.

In order to explore the catalytic properties of the prepared materials, the present work also provides a thorough study about the catalytic activity of the materials in the base-catalyzed Michael addition reaction between chalcone and malononitrile, and the influence of the chemical composition and the textural properties on the catalysts behavior. Moreover, infrared spectroscopy of adsorbed pyrrole has been used to characterize the basic active sites of the catalyst being able to make a correlation between the basic properties and the catalytic activity.

2. Experimental

All the gels were prepared under anaerobic conditions through the use of an air-free system. Silicon diimide gels were prepared according to our previously reported procedure [17] by the reaction of silicon tetrachloride (Sigma-Aldrich, 99 wt%) and gaseous anhydrous ammonia (Air Liquide, H_2O < 400 ppm) using the ionic liquid 1-ethyl-3-methylimidazolium bis(trifluoromethylsulfonyl)imide ($[C_2C_1im][Tf_2N]$) (Sigma-Aldrich, 98 wt%) or the 1-butyl-1-methylpyrrolidinium bis(trifluoromethylsulfonyl)imide ($[C_4C_1pyrr][Tf_2N]$) (Sigma-Aldrich, 98 wt%) as solvent.

The ionic liquid $[C_4C_1pyrr][Tf_2N]$ was only applied when sodium amide was added to the gel to be applied as a mineralizing agent. The silicon-aluminium imide gels were prepared by a modification of our previously reported method [17]. First, 8.65 g of silicon tetrachloride (Sigma-Aldrich, 99 wt%) and 0.68 g of anhydrous aluminium

chloride (Panreac, 98 wt%) were dissolved in 31.7 g of the ionic liquid 1-ethyl-3-methylimidazolium bis(trifluoromethylsulfonyl)imide ($[C_2C_1im][Tf_2N]$) (Sigma-Aldrich, 98 wt%) and reacted with gaseous anhydrous ammonia (Air Liquide, H_2O < 400 ppm) in a vessel kept in an ice bath to avoid the very vigorous course of the reaction.

The resulting silicon diimide and silicon-aluminium imide gels were homogenized inside a nitrogen-filled glove bag and introduced into 60-ml Teflon-lined stainless steel autoclaves which were heated statically at 150 ºC or 180 ºC under autogenous pressure for 43 hours, 7 days or 21 days. In some experiments pyrrolidine (Sigma-Aldrich, ≥99.5 wt%, purified by distillation) and/or sodium amide (Sigma-Aldrich, 95 wt%) were added to the mixture.

For some syntheses, ammonia gas was dissolved in the ionic liquid before the heating process. To dissolve the ammonia, static phase equilibrium cells constructed with Swagelok fittings, one Swagelok ball valve, and glass-lined stainless steel tubing were used. The cells were filled inside the glove bag with the mixture resulting of homogenizing the white gel obtained in the ammonolysis reaction, adding pyrrolidine in some cases. Then, ammonia was dissolved in the ionic liquid by the procedure described in our previous report [17] and the cells were heated as described above.

The obtained products were washed with methanol (Scharlau, 0.028% water as received; it was previously distilled in the presence of activated molecular sieve 3 Å pellets to remove the traces of water) to remove the ammonium chloride, the ionic liquid and the unreacted pyrrolidine and sodium amide if present, and filtered under a nitrogen flow using a stainless steel pressure filter holder. The transfer of the products to the filter holder was performed always in the glove bag, as well as all subsequent manipulations of the washed product. White solids were obtained in all cases. After

washing, the samples were heated under flowing ammonia (100 ml/min) at 600 ºC for 2 h.

In this way, different gels with the molar composition *$SiCl_4$: x $AlCl_3$: y Py: 4 NH_4Cl: (1.5+x) IL: z NH_3: q $NaNH_2$* were prepared, where *x*, *y*, *z* and *q* were varied as stated in Table 1 and *IL* stands for the ionic liquid applied as solvent. All the gels were prepared by using the ionic liquid $[C_2C_1im][Tf_2N]$ except for the gels in which sodium amide was applied as a mineralizing agent where the ionic liquid applied was $[C_4C_1pyrr][Tf_2N]$. Hereafter the samples will be named making reference to the quantity of pyrrolidine, *yPy*, where *y* stands for the Py/Si molar ratio, and to the quantity of sodium amide, *qNa*, where *q* stands for the $NaNH_2$/Si molar ratio, followed by a number indicating the heating temperature and a number indicating the heating time. If ammonia is dissolved in the ionic liquid, the heating time is followed by NH. The samples prepared from a silicon diimide gel were named starting by *Si* while the samples prepared from a silicon-aluminium imide gel were named starting by *SiAl*. As an example, SiAl-0.27Py-180-43h-NH refers to the sample prepared from a silicon-aluminium imide gel with a Py/Si molar ratio of 0.27 heated at 180 ºC for 43 hours with ammonia dissolved in the ionic liquid. The experiments performed are summarized in Table 1. An Al-Mg mixed oxide was also synthesized as reference basic solid material. This sample was obtained by calcination at 550 ºC of a hydrotalcite with Al/(Al+Mg) = 0.33 prepared following a previously reported procedure [21]. The presence of a single phase of high crystallinity was assessed by XRD.

Thermogravimetric analyses of the as-prepared samples were performed in a Perkin-Elmer TGA7 instrument, in an air flow of 40 mL/min, with a heating ramp from 25 to 900 ºC at 20 ºC/min. For the ammonia heat-treated samples, thermogravimetric analysis

were performed in an air flow of 40 mL/min, by using a heating ramp from 25 to 950 ºC at 20 ºC/min and keeping the sample at 950 ºC until constant sample weight.

Chemical CHNS analyses were obtained in a LECO CHNS-932 analyser provided with an AD-4 Perkin-Elmer scale. The silicon and aluminium content of the samples were measured by ICP-AES using an ICP Winlab Optima 3300 DV Perkin-Elmer spectrometer. Samples for ICP-AES analysis were dissolved by alkaline fusion.

Attenuated total reflection Fourier transform infrared (ATR-FTIR) measurements were conducted using a Nicolet Nexus 670 spectrometer provided with a MCT detector and a GladiATR single-bounce monolithic diamond ATR accessory. The spectra were recorded in the 4000-400 cm^{-1} range, at 4 cm^{-1} resolution, by averaging 128 scans.

Nitrogen adsorption isotherms where measured in a Micromeritics ASAP 2420 apparatus at the temperature of liquid nitrogen (-196 ºC). The samples (~ 100 mg) were loaded in the sample tubes in a nitrogen-filled glove bag and degassed in situ at 350 ºC in vacuum for 16 hours prior to analysis. Specific surface areas were determined using the BET method and the external and micropore surface areas were calculated using the t-plot method. The pore volume and the average pore diameter were calculated by applying the BJH protocol to the adsorption branch of the isotherm.

X-ray photoelectron spectroscopy (XPS) analysis was performed using a SPECS GmbH spectrometer equipped with a PHOIBOS 150 9MCD energy analyzer. A non-monochromatic magnesium X-ray source (1253.6 eV) was used with a power of 200 W and voltage of 12 kV. The powder sample was pressed inside a nitrogen-filled glove bag using a hand press and stuck on the sample holder with double-sided adhesive conductive carbon tape. The sample was introduced into the spectrometer without prior thermal treatment. The instrument operated at pressures near 6 x 10^{-9} mbar in the

analysis chamber. Pass energies of 75 and 25 eV were used for acquiring both survey and high-resolution spectra, respectively. The high resolution scans were taken around the emission lines of interest with 0.1 eV steps and 100 ms dwell time per point. SpecsLab Version 2.78 software was used for spectrometer control. The C 1s emission line of adventitious carbon (binding energy of 284.8 eV) was used to calibrate the energy scale of the spectra. The N1s peak was decomposed using the Casa XPS program (Casa Software Ltd) with a Gaussian/Lorentzian (70/30) product function and after subtraction of a Shirley background.

FTIR measurements of adsorbed pyrrole were carried out using a Thermo Nicolet Nexus 670 spectrometer equipped with a MCT detector. Spectra were acquired in the transmission mode, at a resolution of 4 cm^{-1} by averaging 250 scans. Samples were pressed into self-supporting wafers of 2.5-5 mg/cm^2 thickness and placed inside a glass cell provided with KBr windows and greaseless stopcocks. All sample manipulation was done inside a dry nitrogen-filled glove bag to prevent contact with oxygen and moisture. Samples were outgassed at 150 °C for 1 h (pressure less than 10^{-3} mbar) and cooled down to 25 °C and then pyrrole vapor (Aldrich, reagent grade, 98 wt%) was dosed repeatedly to get different equilibrium pressures.

Michael Addition reactions were performed in batch mode using a two-neck round bottom flask (100 mL) immersed in a silicone bath and equipped with a thermometer, a magnetic stirrer and a reflux condenser. In order to avoid the oxidation of the catalysts, the reflux condenser was fitted to a glass silicone-bubbler designed in a way that allows the entry of nitrogen by the top of the condenser and prevents the presence of water and oxygen in the reaction system.

In a typical experiment, 833 mg (4.0 mmol) of trans-chalcone (Sigma-Aldrich, 97 wt%), 264 mg (4.0 mmol) of malononitrile (Sigma-Aldrich, ≥99 wt%) and 150 mg of

anhydrous toluene (Sigma-Aldrich, 99.8 wt%) as internal standard were dissolved in dry methanol (chalcone/methanol weight ratio of 0.05). An aliquot of this solution was taken to determine the composition of the reaction mixture at zero time before adding the solution over the catalyst (catalyst/chalcone weight ratio of 0.04), which was previously introduced in the round bottom flask inside a nitrogen-filled glove bag.

All the test reactions were performed at 60 ºC under magnetic stirring and the progress of the reaction was monitored by withdrawing small aliquots (0.1 cm^3) using a syringe at defined time intervals. The samples were diluted with 0.2 cm^3 of chloroform, filtered and analyzed by gas chromatography using a Varian 430-GC gas chromatograph equipped with a flame ionization detector (FID) and a (95%)-dimethyl-(5%)-diphenylpolysiloxane DB – 5ms capillary column (15 m × 0.25mm ID × 0.25 μm). Under the same reaction conditions, a blank experiment (in the absence of catalyst) was performed resulting in a yield of 0% after 7 h.

To isolate the product from the reaction mixture, the catalyst was filtered and the resulting filtrate was cooled leading to the precipitation of the product. The resulting solid was extracted by filtration and purified by washing with cold methanol and hexane several times. The product 2-(3-oxo-1,3-diphenylpropyl)malononitrile was identified by ^{1}H-NMR spectroscopy (Bruker Avance III-HD NANOBAY 300 MHz). The spectrum (Figure S1 of the Supporting Information) agrees with those reported in literature [22, 23]. ^{1}H-NMR (300 MHz, $CDCl_3$) δ: 7.98-7.95 (m, 2H, ArH), 7.65-7.60 (m, 1H, ArH), 7.54-7.38 (m, 7H, ArH), 4.64 (d, J = 5.1 Hz, 1H, CN-CH), 3.96 (dt, J = 8.1, 5.4 Hz, 1H, Ar-CH), 3.76 – 3.60 (m, 2H, CH_2).

3. Results and discussion

Several silicon diimide and silicon-aluminium imide-type gels have been prepared as summarized in Table 1. The silicon diimide gels were obtained by the ammonolysis reaction of silicon tetrachloride using an ionic liquid (*IL*) as solvent, according to reaction (1), resulting in a white gel of silicon diimide, ammonium chloride and the ionic liquid.

$$SiCl_4 + 6\ NH_3\,(g) \xrightarrow{IL} Si(NH)_2 + 4\ NH_4Cl \qquad (1)$$

For the preparation of the silicon-aluminium imide gels, the silicon tetrachloride was subjected to a joint ammonolysis with anhydrous aluminium chloride, using the ionic liquid $[C_2C_1im][Tf_2N]$ as solvent. In this case, a gel consisting in silicon-aluminium imide ($T(NH)_x$ where T = Si, Al), ammonium chloride and the ionic liquid was obtained.

All the gels were prepared by using the ionic liquid 1-ethyl-3-methylimidazolium bis(trifluoromethylsulfonyl)imide ($[C_2C_1im][Tf_2N]$) ((Figure S2 (a) of the Supporting Information) except for the gels in which sodium amide was applied as a mineralizing agent. This imidazolium-based ionic liquid incorporates a hydrogen substituent at the C2 position which can be easily deprotonated under basic conditions leading to N-heterocyclic carbenes [24]. Therefore, it is necessary to use a different ionic liquid when sodium amide is applied in order to avoid the reaction between this compound and the ionic liquid. Although substitution of the C2 position of the imidazolium cation should prevent side reactions with base compounds, we found that the C2 methyl substituted 1-ethyl-2,3-dimethylimidazolium [Edmim] cation is not completely inert under basic conditions. When the ionic liquid $[Edmim][Tf_2N]$ was kept under stirring at room

temperature during 10 minutes in the presence of an excess of sodium amide ($NaNH_2$/[Edmim][Tf_2N] molar ratio of 2), the [Edmim] cation decomposed completely. This decomposition was confirmed by comparing the ^1H NMR spectrum of the reaction mixture with the spectrum of the pure ionic liquid (Figures S3 and S4 of the Supporting Information). As the substitution of the C2 position did not increase the chemical stability of the imidazolium-based ionic liquid under basic conditions, we focused our attention on the ionic liquids based on a N,N'-dialkylpyrrolidinium cation. This cation, having only one nitrogen atom in a five-member ring structure, should exhibit a lower acidity. When the ionic liquid 1-butyl-1-methylpyrrolidinium bis(trifluoromethylsulfonyl)imide ([C_4C_1pyrr][Tf_2N]) ((Figure S2 (b) of the Supporting Information) is heated at 180 ºC under vigorous stirring for 1 hour in the presence of an excess of sodium amide ($NaNH_2$/[C_4C_1pyrr][Tf_2N]) molar ratio of 2), the [C_4C_1pyrr] cation does not seem to react with the sodium amide as the ^1H NMR spectrum of the reaction mixture shows all the signals corresponding to the pure ionic liquid (Figure S5 of the Supporting Information). Due to the high chemical stability of the pyrrolidinium-based ionic liquid under basic conditions at the temperature required to process the materials (180 ºC), the solvent used when the sodium amide was applied as a mineralizing agent was the ionic liquid 1-butyl-1-methylpyrrolidinium bis(trifluoromethylsulfonyl)imide ([C_4C_1pyrr][Tf_2N]). The experimental procedure of the ionic liquids synthesis and of the study of their chemical stability can be found in the Supporting Information.

3.1. Characterization of the as-prepared samples.

The ATR-FTIR spectra of the as-prepared samples obtained after the solvothermal treatment of the different all-silicon diimide gels (Figure 1) indicate the effective formation of the Si-N network by the presence of various bands attributed to ν(Si-N) modes (905 cm^{-1}, 1083 cm^{-1} and 820 cm^{-1}) [6]. In all the cases, bands corresponding to the $\nu_a(CF_3)$, ν(C-ethyl), $\nu_s(SO_2)$, ν_a(SNS) and ν_s(SNS)/ν(CS)/γ(CH) modes of the $[Tf_2N]^-$ anion [25] appear, evidencing that the ionic liquid is present in all the materials. As the samples were washed with an abundant amount of methanol, this suggests that the ionic liquid is strongly retained in the material. As we have already observed elsewhere [17], changes in the spectral features of the samples take place as a function of the chemical composition and thermal treatment of the gels. Thus, the spectrum of sample Si-150-21d shows similar intensity in the three regions corresponding to ν(Si-N) bands (820, 905 and 1083 cm^{-1}), while samples prepared with other chemical compositions or subjected to different thermal treatment of the gel show a significantly higher absorbance of the 905 cm^{-1} band. This variation might be associated with changes in the polymerization degree of the silicon diimide gel. The mineralizing role of basic compounds as pyrrolidine and ammonia, i.e., its promotion of the condensation of the silicon diimide gel, which has already been observed in the samples studied in our previous report, is also observed in the samples studied in this work. The addition of these compounds seems to catalyze the condensation process of Si-N moieties; the samples Si-0.4Py-180-43h and Si-180-43h-NH, which were prepared in the presence of pyrrolidine and ammonia, respectively, show a strong 905 cm^{-1} band but much weaker 820 and 1085 cm^{-1} bands than the samples obtained in the absence of these compounds, the band at 820 cm^{-1} being hardly observed. On the other hand, the addition of sodium amide doesn't result in any significant change in the polymerization degree and in fact, when pyrrolidine is applied along with sodium amide, the promotion of the

condensation is disfavored since the band at 905 cm^{-1} shows notably lower intensity in the sample Si-0.25Py-0.1Na-180-7d, prepared in the presence of both pyrrolidine and sodium amide, than in the sample prepared under the same experimental conditions but in the absence of any basic compound (Si-180-7d). This observation evidences the complexity of the chemical process that leads to these diimide gels.

The heating temperature also seems to affect the polymerization process as the samples treated at 180 ºC show a relatively stronger 905 cm^{-1} band compared with the ones subjected to a solvothermal treatment at 150 ºC for the same heating time. Moreover, a long heating time of 21 days leads to a decrease in the condensation process, which is more significant when the samples are treated at 150 ºC.

The formation of the Si-N network and the presence of the ionic liquid in the samples are also proven from the ATR-FTIR spectra of the as-prepared samples obtained after the solvothermal treatment of the different silicon-aluminium imide gels (Figure 2). In this case, the effect of ammonia and pyrrolidine on the degree of condensation of the Si(Al)-N network is not so pronounced as in the samples obtained from pure silicon gels. Moreover, the presence of both mineralizing agents in the same gel results in a reduction of the polymerization degree of the silicon-aluminium imide gel since the intensity of the 905 cm^{-1} band is higher in the sample heated under presure of ammonia but in the absence of pyrrolidine as compared to the sample obtained in the presence of both mineralizing agents.

The chemical CHNS analysis results (Table 2) indicate that the as-prepared samples contain a high proportion of ionic liquid as there is a significant amount of sulfur in all of them, which can only come from the anion $[Tf_2N]^-$ of the ionic liquid. This suggests that the ionic liquid might play a structure-forming role during the polymerization process, as will be discussed below. We have already discussed elsewhere [17] that,

based on the amount of carbon present in the samples in relation to the sulfur content, two different anions ($[Tf_2N]^-$ and Cl^-) would compensate the charge of the ionic liquid cations trapped in the solid. Taking this assumption into account, it is possible to determine the total organic content from the chemical analysis. Table 3 shows the results obtained for some selected samples, which are in reasonable agreement with the organic content determined as the total weight loss observed by TG analysis (Supplementary Information, S6). It is also interesting to notice the high proportion of ionic liquid occluded as compared with the amount of silicon and aluminium present in the material. The calculated ionic liquid/Si+Al molar ratio varied from 0.13 to 0.24 depending on the chemical composition and thermal treatment of the gels (Table 3), and it is mainly affected by the heating time, as it increases from 7 to 21 days. This increase of the amount of the ionic liquid occluded is in agreement with the decrease in the condensation process obserbed in the ATR-FTIR spectra of the as-prepared samples since the lower the polymerization, the greater the amount of ionic liquid occluded in the materials. On the other hand, the content of nitrogen measured by the method described in the experimental section is not reliable for these materials, for it was found that it greatly underestimated the amount of nitrogen of a silicon nitride reference sample. Therefore, it should be taken into account that nitrogen content values included in Table 2 might significantly underestimate the actual composition of the samples.

Chemical analysis of the samples obtained from the silicon-aluminium imide gels, indicate the presence of aluminium in the as-prepared samples (Table 2). Although the Si/Al molar ratio of the sample SiAl-180-43h-NH, which was heated under presure of ammonia in the absence of pyrrolidine, is close to that of the starting gel, this value is different for samples synthesized in the presence of pyrrolidine. The use of pyrrolidine

seems to increase the aluminium incorporation, but when ammonia and pyrrolidine are applied together, gels poorer in aluminium are obtained.

3.2. Characterization of the ammonia heat-treated samples.

The occluded organic material was nearly completely removed by heating the as-prepared samples under flowing ammonia at 600 ºC for 2 h, according to the residual carbon and sulfur content of the samples, which are below 1 wt% and 0.02 respectively in most cases (Table 4). The resulting ammonia heat-treated materials were analyzed by nitrogen adsorption-desorption at 77 K in order to determine their textural properties (Table 5). All the samples present a high surface area in the range 267-693 m^2/g and their isotherms show a notable hysteresis loop (Figure S7 of the Supporting Information). Their pore size distributions, evaluated using the BJH method, are relatively narrow and centered in the pore size range of the mesoporous materials (Figure S8 of the Supporting Information). However, there is a significant fraction of the total surface area that corresponds to micropores. The capability of several ionic liquids to act as structure-directing agents in the formation of open-framework structures has already been studied [26, 27], as in the synthesis of zeolite-type materials [28]. Therefore, it can be deduced that the ionic liquid used is this work is able to act as a pore-forming compound in the formation of the T-N (T = Si, Al) network.

The different surface area, pore volume and pore size that the materials exhibit, reveal that the templating action of the ionic liquid is very dependent upon the specific chemical composition and thermal treatment of the synthesis gel. It can be noticed that, in the purely siliceous materials, the surface area increases with the heating temperature for a given synthesis time, but the micropore surface follows the opposite trend, and it

also decreases with the heating time. On the other hand, the samples prepared by using pyrrolidine or ammonia as the only mineralizing agent are the ones with the highest surface area, above 600 m^2/g, and pore volume. Moreover, applying sodium amide, either alone or together with pyrrolidine, does not seem to have any benefit from the point of view of the textural properties, as both surface area and pore volume are even smaller than those of the sample obtained under the same experimental conditions but in the absence of this compound.

In the case of the aluminium-containing materials, heating the synthesis mixture having both pyrrolidine and ammonia together seems to be more effective in increasing the surface area than using either reagents separately. Nevertheless, the effect in the textural properties of the aluminium-containing materials caused by these base compounds is not as prominent as in the purely siliceous samples since the surface area of the sample SiAl-180-43h-NH, prepared in the presence of ammonia, is not as high as the one exhibited by the purely siliceous sample prepared under the same experimental conditions. Moreover, the Al-materials do not practically contain micropores as compared to the purely siliceous samples.

As it was mentioned above, direct determination of the nitrogen content of the samples by CHNS analysis gave unreliable results. Therefore, the nitrogen content of the ammonia heat-treated materials was estimated taking into account the content of silicon, aluminium, sulfur, hydrogen and carbon as determined from chemical analysis. As is shown in Table 4, a N/(Si+Al) molar ratio higher than 2 is obtained for all the samples, being significantly higher than in some mesoporous materials prepared by a different synthesis route but subjected to a heat treatment under flowing ammonia at the same temperature [10].

The ATR-FTIR spectra of the ammonia heat-treated samples (Figure 3) show the bands corresponding to various skeletal ν(Si-N) modes of the Si-N groups of the network and a band at 1209 cm^{-1} which correspond to a δ(NH) mode [10].

The stability of the ammonia heat-treated samples in air was studied in our previous work by recording an ATR-FTIR spectrum of one sample after being exposed to air for 1, 24 and 72 hours [17]. An air-exposure of 1 hour did not result in any perceptible change in the FTIR spectrum. However, prolonged exposure led to the appearance of characteristic Si-O vibration bands, which are the consequence of bulk partial oxidation and/or hydrolysis of the sample due to exposure to oxygen and water vapor. Here, in order to explore which one of these compounds is responsible for the modification of the samples, we have studied the stability of sample Si-0.4Py-180-43h under two different conditions. To evaluate its resistance to the combined oxidation by oxygen and hydrolysis by ambient water, we have recorded an ATR-FTIR spectrum of the sample after being exposed to air for 24 hours. To study its oxidation due only to oxygen, the sample was exposed to air using a system provided with a drying tube with 3 Å molecular sieve to remove the ambient water. Figure 4 shows that the exposure to air under anhydrous conditions leads to the appearance of characteristic Si-O vibration bands at ca. 1200, 1060, 950 and 800 cm^{-1}, attributed to υ_{as}(Si-O-Si), υ(Si-O), δ(Si-OH) and υ_s'(Si-O-Si), respectively [29-31]. These bands show higher intensity (especially the band at 1060 cm^{-1}) when the sample is exposed to both oxygen and ambient water. This means that not only the oxygen but also the ambient water lead to the decomposition of the material.

The chemical environments of nitrogen, silicon and aluminium on the materials surface were investigated by XPS. The N 1s, Si 2p and Al 2p core-level spectra of some selected ammonia heat-treated samples are shown in Figures 5, 6 and S9, respectively.

Analysis of the asymmetric N 1s band (Figure 5) reveals two components attributed to two different bonding states of nitrogen atoms (Table 6). The first component at high binding energy (400 - 399 eV) corresponds to T-NH_2 terminal groups on the materials surface, while the lower binding energy component is attributed to T-NH-T groups. In the samples based on a Si-N network, this last component is located between 398 and 398.3 eV [32]. However, when aluminium atoms are incorporated to the network, the position of this band shifts towards lower binding energies (~ 397.6 eV) [33]. Aluminium atoms, being less electronegative than silicon, cause an increase of the electron density on the nitrogen atoms resulting in a small decrease in the binding energy of the N 1s peak. Hence, the electron donor ability of the nitrogen atoms bonded to aluminium atoms will be higher than that for the purely siliceous materials. As it will be discussed below, this higher electron donor ability will result in an increase of the basic strength of the active sites of these materials. It can be noticed that the contribution of the first component, which is due to the presence of T-NH_2 terminal groups, is significantly smaller in the samples prepared by heating the synthesis mixture under pressure of ammonia (Si-180-43h-NH, SiAl-180-43h-NH and SiAl-0.27Py-180-43h-NH) and in that prepared having both pyrrolidine and sodium amide together (Si-0.25Py-0.1Na-180-7d). It can be concluded that the relative proportion of the two N 1s components depends on the chemical composition of the synthesis gel. On the other hand, the abundance of terminal –NH_2 groups, which in some samples account for nearly 50% of the total N atoms, is in agreement with the N/T ratio being higher than 2, as it was discussed above.

On the other hand, Si 2p XPS spectra (Figure 6) show only one symmetric peak evidencing a quite homogeneous chemical environment for the silicon atoms of the surface. The binding energy values for the Si 2p peak of the purely siliceous materials

are close to 103 eV (Table 7). Taking into account that a binding energy of 101.7 eV has been assigned to the Si 2p core-level of a Si-NNNN configuration of Si_3N_4 [34] and that the BE for silicon dioxide (SiO_2) is 103.9 eV [35], the Si 2p peaks of the ammonia heat-treated samples can be attributed to silicon atoms in a polysilazane-type environment ($Si(NH)_x$). It can be noticed that in the samples with a high contribution of the N 1s component due to T–NH–T groups (Si-180-43h-NH and Si-0.25Py-0.1Na-180-7d), a slight shift of the Si 2p peak towards lower binding energy (102.7 eV) takes place due to the lower electronegativity of the T–NH–T group as compared to the T–NH_2 terminal groups. When aluminium atoms are present in the samples, a more remarkable shift of the Si 2p peak towards lower binding energies takes place. As has been discussed for the N 1s spectra, aluminium atoms, being less electronegative than silicon, cause an increase of the electron density on the silicon atoms, resulting in a significant decrease in the Si 2p binding energy, as happens in the case of the sialon-type materials [33, 36]. This change in the Si 2p peak position is an undeniable proof of the presence of Al atoms bonded to Si atoms through –(NH)- groups on the materials surface.

The formation of an $Al(NH)_x$ environment was also confirmed by the analysis of the Al 2p spectra which show only one symmetric peak located at ~ 74.0 eV (Supplementary Information, Figure S9 and Table 7). As several XPS studies performed on aluminium nitride (AlN) films, have shown an Al 2p peak located between 73.7 and 73.3 eV [37, 38] while a binding energy of 75.9 eV has been assigned to aluminium bound to oxygen in γ-Al_2O_3 [39], the Al 2p peak of the materials studied in this work is assigned to aluminium in an intermediate electron-withdrawing environment such as aluminium bound to –(NH)- groups ($Al(NH)_x$).

Table 7 also shows the Si/Al molar ratio on the materials' surfaces determined by XPS, which is is close to that of the bulk composition determined by ICP analysis.

3.3. Catatytic activity

The properties of the ammonia heat-treated materials as solid base catalysts have been evaluated by using the Michael addition reaction between chalcone and malononitrile as a probe reaction (Scheme 1 of the Supporting Information).

As the desired 1,4 – addition product was the only product detected in any of the reactions studied, the evolution of the Michael addition reaction is given by the yield of this product. Figure 7 shows the evolution with time of the yield of the 1,4 – addition product for the ammonia heat-treated catalysts using a catalyst/chalcone weight ratio of 0.04. All the catalysts show high catalytic activity, reaching a yield of at least 80% in some cases, while a mesoporous silica MCM-41 used for comparison purposes, which would be an oxygen-based analogue of the Si-N based materials, showed no catalytic activity at the same reaction conditions. This result reveals that the incorporation of nitrogen in a silicon-based network results in the generation of basic active sites.

The comparison between the catalytic activity of the different catalysts would show the influence of the surface area and the chemical composition of the materials. At short reaction times ($t < 1$ h), the reaction yield increases very fast, and a smooth increase of yield as a function of time is observed as the reaction is prolonged beyond 1 or 2 hours. The largest differences in activity mainly take place at the first stages of the reaction ($t < 1$ h), which can mainly be due to differences in the surface area of the materials but also to differences in the intrinsic catalytic activity of the active sites. Figure 8, which represents the reaction yield versus the specific surface area of the catalysts for a specific reaction time ($t = 15$ min), shows that in the case of the purely siliceous

materials there is a trend for the reaction yield to increase with the specific surface area, with the exception of sample Si-180-43h-NH which was prepared in the presence of ammonia. This sample exhibits higher catalytic activity than other catalysts with similar surface area. This effect can be due to the high proportion of Si-NH-Si groups on the material surface as compared with the remaining Si-N based catalysts, according to XPS results discussed above. In these groups, the electron donor ability of the nitrogen atoms would be higher than for the Si-NH_2 terminal groups, which should result in a higher basic strength of the active sites.

These conclusions are supported by additional characterization results obtained by FTIR analysis of samples kept in a vacuum cell under controlled atmosphere and using pyrrole as a probe to evaluate the relative strength of the basic sites. Spectra corresponding to sample Si-150-7d have been plotted in Figure 9 as a representative example, together with the spectrum of pyrrole vapor used as reference (spectra of other samples have been included in the supplementary information, Figure S10). The spectra of samples previously degassed at 150°C show a strong band at ca. 3380 cm^{-1} that can be assigned to the N-H stretching mode of Si-NH-Si groups and two bands at 3490 and 3640 cm^{-1} (the later one being notably broader) that are attributed to the symmetric and asymmetric H-N-H stretching modes of Si-NH_2 species (supplementary information, Figure S10). Additionally, weak bands can be observed at 3740 cm^{-1} and at ca. 3700 cm^{-1} (broad shoulder), corresponding to isolated and perturbed silanol species, which reveals that samples are slightly oxidized. The relative intensities of the Si-NH-Si and Si-NH_2 stretching bands evidence that most of the nitrogen atoms in sample Si-180-43h-NH are present as bridging Si-NH-Si species, that the fraction of terminal Si-NH_2 groups is slightly higher in sample Si-0.25Py-0.1Na-180-7d and that it increases notably for samples Si-150-7d and Si-0.1Na-180-7d, in agreement with the relative proportions

of the two components observed in the N1s core-level spectra (Table 6). The relative strength of basic sites present in these samples was evaluated by adsorption of pyrrole, for it is known that the interaction of the NH group of pyrrole with an electron donor site produces a bathochromic shift of its stretching vibration band with respect to the molecule in the vapor phase, and the magnitude of this shift can be used as a measure of the strength of the basic site [40]. The FTIR spectra recorded after dosing of pyrrole vapor into the cell showed the development of bands that overlap with those of the NH and NH_2 groups of the samples (supplementary information, Figure S10). The difference spectra obtained by subtracting the spectrum of the corresponding degassed sample show that the band corresponding to the ν(NH) mode of adsorbed pyrrole interacting with basic sites appears at wavenumber values in the range 3450-3470 cm^{-1}, and that its exact position varies from one sample to another. In addition, an overlapping band that grows as the equilibrium pressure increases can be observed at 3410 cm^{-1}, which is assigned to physisorbed pyrrole [40]. The calculated shifts for the ν(NH) band of pyrrole adsorbed on basic site with respect to free pyrrole are collected in Table 8. The results show that the largest shift is obtained for sample Si-180-43h-NH (-78 cm^{-1}), proving that this sample possess the strongest basicity among the Si-N samples. The data also confirm that the overall basic strength of the catalysts decreases as the ratio of bridging Si-NH-Si to terminal Si-NH_2 groups decreases, in agreement with the expected higher electron donor ability of the nitrogen atom in Si-NH-Si moieties. The variation in the magnitude of the shift of the ν(NH) band of pyrrole suggests that there are significant differences in basic strength among the samples. For comparison purposes, adsorption of pyrrole was also carried out on a strong basic solid material, an Al-Mg mixed oxide obtained by calcination of a hydrotalcite material with Mg/Al ratio of 2. For this sample, adsorption of pyrrole gave rise to the development of

a strong band at 3388 cm^{-1}, indicating a -142 cm^{-1} shift of the ν(NH) band of pyrrole (supplementary information, Figure S10), in agreement with previous results obtained with similar samples [41]. This shift is notably larger than the maximum value obtained for the Si-N materials (-78 cm^{-1}), which suggests that these materials exhibit moderate basic strength.

Figure 8 shows that the active sites of two of the aluminium-containing samples exhibit a higher intrinsic catalytic activity as compared with the Si-N based materials. In this case, the relative proportion of the T-NH-T groups is not the only factor influencing the catalytic activity of the catalysts. The incorporation of aluminium atoms, which are less electronegative than silicon, causes an increase of the electron density on the nitrogen atoms bound to aluminium atoms resulting in an enhancement of the intrinsic catalytic activity of the active sites. Indeed, the calculated shift of the NH stretching of pyrrole adsorbed on sample SiAl-0.27Py-180-43h (Table 8) is higher than the one expected for Si-N samples with similar molar ratio of bridging T-NH-T to terminal T-NH_2 sites (as determined by XPS: Table 6). Nevertheless, this shift is slightly smaller than that obtained for the Si-N with the highest content of Si-NH-Si groups, which indicates that the basic strength of sample SiAl-0.27Py-180-43h is close but slightly lower than that of sample Si-180-43h-NH.

Comparing the two aluminium-containing samples, sample SiAl-0.27Py-180-43h exhibits a higher catalytic activity in spite of its lower surface area and its higher proportion of T-NH_2 terminal groups. As the Si/Al molar ratio of this sample is significantly lower than that of the remaining aluminium-containing samples, it can be concluded that an increase of the aluminium content leads to the formation of active sites with higher overall intrinsic activity. In this regard, the calculated reaction yield/S_{BET} ratio for a specific reaction time (t = 15 min) has been plotted in Figure 10 as

a function of the Al/Si molar ratio for three of the catalysts. It can be seen that the intrinsic catalytic activity of a purely siliceous catalyst like sample Si-180-7d is considerably lower than that of the aluminium-containing samples, and the activity of the latter increases with their aluminium content.

Sample SiAl-180-43h-NH was selected to investigate the influence of the solvent on the reaction yield. Table 1 of the Supporting Information shows the activity of this catalyst for the Michael addition reaction between chalcone and malononitrile in different solvents. As we previously discussed, when the reaction is conducted in methanol for a catalyst/chalcone weight ratio of 0.08 the reaction yield is ~ 98 %. However, when THF, CH_2Cl_2 or $CHCl_3$ (all of them previously dried) is used as solvent, the Michael addition reaction between chalcone and malononitrile does not take place even if the catalyst/chalcone ratio is increased to 0.16. Several reports have shown this great influence of the solvent nature on the catalytic behavior. For example, no 1,4 – addition product formation was observed in aprotic solvents when using different chiral amines as basic catalysts, whereas the reaction proceeds very well in methanol [42]. Moreover, some reports indicate that the use of an aprotic solvent leads to a decrease in the yield of the 1,4 – addition product [22, 43]. According to the classical mechanism of the Michael addition reaction, the abstraction of a proton from the donor by the basic sites (T-NH-T) of the catalyst generates a carbanion which can be stabilized by the cationic charge created in the lattice (Scheme 2 of the Supporting Information, step 1). The carbanion then reacts in a 1,4-conjugate addition to the chalcone (step 2). The resulting anion would be protonated giving the final product and regenerating the active site (step 3). Based on this mechanism we hypothesize that methanol, being a polar protic solvent, can stabilize the charged intermediates by hydrogen bonding and promote rapid proton

transfer [44]. In aprotic and less polar solvents, the formation of the intermediates is not so favored.

As mentioned above, the initial step of the Michael addition reaction is deprotonation of the donor to form a carbanion. To carry out this step, the catalysts must have a pK_a for their conjugate acid in the same range as that of the Michael donor. The lower the pK_a value of the donor, the easier it is to abstract a proton, so the basic strength of the catalysts could be estimated by varying the pKa of the donors. When malononitrile (pK_a 11) is the donor, the Michael addition to chalcone takes place with a high yield (~ 98 %.) over SiAl-180-43h-NH in methanol. On the contrary, when using diethylmalonate (pK_a 13.3), the reaction does not occur even if the catalyst/chalcone ratio is increased to 0.16. Since malononitrile is a weak acid compared with other Michael donors [45], such as cyanoacetamide (pK_a 2.96), it can be estimated that the strength of the basic sites on SiAl-180-43h-NH is considerably high, although it is not high enough to deprotonate an acid as weak as the diethylmalonate. Therefore, the basic strength of these N-containing materials should be in the range $11 < pK_a < 13.3$. To compare the catalytic activity of the catalysts with well-known basic catalysts, Michael addition reaction was performed at the same conditions over the sodium form of zeolite (Aldrich 13X zeolite powder) and an Al-Mg mixed oxide (obtained by calcination of a hydrotalcite material with Mg/Al ratio of 2). Figure 11 and Table 9 shows the yield of the 1,4 – addition product for these catalysts and for SiAl-0.27Py-180-43h, Si-180-21d and Si-180-43h-NH after 15 min and 7 hours of reaction. It can be noticed that at the first stages of the reaction (t = 15 min), the catalysts prepared in this work show lower catalytic activity than the sodium zeolite and the calcined hydrotalcite, the latter of which gave the highest yield. However, when the reaction time comes to 7 hours, the yield is almost the same for the five materials (Table 9). Considering the calculated reaction yield/S_{BET} ratio of the

materials, it can be observed that the intrinsic catalytic activity of the Al-Mg mixed oxide is notably higher than that of the other materials (Table 9), in agreement with its higher basic strength estimated by FTIR of adsorbed pyrrole and with previous catalytic studies [46]. However, despite having lower aluminium content, the SiAl-0.27Py-180-43h catalyst exhibits an intrinsic catalytic activity which is quite close at least, if not higher, than that of the sodium zeolite.

As we mentioned above, the ammonia heat-treated samples undergo oxidation and hydrolysis when exposed to the air, leading to the appearance of Si-O groups and to the consequent reduction of the number of T-NH active sites. To study the influence of this alteration of the material upon the reaction yield, we have performed the Michael addition reaction over the Si-0.4Py-180-43h sample before and after being exposed to air for 15 days. This prolonged air exposure did not result in any significant change of the FTIR spectrum with respect to the one recorded after 24 hours air-exposure (shown in Figure 4). Figure 12, which represents the reaction yield versus time, shows that the catalytic activity is reduced significantly when the sample is oxidized reaching a yield of ~ 33% after 7 hours of reaction, while the fresh sample reached a yield close to 70%. This result reveals that air-exposure leads to a significant reduction of the number of T-NH active sites but not to the complete oxidation of the sample. Although the bands corresponding to the T-NH groups are not clearly observed in the FTIR spectrum of the oxidized sample, they might be obscured due to overlapping with the wide Si-O bands as the material should have some T-NH active groups which have resisted the oxidation and are active to catalyze the reaction.

Conclusions

All-silicon and silicon-aluminium porous materials containing a framework formed by T-NH-T linkages can be easily prepared by the reaction between ammonia and silicon and aluminium chlorides in an ionic liquid under controlled reaction conditions. The ionic liquid occluded in the as-made materials can be removed by heating in an ammonia flow at 600 ºC, leaving materials with a high surface area and porosity. It has been found that the textural properties of the resulting solids are very much dependent upon the specific synthesis conditions and the chemical composition of the gel, and in particular of the aluminium content of the framework. In this latter case, when aluminium is present in the solid, mesoporous materials containing no micropores have been obtained.

Beside the presence of T-NH-T units, a large amount of terminal T-NH_2 groups are also evidenced by IR and XPS. These groups can be considered as defects that interrupted the framework very much in the same way as Si-OH are commonly found in silicon and oxygen-based mesoporous materials. The relative content of these defects is also strongly related to the specific synthesis conditions and chemical composition of the gels.

These nitrogen-containing materials exhibit basic properties owing to the presence of two types of N-groups, the bridging –NH- units and the T-NH_2 terminal groups. The overall basic strength of these materials has been shown by pyrrole adsorption to increase with the fraction of T-NH-T groups and the aluminium content of the framework. Moreover, this basic strength is lower than that of a calcined hydrotalcite (Al/(Al+Mg) = 0.33). However, these materials are active catalysts in the Michael addition reaction between chalcone and malononitrile (pK_a 11) carried out in methanol, although they turned to be inactive when diethylmalonate having a weaker acidity (pK_a 13.3) is used as the donor. Therefore, the basic sites of these materials should have pK_a

values within that range. It is also noteworthy that no products other than that resulting from the Michael addition are detected. The reaction is also very sensitive to the nature of the solvent, for it does not proceed in dichloromethane, chloroform and tetrahydrofuran.

Acknowledgments

A. Saugar, C. Márquez-Álvarez and J. Pérez-Pariente acknowledge the Spanish Ministry of Economy and Competitiveness for the funding through Project MAT2012-31127. A. Saugar also acknowledges this Ministry for a research grant to stay at the Prof. Welton laboratory at Imperial College.

References

[1] J.S. Bradley, O. Vollmer, R. Rovai, U. Specht, F. Lefebvre, Advanced Materials. 10 (1998) 938-942.

[2] O. Vollmer, F. Lefebvre, J.S. Bradley, Journal of Molecular Catalysis A: Chemical. 146 (1999) 87-96.

[3] H.N. Han, D.A. Lindquist, J.S. Haggerty, D. Seyferth, Chemistry of Materials. 4 (1992) 705-711.

[4] R. Rovai, C.W. Lehmann, J.S. Bradley, Angewandte Chemie International Edition. 38 (1999) 2036-2038.

[5] F. Cheng, S. Clark, S.M. Kelly, J.S. Bradley, F. Lefebvre, Journal of the American Ceramic Society. 87 (2004) 1413-1417.

[6] V. Rocher, S.M. Kelly, A.L. Hector, Microporous and Mesoporous Materials. 156 (2012) 196-201.

[7] K.S. Mazdiyasni, C.M. Cooke, Journal of the American Ceramic Society. 56 (1973) 628-633.

[8] W. Schnick, H. Huppertz, Chemistry – A European Journal. 3 (1997) 679-683.

[9] S. Kaskel, D. Farrusseng, K. Schlichte, Chemical Communications. (2000) 2481-2482.

[10] S. Kaskel, K. Schlichte, B. Zibrowius, Physical Chemistry Chemical Physics. 4 (2002) 1675-1681.

[11] S. Kaskel, Journal of Catalysis. 201 (2001) 270-274.

[12] D. Farrusseng, K. Schlichte, B. Spliethoff, A. Wingen, S. Kaskel, J.S. Bradley, F. Schüth, Angewandte Chemie International Edition. 40 (2001) 4204-4207.

[13] J.S. Bradley, F. Cheng, S.J. Archibald, R. Supplit, R. Rovai, C.W. Lehmann, C. Kruger, F. Lefebvre, Dalton Transactions. (2003) 1846-1851.

[14] F. Cheng, S.M. Kelly, F. Lefebvre, S. Clark, R. Supplit, J.S. Bradley, Journal of Materials Chemistry. 15 (2005) 772-777.

[15] S. Kaskel, Christian W. Lehmann, G. Chaplais, K. Schlichte, M. Khanna, European Journal of Inorganic Chemistry. 2003 (2003) 1193-1196.

[16] S. Kaskel, G. Chaplais, K. Schlichte, Chemistry of Materials. 17 (2005) 181-185.

[17] A.I. Saugar, A. Mayoral, J. Pérez-Pariente, Microporous and Mesoporous Materials. 186 (2014) 146-154.

[18] S. Sowmiah, V. Srinivasadesikan, M.C. Tseng, Y.H. Chu, Molecules (Basel, Switzerland). 14 (2009) 3780-3813.

[19] A. Yokozeki, M.B. Shiflett, Industrial & Engineering Chemistry Research. 46 (2007) 1605-1610.

[20] G. Li, Q. Zhou, X. Zhang, LeiWang, S. Zhang, J. Li, Fluid Phase Equilibria. 297 (2010) 34-39.

[21] S. Miyata, Clays and Clay Minerals. 28 (1980) 50-56.

[22] W. Yang, Y. Jia, D.-M. Du, Organic & Biomolecular Chemistry. 10 (2012) 332-338.

[23] X. Li, L. Cun, C. Lian, L. Zhong, Y. Chen, J. Liao, J. Zhu, J. Deng, Organic & Biomolecular Chemistry. 6 (2008) 349-353.

[24] S. Chowdhury, R.S. Mohan, J.L. Scott, Tetrahedron. 63 (2007) 2363-2389.

[25] O. Höfft, S. Bahr, V. Kempter, Langmuir. 24 (2008) 11562-11566.

[26] Z. Ma, J. Yu, S. Dai, Advanced Materials. 22 (2010) 261-285.

[27] S. Dai, Y.H. Ju, H.J. Gao, J.S. Lin, S.J. Pennycook, C.E. Barnes, Chemical Communications. (2000) 243-244.

[28] E.R. Cooper, C.D. Andrews, P.S. Wheatley, P.B. Webb, P. Wormald, R.E. Morris, Nature. 430 (2004) 1012-1016.

[29] P.N. Sen, M. Thorpe, Physical review. B, Solid state. 15 (1977) 4030-4038.

[30] R.B. Laughlin, J. Joannopoulos, Physical review. B, Solid state. 16 (1977) 2942-2952.

[31] P. McMillan, The American mineralogist. 69 (1984) 622-644.

[32] J.L. Bischoff, F. Lutz, D. Bolmont, L. Kubler, Surface Science. 251–252 (1991) 170-174.

[33] T. Hagio, A. Takase, S. Umebayashi, J Mater Sci Lett. 11 (1992) 878-880.

[34] T.T.T. Hien, C. Ishizaki, K. Ishizaki, Nippon Seramikkusu Kyokai Gakujutsu Ronbunshi/Journal of the Ceramic Society of Japan. 113 (2005) 647-653.

[35] D.F. Mitchell, K.B. Clark, J.A. Bardwell, W.N. Lennard, G.R. Massoumi, I.V. Mitchell, Surface and Interface Analysis. 21 (1994) 44-50.

[36] C. Qin, G. Wen, X. Wang, L. Song, X. Huang, Journal of Materials Chemistry. 21 (2011) 5985-5991.

[37] L. Rosenberger, R. Baird, E. McCullen, G. Auner, G. Shreve, Surface and Interface Analysis. 40 (2008) 1254-1261.

[38] D. Manova, V. Dimitrova, W. Fukarek, D. Karpuzov, Surface and Coatings Technology. 106 (1998) 205-208.

[39] B. Ealet, M.H. Elyakhloufi, E. Gillet, M. Ricci, Thin Solid Films. 250 (1994) 92-100.

[40] B. Camarota, Y. Goto, S. Inagaki, B. Onida, Langmuir. 27 (2011) 1181-1185.

[41] D. Tichit, M.N. Bennani, F. Figueras, J.R. Ruiz, Langmuir. 14 (1998) 2086-2091.

[42] S. Colonna, H. Hiemstra, H. Wynberg, Journal of the Chemical Society, Chemical Communications. (1978) 238-239.

[43] H. Keipour, M.A. Khalilzadeh, A. Hosseini, A. Pilevar, D. Zareyee, Chinese Chemical Letters. 23 (2012) 537-540.

[44] B.D. Mather, K. Viswanathan, K.M. Miller, T.E. Long, Progress in Polymer Science. 31 (2006) 487-531.

[45] B.M. Choudary, M. Lakshmi Kantam, C.R. Venkat Reddy, K. Koteswara Rao, F. Figueras, Journal of Molecular Catalysis A: Chemical. 146 (1999) 279-284.

[46] A. Corma, V. Fornés, R.M. Martín-Aranda, F. Rey, Journal of Catalysis. 134 (1992) 58-65.

TABLES

Table 1. Experimental conditions used for the preparation of silicon- and silicon-aluminium imidonitride materials from gels with the following molar composition: *$SiCl_4$: x $AlCl_3$ y Py: 4 NH_4Cl: (1.5+x) IL: z NH_3: q $NaNH_2$*, where *Py* stands for pyrrolidine applied as a potential structure directing agent, *z* stands for the quantity of ammonia dissolved in the gel before the heating process and *q* stands for the sodium amide applied as a potential mineralizing agent. *IL* refers to the ionic liquid applied as solvent (*$[C_2C_1im][Tf_2N]$* or *$[C_4C_1pyrr][Tf_2N]$*).

Sample	*x*	*y*	*z*	*q*	T^a / °C	t^b
Si-150-7d	0	0	0	0	150	7 days
Si-150-21d	0	0	0	0	150	21 days
Si-180-7d	0	0	0	0	180	7 days
Si-180-21d	0	0	0	0	180	21 days
Si-0.4Py-180-43h	0	0.4	0	0	180	43 hours
Si-180-43h-NH	0	0	3.0	0	180	43 hours
Si-0.1Na-180-7d[c]	0	0	0	0.1	180	7 days
Si-0.25Py-0.1Na-180-7d[c]	0	0.25	0	0.1	180	7 days
SiAl-0.27Py-180-43h	0.1	0.27	0	0	180	43 hours
SiAl-180-43h-NH	0.1	0	3.6	0	180	43 hours
SiAl-0.27Py-180-43h-NH	0.1	0.27	3.6	0	180	43 hours

[a] Heating temperature.

[b] Heating time.

[c] *IL*: *$[C_4C_1pyrr][Tf_2N]$*.

Table 2. Elemental composition of the as-prepared samples determined by CHNS chemical analysis and ICP-OES (Si and Al).

As-prepared sample	*Chemical CHNS analysis*				*ICP*		
	C (wt%)	*H (wt%)*	*N (wt%)*	*S (wt%)*	*Si (wt%)*	*Al (wt%)*	*Si/Al*[a]
Si-150-7d	15.80	5.00	13.64	1.00	38.1	-	-
Si-150-21d	20.33	6.10	8.83	0.80	40.5	-	-
Si-180-7d	14.20	4.69	15.88	1.12	36.6	-	-
Si-180-21d	16.94	4.94	13.33	1.35	30.6	-	-
Si-0.4Py-180-43h	9.12	3.67	19.25	1.86	29.5	-	-
Si-180-43h-NH	11.90	4.20	16.85	1.03	31.6	-	-
Si-0.1Na-180-7d	19.16	6.41	11.76	0.88	32.3	-	-
Si-0.25Py-0.1Na-180-7d	18.26	6.01	12.55	0.81	35.1	-	-
SiAl-180-43h-NH	11.26	4.46	15.57	0.89	30.9	2.9	10.2
SiAl-0.27Py-180-43h-NH	13.26	4.8	14.24	0.68	29.6	2.3	12.4
SiAl-0.27Py-180-43h	15.95	4.99	12.43	1.13	26.0	3.1	8.1

[a] Molar ratio between the silicon and the aluminium content.

Table 3. Organic content of selected as-prepared samples determined from CHNS and ICP-OES analyses and from TG results.

As-prepared sample	*Chemical CHNS and ICP analyses*			*TG*
	$Cat^+[Tf2N]^-$ (wt%)	*Cat^+Cl^- (wt%)*	*Org/(Si+Al)*[a]	*Organic*[b] *(wt%)*
Si-150-7d	6.11	29.08	0.16	30.91
Si-150-21d	4.89	38.90	0.19	42.96
Si-180-7d	6.84	25.46	0.15	29.45
Si-180-21d	8.25	30.33	0.21	40.85
Si-180-43h-NH	6.29	21.06	0.14	26.21
Si-0.1Na-180-7d	5.80	28.49	0.15	37.08
SiAl-180-43h-NH	5.44	20.18	0.13	25.37

Cat^+: $[C_2C_1im]^+$or $[C_4C_1pyrr]^+$.

[a] Molar ratio between the organic species (Cat+[Tf2N]- and Cat+Cl-) content estimated from the CHNS analysis and the silicon and aluminium content of the material determined by ICP-OES.

[b] Weight loss in the TG analysis performed in an air flow from 25 to 900ºC.

Table 4. Elemental composition of the ammonia heat-treated samples determined by CHNS chemical analysis and ICP-OES (Si and Al).

Ammonia heat-treated sample	*Chemical CHNS analysis*				*ICP-OES*			
	C (wt%)	*H (wt%)*	*N (wt%)*	*S (wt%)*	*Si (wt%)*	*Al (wt%)*	*N/(Si+Al)*[a]	*Si/Al*[b]
Si-150-7d	1.06	1.16	7.32	0.02	48.5	-	2.04	-
Si-150-21d	0.47	1.52	4.61	0.01	38.3	-	3.10	-
Si-180-7d	0.53	1.40	14.1	0.00	44.1	-	2.45	-
Si-180-21d	0.77	1.60	9.51	0.02	39.4	-	2.96	-
Si-0.4Py-180-43h	1.77	1.75	14.05	0.01	36.9	-	3.24	-
Si-180-43h-NH	0.42	1.76	16.88	0.02	43.5	-	2.50	-
Si-0.1Na-180-7d	0.67	1.13	10.43	0.02	42.2	-	2.66	-
Si-0.25Py-0.1Na-180-7d	0.93	1.05	10.67	0.03	42.2	-	2.80	-
SiAl-180-43h-NH	0.51	1.44	11.37	0.01	38.1	3.6	2.70	10.2
SiAl-0.27Py-180-43h-NH	0.43	1.34	11.24	0.01	39.7	3.0	2.59	12.7
SiAl-0.27Py-180-43h	0.42	1.28	8.06	0.01	37.4	5.2	2.61	6.91

[a] Nitrogen to silicon (or silicon plus aluminium) molar ratio. Nitrogen content estimated taking into account the content of silicon, aluminium, sulfur, hydrogen and carbon determined by chemical analysis.

[b] Molar ratio between the silicon content and the aluminium content.

Table 5. Specific surface area, external surface, micropore area, pore volume and average pore diameter of the ammonia heat-treated samples.

Ammonia heat-treated sample	S_{BET} (m^2/g)	S_{ext} [a] (m^2/g)	S_{micro} [b] (m^2/g)	V_p [c] (cm^3/g)	Average pore diameter (nm)
Si-150-7d	267	202	65	0.57	9.0
Si-150-21d	306	119	187	0.44	9.4
Si-180-7d	626	569	57	1.25	7.2
Si-180-21d	537	440	97	1.04	7.5
Si-0.4Py-180-43h	693	653	40	1.54	7.9
Si-180-43h-NH	630	574	56	1.44	8.2
Si-0.1Na-180-7d	460	410	50	0.87	7.4
Si-0.25Py-0.1Na-180-7d	497	465	32	1.11	8.0
SiAl-0.27Py-180-43h	267	267	0	0.60	7.7
SiAl-180-43h-NH	325	319	6	0.90	9.7
SiAl-0.27Py-180-43h-NH	448	444	4	1.25	8.7

[a] Non-micropore (external and mesopore) surface area.

[b] Micropore surface area.

[c] Pore volume.

Table 6. Binding energy (B.E.) and relative contribution of N1s components of the XPS spectra.

Ammonia heat-treated sample	*Component 1*		*Component 2*	
	B.E. (eV)	*%*	*B.E. (eV)*	*%*
Si-150-7d	399.7	63	398.3	37
Si-180-7d	399.4	59	398.0	41
Si-180-21d	399.8	54.6	398.3	45.4
Si-0.4Py-180-43h	400.0	51.5	398.1	48.5
Si-0.1Na-180-7d	399.8	48	398.2	52
Si-0.25Py-0.1Na-180-7d	398.8	22.6	397.8	77.4
Si-180-43h-NH	398.9	20.3	398.0	79.7
SiAl-0.27Py-180-43h	399.4	31.4	397.7	68.6
SiAl-0.27Py-180-43h-NH	399.4	18.8	397.6	81.2
SiAl-180-43h-NH	399.1	14.3	397.4	85.7

Table 7. Binding energy (B.E.) of Si 2p and Al 2p bands of the XPS spectra and molar ratio between silicon and aluminium on the materials surface determined by XPS.

Sample	*B.E (eV)*		*Si/Al*
	Al 2p	*Si 2p*	
Si-150-7d	-	103.4	-
Si-180-7d	-	103.4	-
Si-180-21d	-	103.4	-
Si-0.4Py-180-43h	-	103.3	-
Si-0.1Na-180-7d	-	103.2	-
Si-0.25Py-0.1Na-180-7d	-	102.7	-
Si-180-43h-NH	-	102.7	-
SiAl-0.27Py-180-43h	74.2	102.3	7.8
SiAl-0.27Py-180-43h-NH	74.1	102.3	11.8
SiAl-180-43h-NH	74.0	102.0	11.1

Table 8. Shift of the N-H stretching mode of pyrrole upon adsorption on Si(Al)-N materials and an Al-Mg mixed oxide (calcined hydrotalcite).

Sample	$\Delta\nu\ (cm^{-1})$
Si-150-7d	-57
Si-0.1Na-180-7d	-58
Si-0.25Py-0.1Na-180-7d	-63
Si-180-43h-NH	-78
SiAl-0.27Py-180-43h	-73
Calcined hydrotalcite	-142

Table 9. Activity of Si(Al)-N materials and reference basic solid catalysts for the Michael addition reaction between chalcone and malononitrile.

Sample	*Physicochemical properties*		*t = 15 min*		*t = 7 hours*	
	$S_{BET}\ (m^2/g)$	*Si/Al*[a]	*Yield*[b] *(%)*	$Yield/S_{BET}$	*Yield*[b] *(%)*	$Yield/S_{BET}$
Si-180-21d	537	-	19	0.03	81	0.15
Si-180-43h-NH	630	-	39	0.06	83	0.13
SiAl-0.27Py-180-43h	266	6.91	37	0.14	89	0.33
Sodium zeolite	681	1.2	43	0.06	85	0.12
Calcined hydrotalcite	202	-	50	0.24	86	0.42

[a] Silicon to aluminium molar ratio determined by ICP.

[b] Reaction conditions: Chalcone/malononitrile molar ratio: 1, catalyst/chalcone weight ratio: 0.04; chalcone/solvent weight ratio: 0.05, reaction temperature: 60 ºC.

Figure Captions.

Fig. 1. ATR-FTIR spectra of the as-prepared samples obtained from silicon diimide-type gels; (a) Si-150-21d, (b) Si-180-21d, (c) Si-0.25Py-0.1Na-180-7d, (d) Si-150-7d, (e) Si-180-7d, (f) Si-0.1Na-180-7d, (g) Si-0.4Py-180-43h and (h) Si-180-43h-NH.

Fig. 2. ATR-FTIR spectra of the as-prepared samples obtained from silicon-aluminium imide-type gels; (a) SiAl-0.27Py-180-43h, (b) SiAl-0.27Py-180-43h-NH and (c) SiAl-180-43h-NH.

Fig. 3. ATR-FTIR spectra of the ammonia heat-treated samples; (a) SiAl-0.27Py-180-43h-NH, (b) Si-150-21d, (c) SiAl-180-43h-NH and (d) Si-180-7d.

Fig. 4. FTIR spectra of the ammonia heat-treated sample Si-0.4Py-180-43h before and after being exposed to air for 24h in the presence and in the absence of ambient water.

Fig. 5. N 1s XPS spectra of the some selected ammonia heat-treated samples.

Fig. 6. Si 2p XPS spectra of some selected ammonia heat-treated samples; (a) SiAl-180-43h-NH, (b) SiAl-0.27Py-180-43h-NH, (c) Si-180-43h-NH and (d) Si-0.4Py-180-43h.

Fig. 7. Yield of the 1,4 – addition product vs reaction time of the ammonia heat-treated catalysts. Reaction conditions: reaction temp: 60 ºC, chalcone/malononitrile molar ratio: 1, catalyst/chalcone weight ratio: 0.04, chalcone/methanol weight ratio: 0.05.

Fig. 8. Influence of the specific surface area of the catalyst on the yield of the 1,4 – addition product for the Si-N based materials (full symbols) and for the aluminium-

containing materials (open symbols) after 15 min of reaction. Reaction conditions: reaction temp: 60 ºC, chalcone/malononitrile molar ratio: 1, catalyst/chalcone weight ratio: 0.04, chalcone/methanol weigth ratio: 0.05.

Fig. 9. FTIR spectra of sample Si-150-7d (3.1 mg/cm^2 thickness) after degassing at 150°C (a) and in contact with pyrrole vapor at 25ºC and equilibrium pressure of ca. 1 mbar (b) and ca. 10 mbar (c). Difference spectra c-a and b-a are shown to facilitate determination of the shift of the NH stretching band of pyrrole. The spectrum of pyrrole vapor (6 mbar) is also shown for reference (NH stretching band centered at 3530 cm^{-1}). The arrow indicates the shifts of the ν(NH) band of pyrrole due to H-bonding with basic sites. At high equilibrium pressure, the 3410 cm^{-1} band (marked with an asterisk) corresponding to physisorbed pyrrole [40] becomes dominant.

Fig. 10. Calculated reaction yield/S_{BET} ratio for t = 15 min vs Al/Si molar ratio for the Si-N based materials (full symbols) and for the aluminium-containing materials (open symbols). Reaction conditions: reaction temp: 60 ºC, chalcone/malononitrile molar ratio: 1, catalyst/chalcone weight ratio: 0.04, chalcone/methanol weigth ratio: 0.05.

Fig. 11. Yield of the 1,4 – addition product vs reaction time of SiAl-0.27Py-180-43h, Si-180-43h-NH and two reference basic catalysts; sodium zeolite and calcined hydrotalcite. Data corresponding to the first hour of reaction are shown in the right figure for clarity. Lines are guide for the eyes. Reaction conditions: reaction temp: 60 ºC, chalcone/malononitrile molar ratio: 1, catalyst/chalcone weight ratio: 0.04, chalcone/methanol weigth ratio: 0.05.

Fig. 12. Yield of the 1,4 – addition product vs reaction time of SiAl-0.4Py-180-43h before and after being exposed to ambient air for 15 days (lines are guide for the eyes). Reaction conditions: reaction temp: 60 ºC, chalcone/malononitrile molar ratio: 1, catalyst/chalcone weight ratio: 0.04, chalcone/methanol weigth ratio: 0.05.

FIGURES

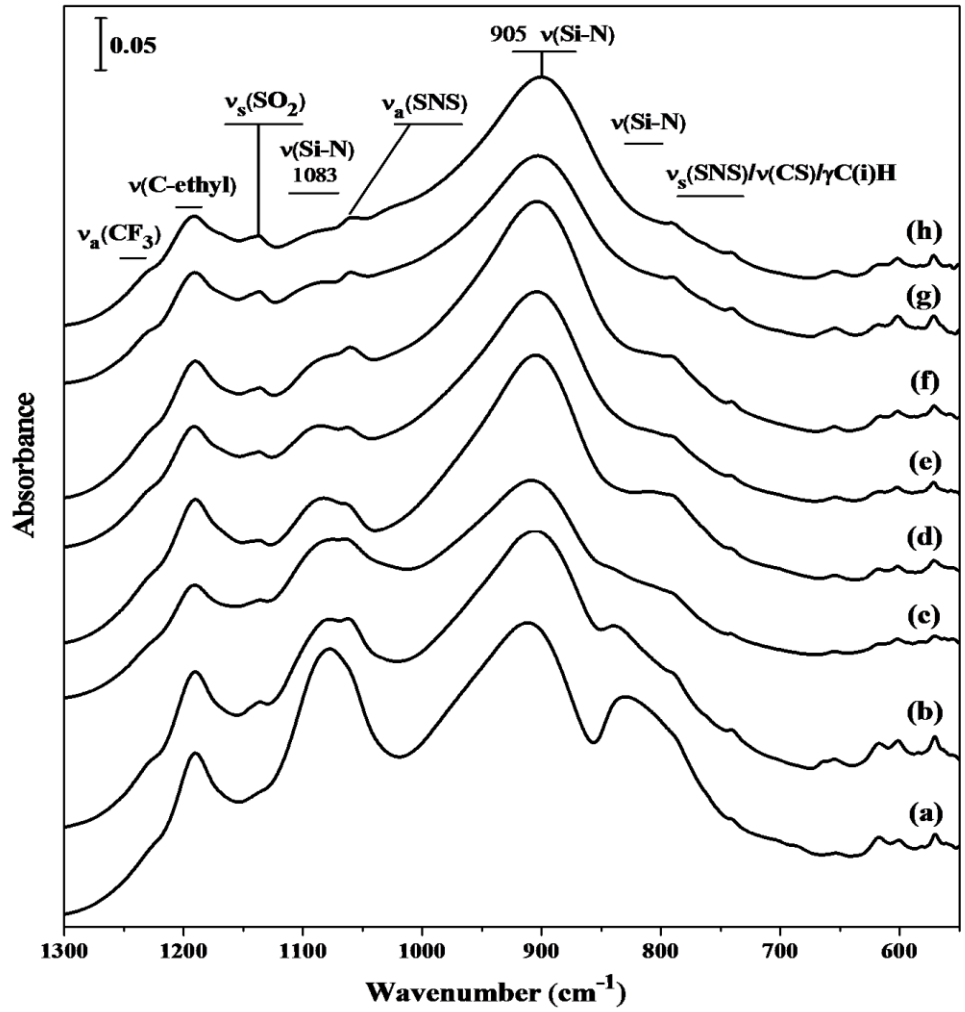

Fig. 1.

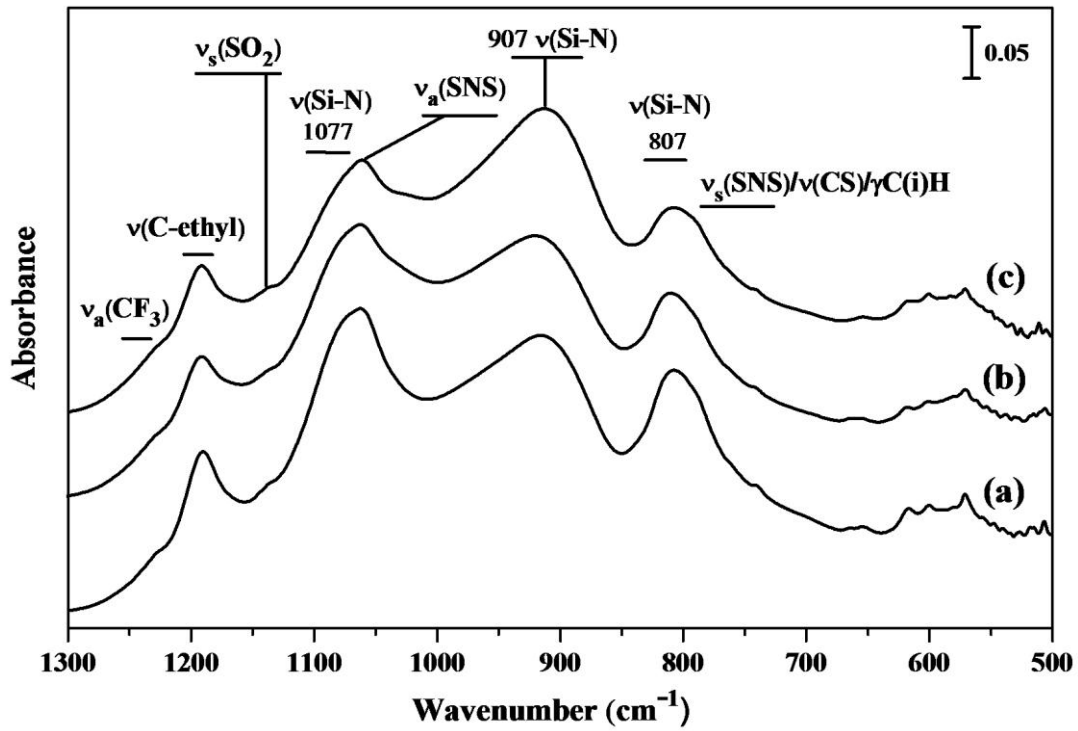
νs(SO2)
907 ν(Si-N)
0.05
ν(Si-N)
1077
νa(SNS)
ν(Si-N)
807
νs(SNS)/ν(CS)/γC(i)H
ν(C-ethyl)
νa(CF3)
(c)
(b)
(a)
Absorbance
1300
1200
1100
1000
900
800
700
600
500
Wavenumber (cm-1)

Fig. 2.

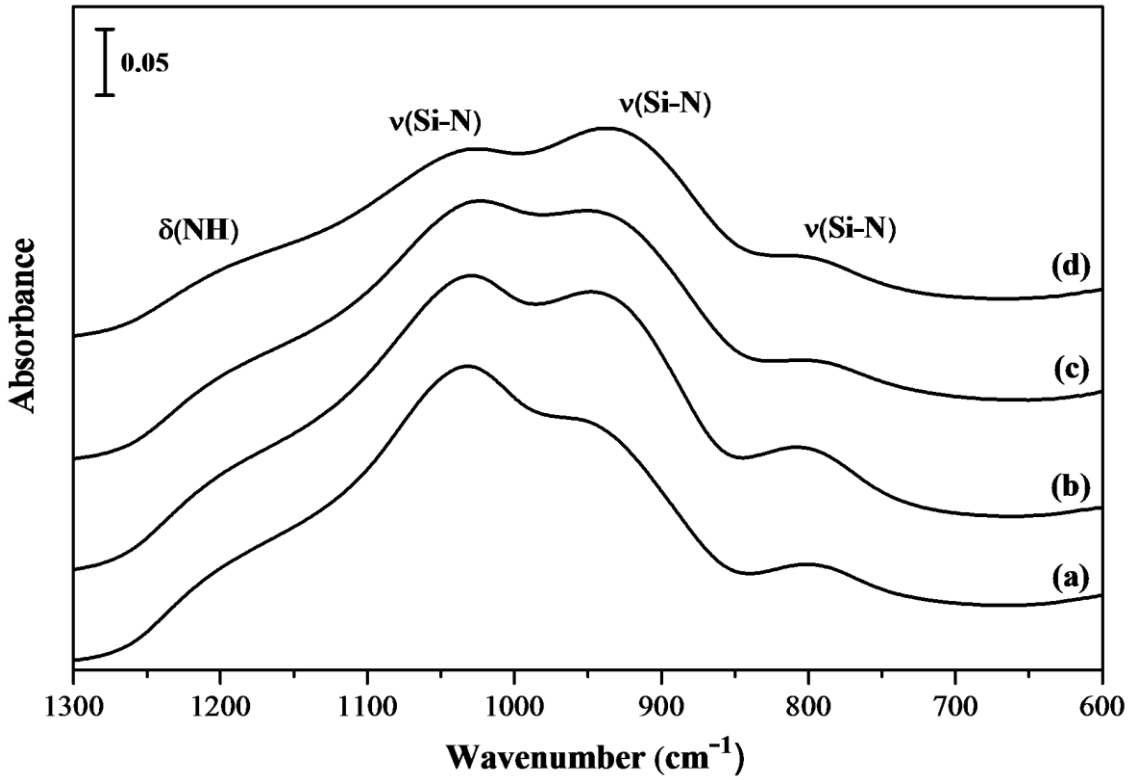
0.05
ν(Si-N)
ν(Si-N)
δ(NH)
ν(Si-N)
(d)
(c)
(b)
(a)
Absorbance
1300
1200
1100
1000
900
800
700
600
Wavenumber (cm-1)

Fig. 3.

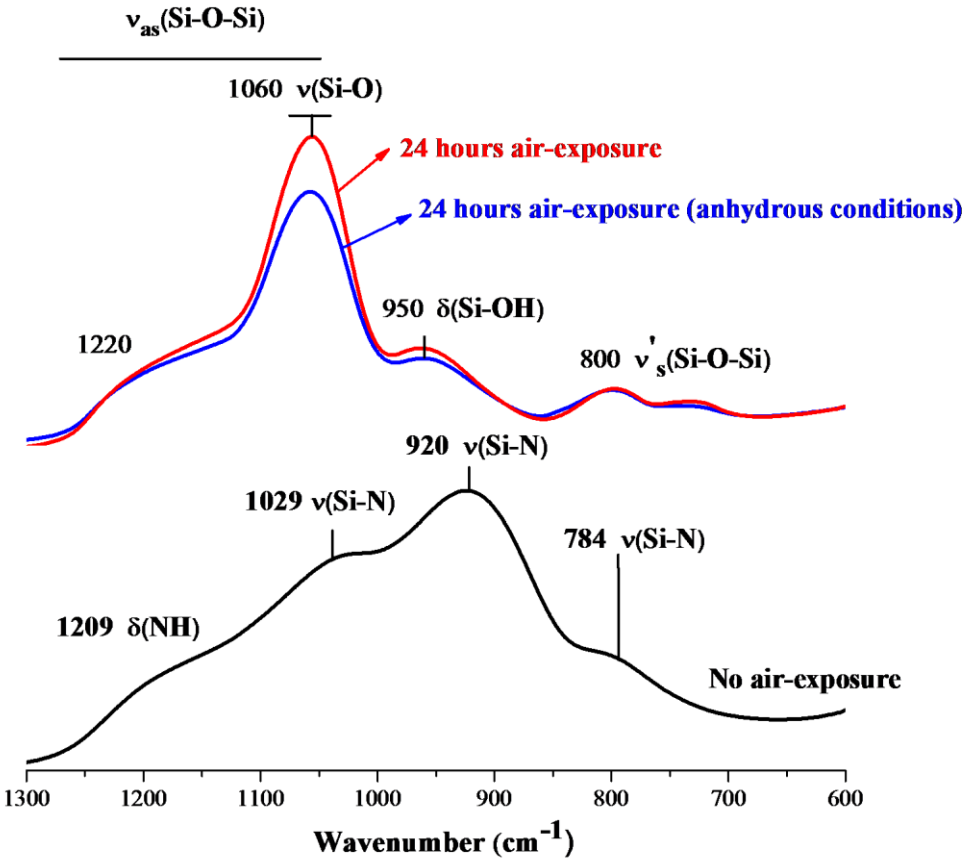
ν_{as}(Si-O-Si)
1060 ν(Si-O)
24 hours air-exposure
24 hours air-exposure (anhydrous conditions)
950 δ(Si-OH)
1220
800 ν'_s(Si-O-Si)
920 ν(Si-N)
1029 ν(Si-N)
784 ν(Si-N)
1209 δ(NH)
No air-exposure
1300
1200
1100
1000
900
800
700
600
Wavenumber (cm^{-1})

Fig. 4.

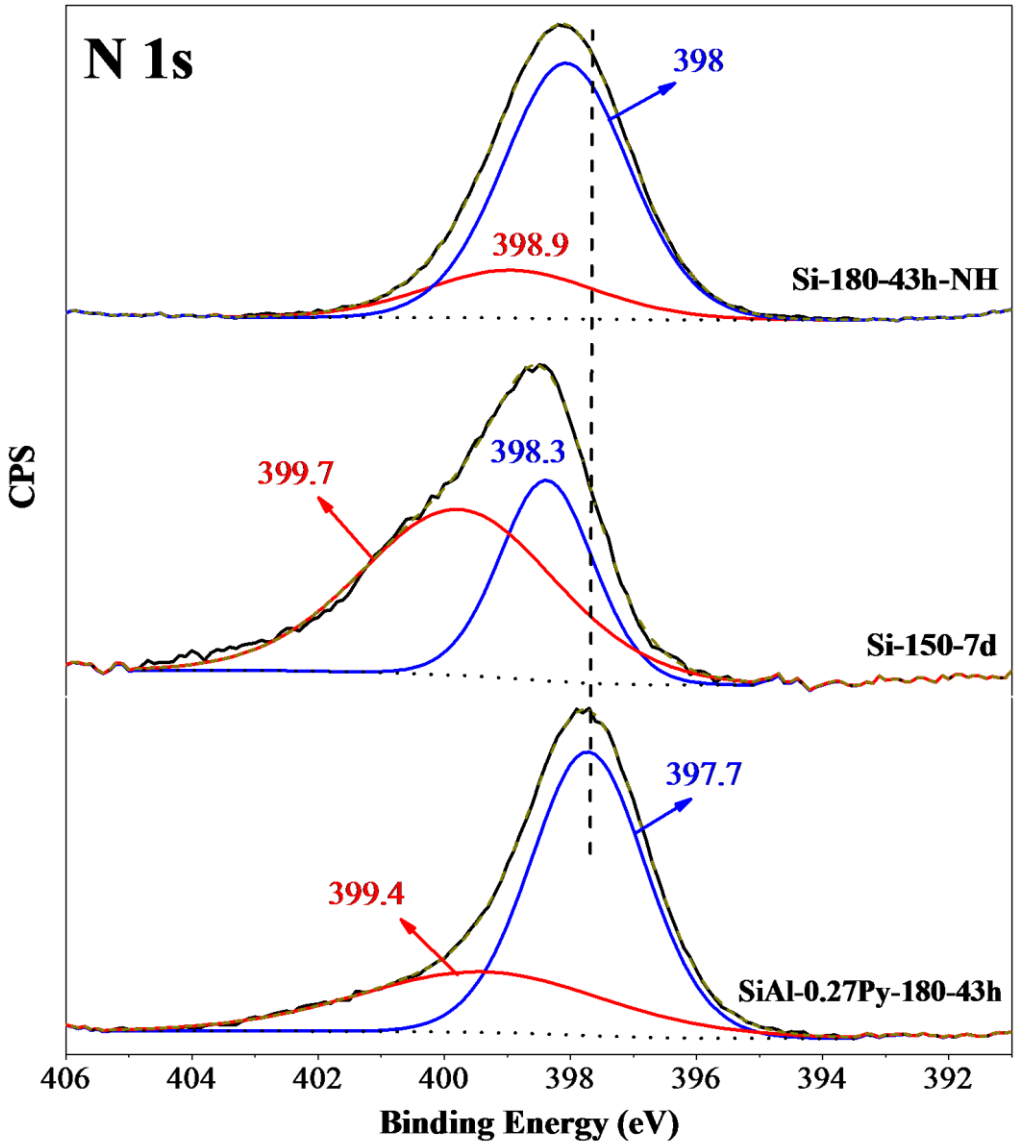
N 1s
398
398.9
Si-180-43h-NH
399.7
398.3
Si-150-7d
397.7
399.4
SiAl-0.27Py-180-43h
CPS
406
404
402
400
398
396
394
392
Binding Energy (eV)

Fig. 5.

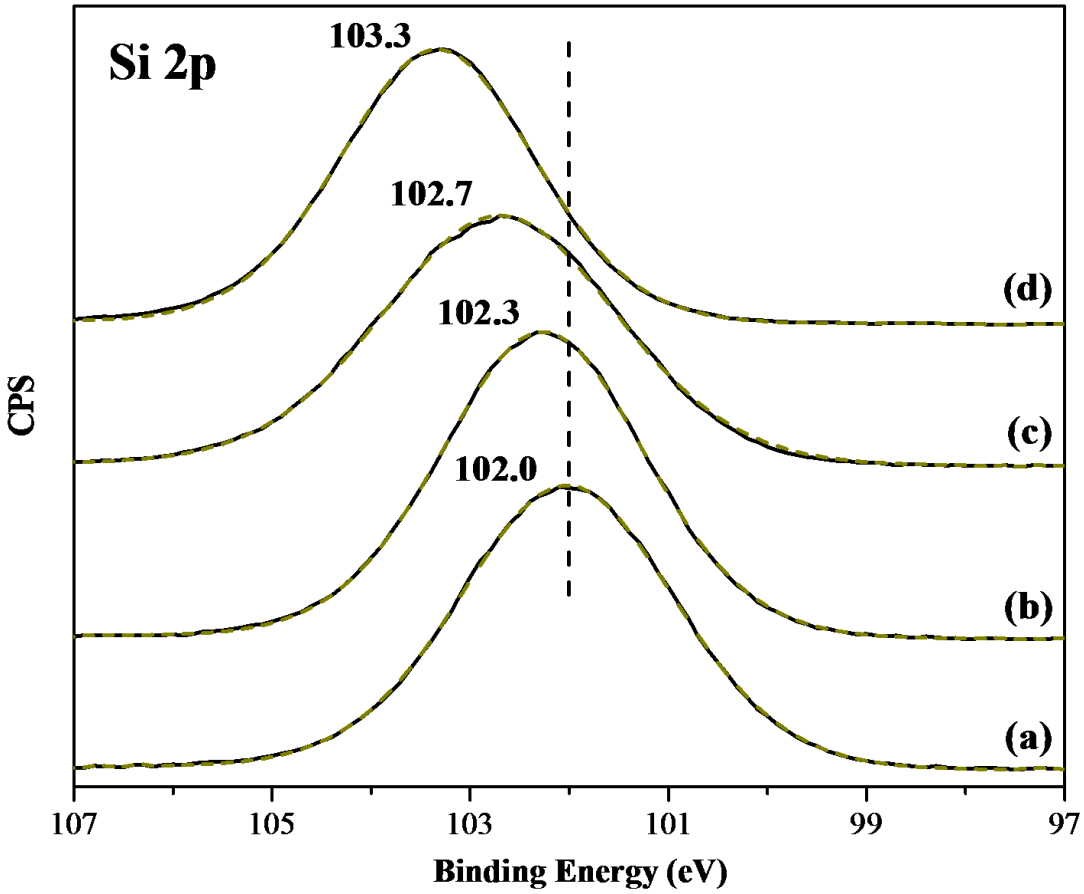
Si 2p
103.3
102.7
102.3
102.0
(d)
(c)
(b)
(a)
CPS
107
105
103
101
99
97
Binding Energy (eV)

Fig. 6.

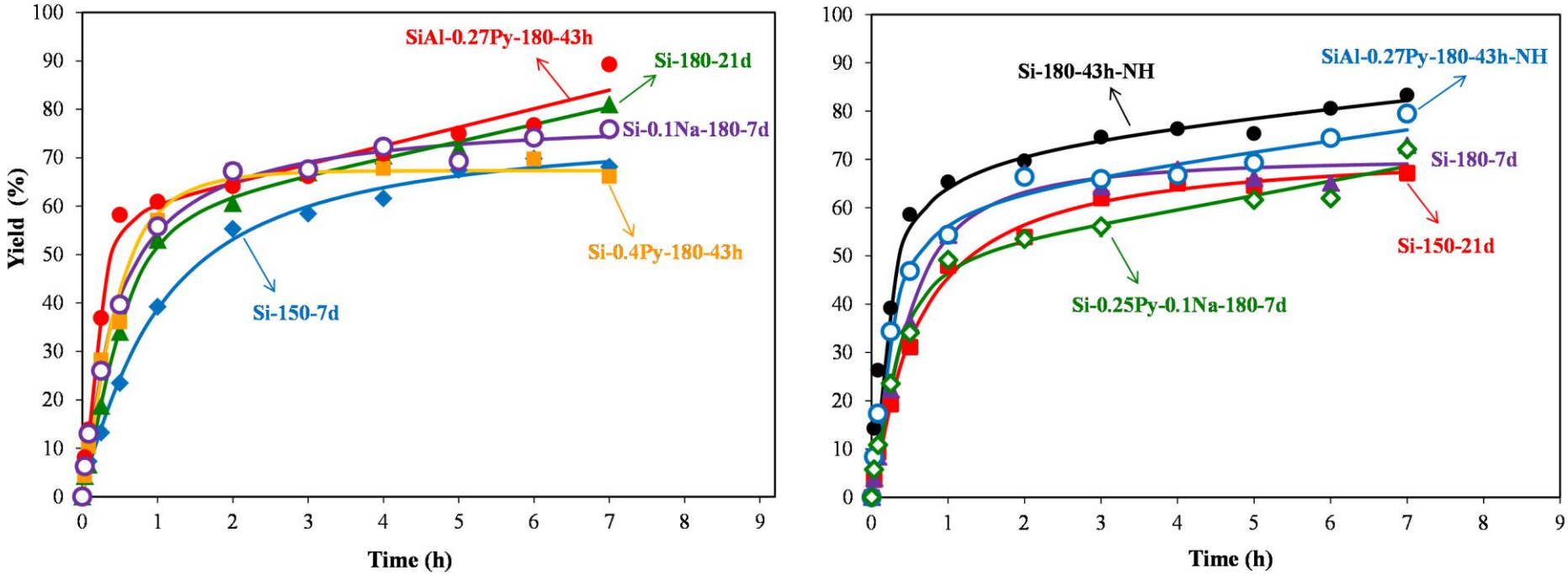
Yield (%)
Time (h)
SiAl-0.27Py-180-43h
Si-180-21d
Si-0.1Na-180-7d
Si-0.4Py-180-43h
Si-150-7d
Si-180-43h-NH
SiAl-0.27Py-180-43h-NH
Si-180-7d
Si-150-21d
Si-0.25Py-0.1Na-180-7d

Fig. 7.

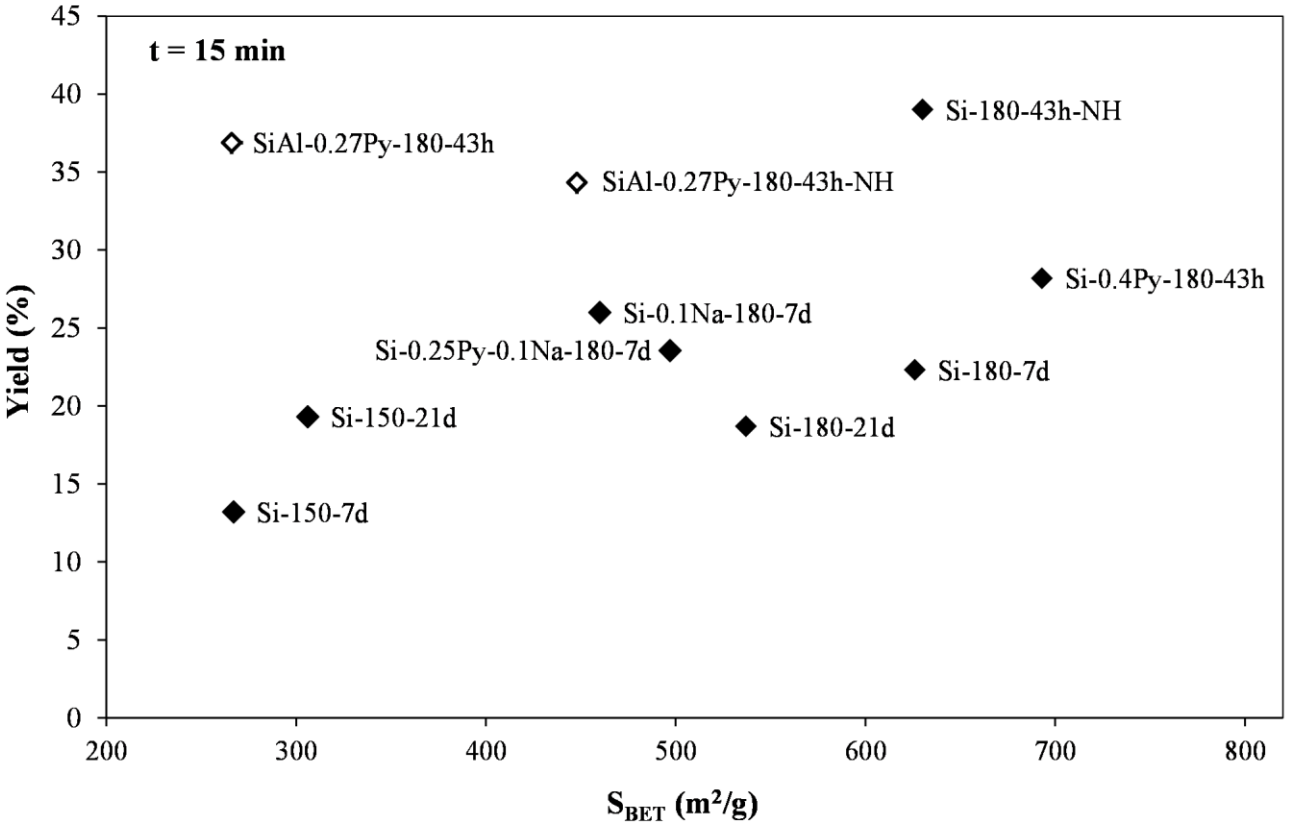
t = 15 min
Si-180-43h-NH
SiAl-0.27Py-180-43h
SiAl-0.27Py-180-43h-NH
Si-0.4Py-180-43h
Si-0.1Na-180-7d
Si-0.25Py-0.1Na-180-7d
Si-180-7d
Si-150-21d
Si-180-21d
Si-150-7d
Yield (%)
S_{BET} (m^2/g)
0
5
10
15
20
25
30
35
40
45
200
300
400
500
600
700
800

Fig. 8.

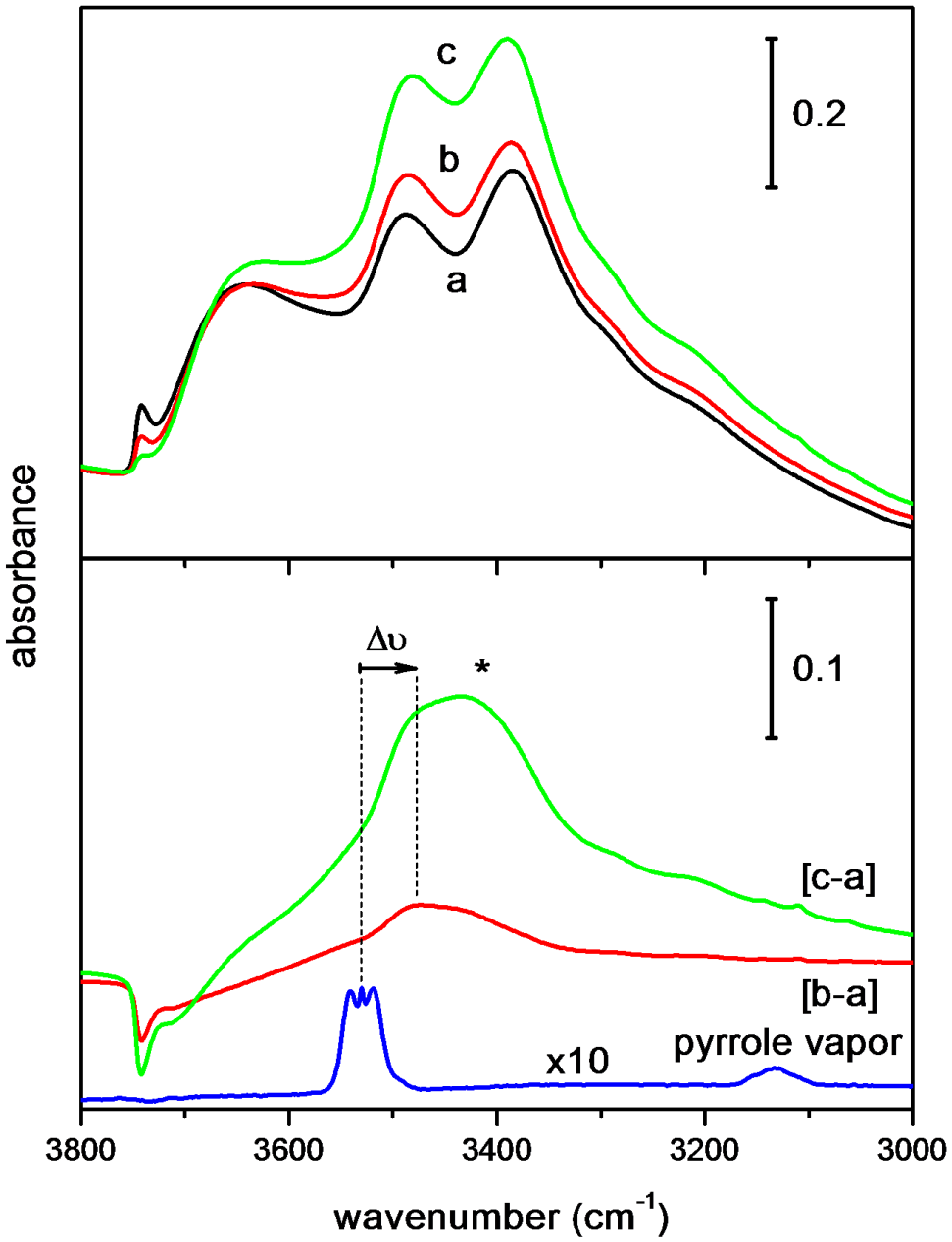
c
b
a
0.2
absorbance
Δυ
*
0.1
[c-a]
[b-a]
pyrrole vapor
x10
3800
3600
3400
3200
3000
wavenumber (cm-1)

Fig 9.

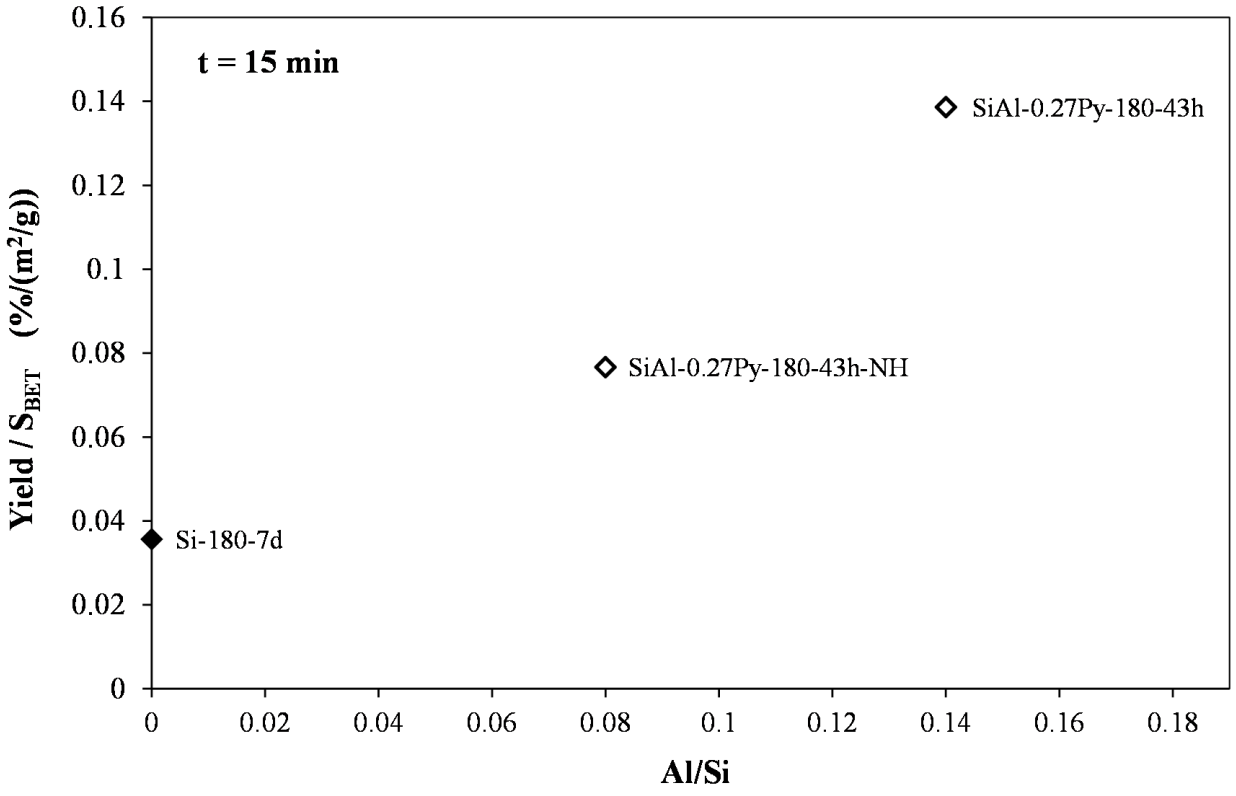
t = 15 min
SiAl-0.27Py-180-43h
SiAl-0.27Py-180-43h-NH
Si-180-7d
Yield / S_{BET} (%/(m²/g))
Al/Si
0.16
0.14
0.12
0.1
0.08
0.06
0.04
0.02
0
0
0.02
0.04
0.06
0.08
0.1
0.12
0.14
0.16
0.18

Fig. 10.

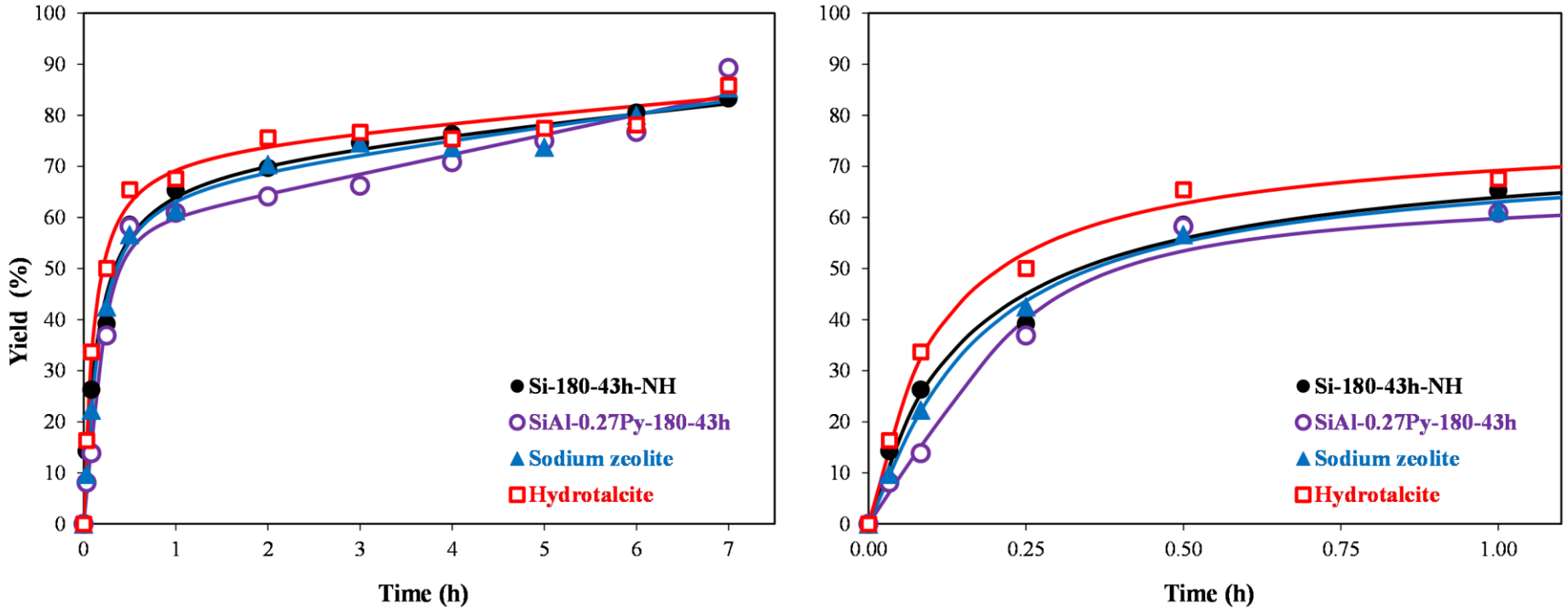
Yield (%)
Time (h)
Si-180-43h-NH
SiAl-0.27Py-180-43h
Sodium zeolite
Hydrotalcite
Time (h)
Si-180-43h-NH
SiAl-0.27Py-180-43h
Sodium zeolite
Hydrotalcite

Fig. 11.

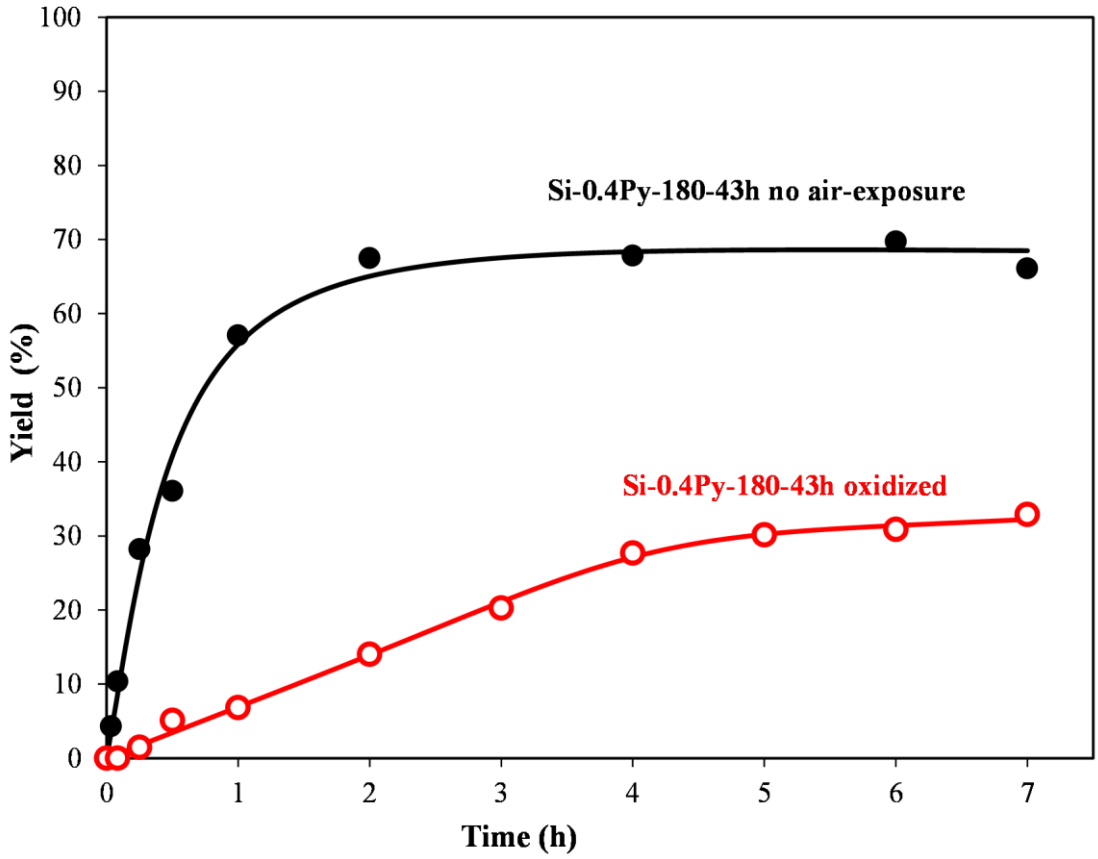
Yield (%)
Time (h)
Si-0.4Py-180-43h no air-exposure
Si-0.4Py-180-43h oxidized
0
10
20
30
40
50
60
70
80
90
100
0
1
2
3
4
5
6
7

Fig. 12.

Supporting Information

Basicity and catalytic activity of porous materials based on a (Si,Al)-N framework

A.I. Saugar [a], C. Márquez-Álvarez [a], I.J. Villar-Garcia [b], T. Welton [b], J. Pérez-Pariente [a]

[a] Instituto de Catálisis y Petroleoquímica, CSIC, C/Marie Curie 2, 28049-Cantoblanco, Spain. [b] Department of Chemistry, Imperial College London, Exhibition Road, South Kensington SW7 2AZ, United Kingdom.

Identification of 2-(3-Oxo-1,3-diphenylpropyl)malononitrile

The identification of the product obtained in the Michael addition reaction was carried out by ^{1}H NMR spectroscopy, using a Bruker Avance III-HD 300 MHz NanoBay equipment operating at 300 MHz.

Figure S1 shows the ^{1}H NMR spectrum of the isolated product of the reaction mixture dissolved in deuterated chloroform. The chemical shifts of the spectrum signals correspond to those reported in literature for the 2-(3-oxo-1,3-diphenylpropyl)malononitrile addition product [1, 2]. ^{1}H-NMR (300 MHz, $CDCl_3$) δ: 7.98-7.95 (m, 2H, ArH), 7.65-7.60 (m, 1H, ArH), 7.54-7.38 (m, 7H, ArH), 4.64 (d, J = 5.1 Hz, 1H, CN-CH), 3.96 (dt, J = 8.1, 5.4 Hz, 1H, Ar-CH), 3.76 – 3.60 (m, 2H, CH_2).

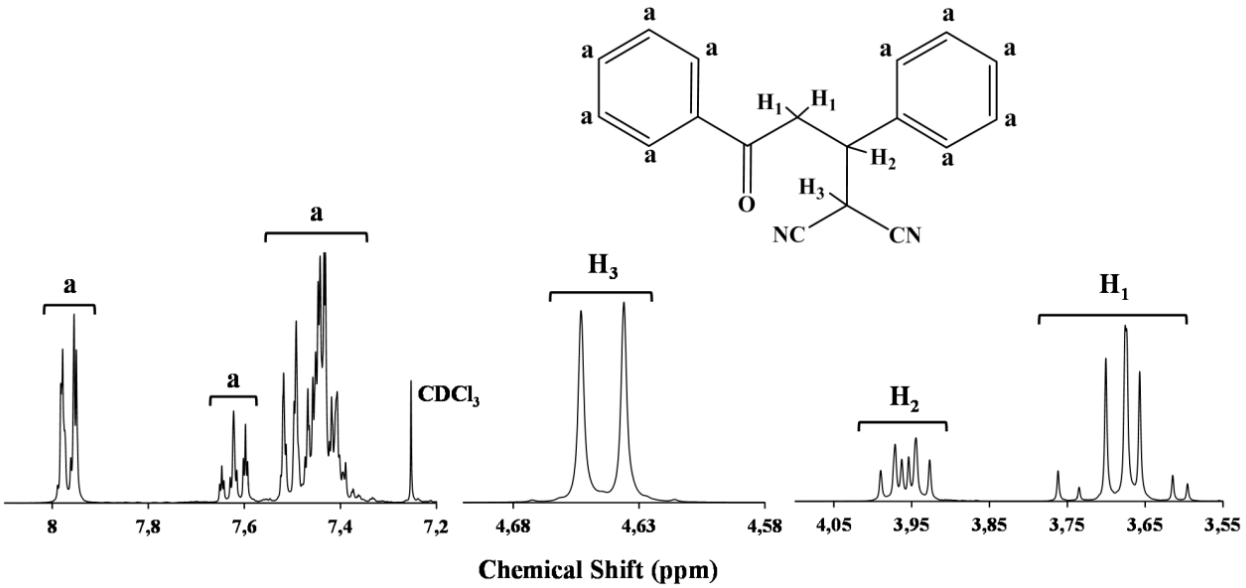

Figure S1. ^{1}H-NMR (300 MHz, $CDCl_3$) spectrum of the product 2-(3-oxo-1,3 diphenylpropyl)malono-nitrile obtained in the Michael addition reaction.

Synthesis of the ionic liquid compounds.

All the gels were prepared by using the ionic liquids 1-ethyl-3-methylimidazolium bis(trifluoromethylsulfonyl)imide ($[C_2C_1im][Tf_2N]$) (Figure S2 (a)) and 1-butyl-1-methylpyrrolidinium bis(trifluoromethylsulfonyl)imide, $[C_4C_1pyrr][Tf_2N]$ (Figure S2 (b)).

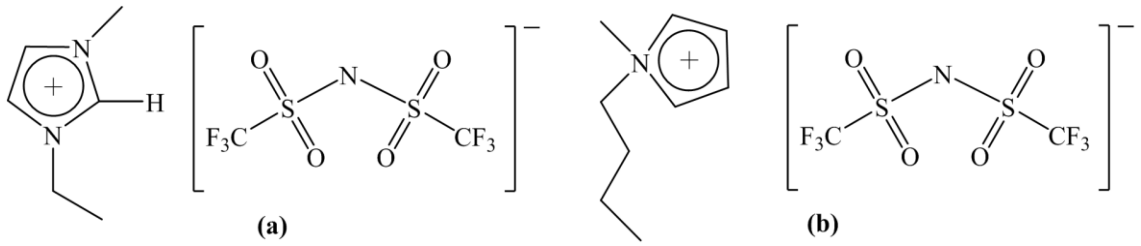

Figure S2. Molecular structure of the ionic liquid (a) 1-ethyl-3-methylimidazolium bis(trifluoromethylsulfonyl)imide ($[C_2C_1im][Tf_2N]$) and (b) 1-butyl-1-methylpyrrolidinium bis(trifluoromethylsulfonyl)imide ($[C_4C_1pyrr][Tf_2N]$).

The ionic liquids 1-ethyl-2,3-dimethylimidazolium bis(trifluoromethylsulfonyl)imide, [Edmim][Tf_2N] and 1-butyl-1-methylpyrrolidinium bis(trifluoromethylsulfonyl)imide, [C_4C_1pyrr][Tf_2N] were synthesized from the corresponding bromide salts. Bromoethane and bromobutane were previously distilled over phosphorous pentoxide and N-methylpyrrolidine was distilled over calcium hydride. All other reagents were purchased from commercial sources and used without further purification.

NMR spectra were recorded on a Bruker AVANCE III 600 MHz equipment operating at 400 MHz for ^{1}H NMR and 100 MHz for ^{13}C NMR at room temperature.

Synthesis of 1-ethyl-2,3-dimethylimidazolium bromide [Edmim][Br].

Into a round bottom flask equipped with a septum, a magnetic stirrer and a reflux condenser, 0.22 mol of 1,3-dimethylimidazole and 75 ml of dry ethyl acetate were placed under nitrogen atmosphere. An excess of 1-bromoethane (0.67 mol) was added drop wise by a dropping funnel with pressure compensation. The reaction mixture was vigorously stirred and heated at 35 °C for 20 h. The mixture was allowed to cool to room temperature and the resulting residue was filtered and dried under vacuum. The recrystallization of the residue was done by solving the compound in a small quantity of acetonitrile and by adding a small amount of ethyl acetate to the solution. This solution was cooled in a freezer, and white crystals of the ionic liquid were formed. After filtration, the remaining solvent was removed by evaporation on a rotavap under reduced pressure giving the 1-ethyl-2,3-dimethylimidazolium bromide as white crystals. ^{1}H-NMR (400 MHz, $CDCl_3$) δ: 7.42 (d, 1H), 7.37 (d, 1H), 3.98 (q, 2H), 3.65 (s, 3H), 2.47 (s, 3H), 1.17 (t, 3H). ^{13}C-NMR (100 MHz, $CDCl_3$) δ: 143.1, 122.7, 120.5, 43.8, 35.8, 15.1, 10.6.

Synthesis of 1-ethyl-2,3-dimethylimidazolium bis(trifluoromethylsulfonyl)imide [Edmim][Tf_2N].

Into a round bottom flask cooled in a water bath, 31.6 mmol of 1-ethyl-2,3-dimethylimidazolium bromide were dissolved in water (30 ml). A solution of $LiNTf_2$ (37.9 mmol) in water (100 ml) was added drop wise by a dropping funnel with pressure compensation to the vigorously stirred mixture. After the reaction mixture had been stirred for 48 h, the mixture was extracted with dicloromethane. The organic phase was washed with water (2 × 30 ml) and the solvent was removed by evaporation on a rotavap under reduced pressure. The resulting residue was dried under vacuum giving the 1-ethyl-2,3-dimethylimidazolium bis(trifluoromethylsulfonyl)imide. The corresponding ^{1}H-NMR spectrum is shown in Figure S3. ^{1}H-NMR (400 MHz, $(CD_3)_2SO$) δ: 7.66 (d, 1H), 7.62 (d, 1H), 4.15 (q, 2H), 3.75 (s, 3H), 2.59 (s, 3H), 1.35 (t, 3H). ^{13}C-NMR (100 MHz, $(CD_3)_2SO$) δ: 143.3, 121.5, 119.3, 119.1 (q, J = 320.7 Hz), 42.6, 33.6, 13.3, 7.79.

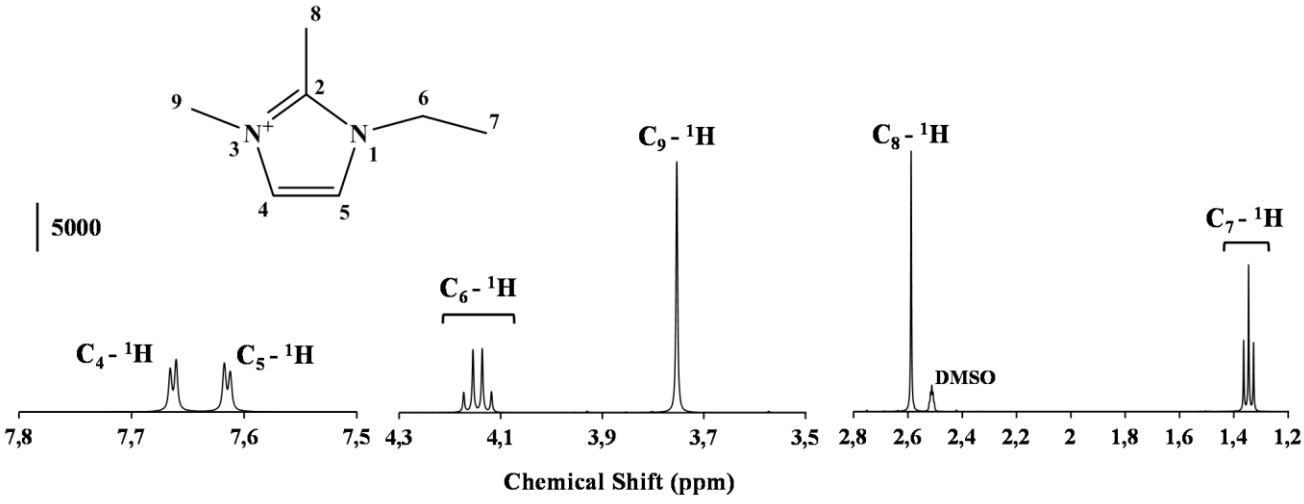

Figure S3. ^{1}H-NMR (400 MHz, $(CD_3)_2SO$) spectrum of the 1-ethyl-2,3-dimethylimidazolium cation $[Edmim]^+$.

Synthesis of 1-butyl-1-methylpyrrolidinium bromide [C_4C_1pyrr][Br].

Into a round bottom flask equipped with a septum, a magnetic stirrer and a reflux condenser, 0.22 mol of N-methylpyrrolidine and 75 ml of dry ethyl acetate were placed under nitrogen atmosphere. An excess of 1-bromobutane (0.67 mol) was added drop wise by a dropping funnel with pressure compensation. The reaction mixture was vigorously stirred and heated at 45 °C for 20 h. The mixture was allowed to cool to room temperature and the resulting residue was filtered and dried under vacuum. The residue was purified by recrystallization, using the same procedure as described for *[Edmim][Br]*, giving the 1-butyl-1-methylpyrrolidinium bromide. ^{1}H-NMR (400 MHz, $(CD_3)_2SO$ capillary) δ: 0.38 (t, 3H), 0.80 (sxt, 2H), 1.16-1.22 (m, 2H), 1.57-1.68 (m, 4H), 2.59 (s, 3H), 2.93-2.98 (m, 2H), 3.03-3.11 (m, 4H). ^{13}C-NMR (100 MHz, $(CD_3)_2SO$ capillary) δ:62.32, 62.58, 46.73, 23.90, 19.99, 17.98, 11.31.

Synthesis of 1-butyl-1-methylpyrrolidinium bis(trifluoromethylsulfonyl)imide [C_4C_1pyrr][Tf_2N].

Into a round bottom flask cooled in a water bath, 33 mmol of 1-butyl-1-methylpyrrolidinium bromide were dissolved in water. A solution of $LiNTf_2$ (39.5 mmol) in water (100 ml) was added drop wise by a dropping funnel with pressure compensation to the vigorously stirred mixture. After the reaction mixture had been stirred for 48 h, the mixture was extracted with dicloromethane. The organic phase was washed with water (2 × 30 ml) and the solvent was removed by evaporation on a rotavap under reduced pressure. The resulting residue was dried under vacuum giving the 1-butyl-1-methylpyrrolidinium bis(trifluoromethylsulfonyl)imide. The corresponding ^{1}H-NMR spectrum it is shown in Figure S5 a). ^{1}H-NMR (400 MHz,

$(CD_3)_2SO$) δ: 3.55-3.35 (m, 4H), 3.35-3.25 (m, 2H), 2.98 (s, 3H), 2.19-2.00 (m, 4H), 1.79-1.61 (m, 2H), 1.33 (sxt, 2H), 0.94 (t, 3H). ^{13}C-NMR (100 MHz, $(CD_3)_2SO$) δ: 119.9 (q, J = 321.8 Hz), 63.8, 63.4, 47.9, 25.37, 21.51, 19.73, 13.82.

Study of the chemical stability of the ionic liquids under basic conditions

The chemical stability of the ionic liquids [Edmim][Tf_2N] and [C_4C_1pyrr][Tf_2N] was studied by using the previously synthesized ionic liquids compounds. Sodium amide was purchased from Sigma-Aldrich as a toluene suspension which was previously filtered via cannula filtration giving a white powder.

Chemical stability of [Edmim][Tf_2N]

I Into a round bottom flask equipped with a septum, a magnetic stirrer and a thermometer, 1.44 mmol of [Edmim][Tf_2N] and an excess of sodium amide (2.88 mmol) were placed under nitrogen atmosphere. After the reaction mixture was stirred for 10 minutes at room temperature, a small aliquot was withdrawn using a syringe and dissolved in deuterated dimethylsulfoxide. The corresponding ^{1}H-NMR spectrum is shown in Figure S4 b).

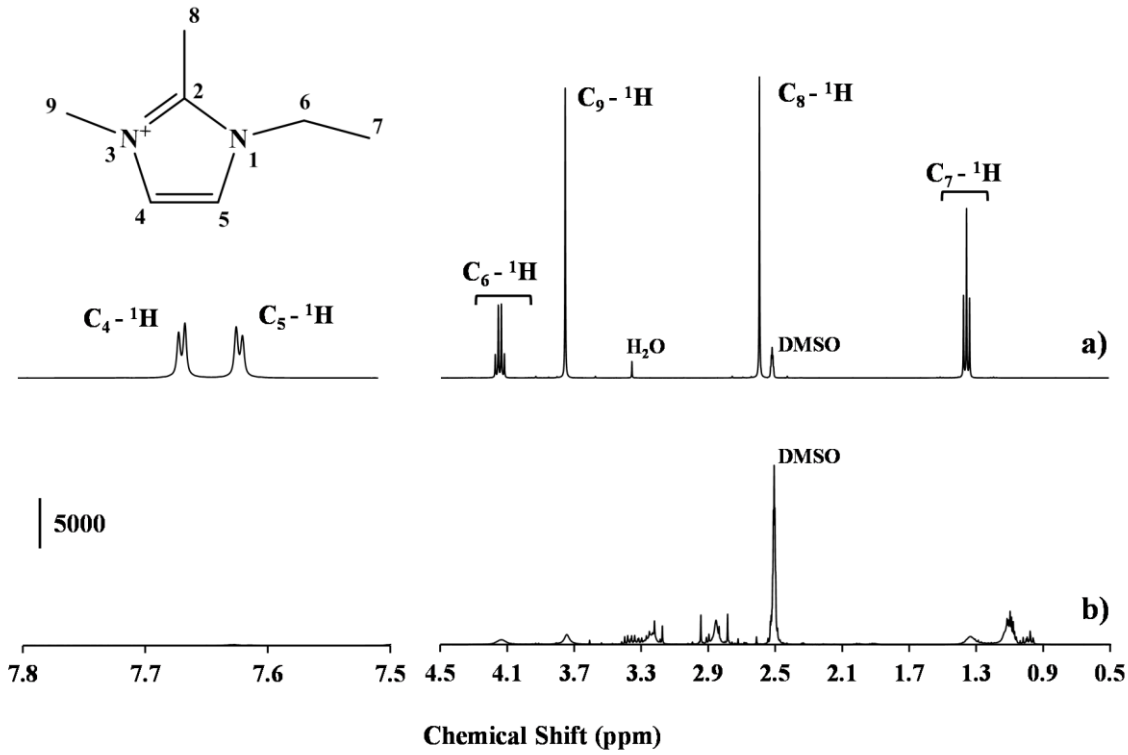

Figure S4. ^{1}H-NMR (400 MHz, $(CD_3)_2SO$) spectrum of a) the 1-ethyl-2,3-dimethylimidazolium cation $[Edmim]^+$ and b) the mixture obtained after stirring the ionic liquid $[Edmim][Tf_2N]$ at room temperature during 10 minutes in the presence of an excess of sodium amide ($NaNH_2$/$[Edmim][Tf_2N]$ molar ratio of 2).

Chemical stability of $[C_4C_1pyrr][Tf_2N]$.

Using the same experimental set up as described for the chemical stability study of $[Edmim][Tf_2N]$, 1.44 mmol of $[C_4C_1pyrr][Tf_2N]$ and an excess of sodium amide (2.88 mmol) were heated at 180 ºC under vigorous stirring for 1 hour. A small aliquot of the reaction mixture was withdrawn using a syringe and dissolved in deuterated dimethylsulfoxide. The corresponding ^{1}H-NMR spectrum it is shown in Figure S5 b).

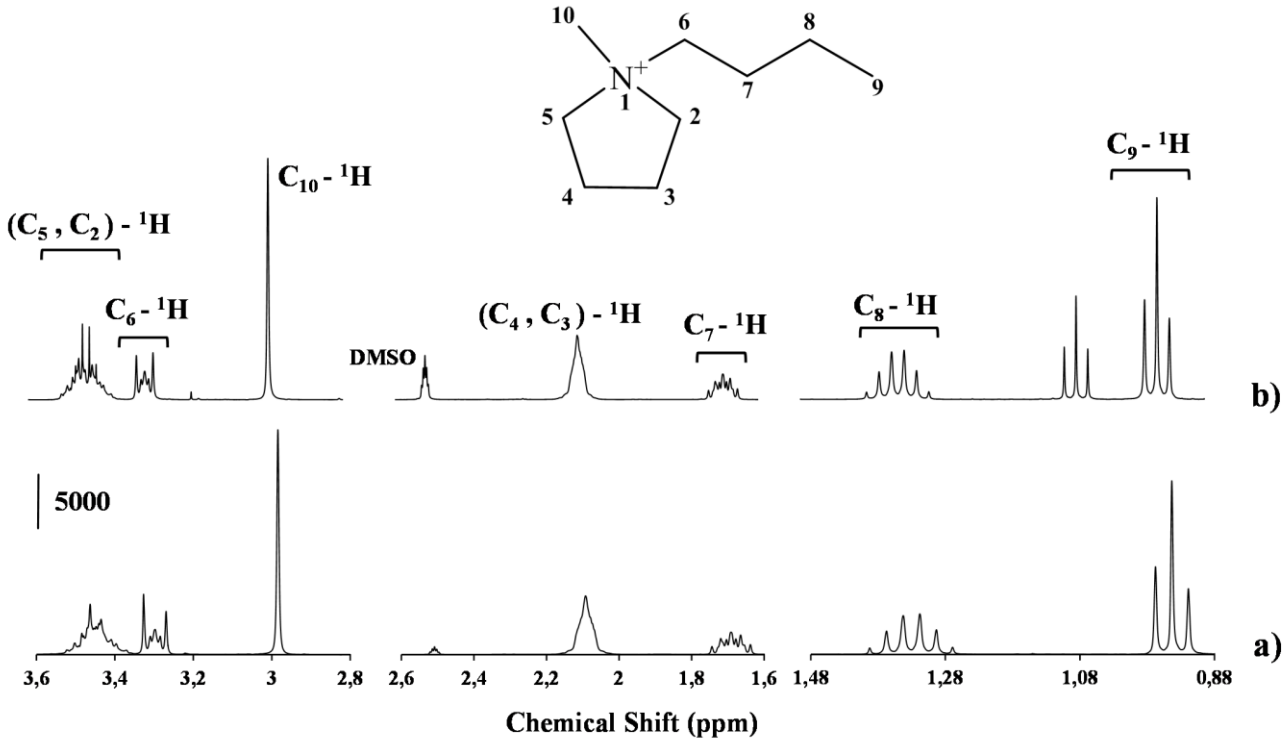

Figure S5. ^{1}H-NMR (400 MHz, $(CD_3)_2SO$) spectrum of a) the 1-butyl-1-methylpyrrolidinium cation $[C_4C_1pyrr]^+$ and b) the mixture obtaining after heating the ionic liquid $[C_4C_1pyrr][Tf_2N]$ at 180 ºC under vigorous stirring for 1 hour in the presence of an excess of sodium amide ($NaNH_2$/$[C_4C_1pyrr][Tf_2N]$) molar ratio of 2).

Thermogravimetric analyses of the as-prepared samples

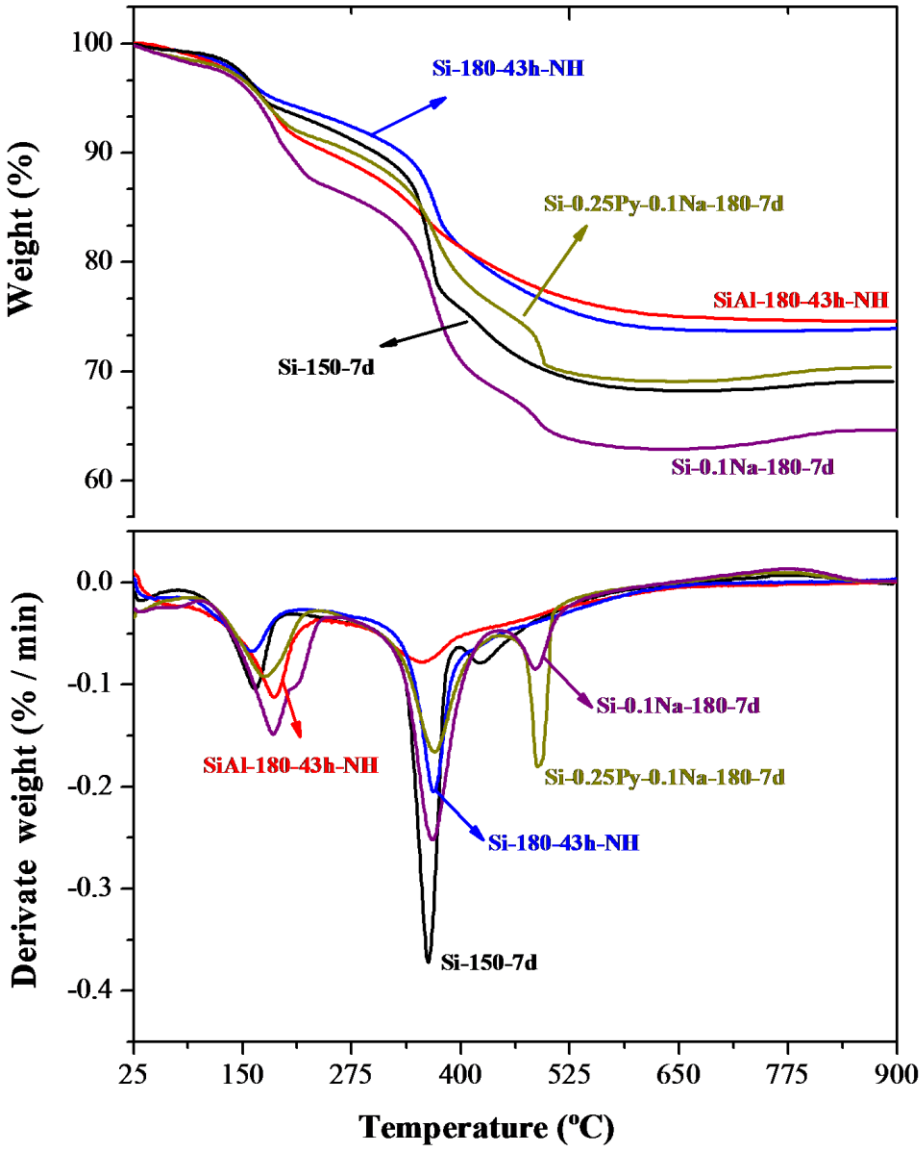

Figure S6. Thermogravimetry plots (top) and derivative of the TG curves (bottom) of some selected as-prepared samples.

Nitrogen adsorption-desorption measurements.

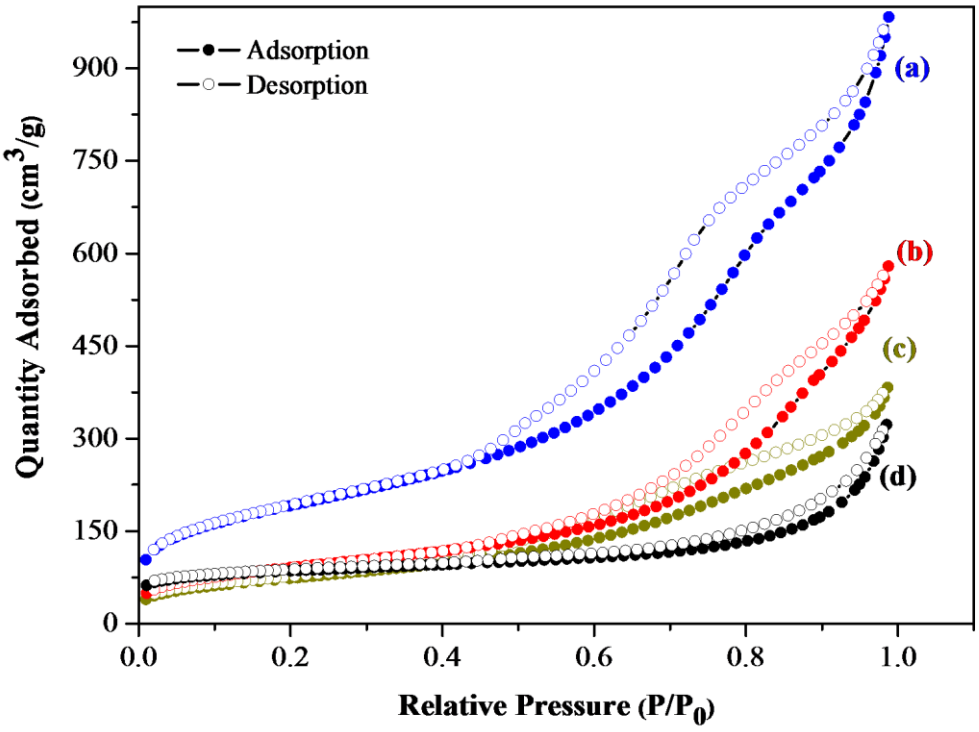

Figure S7. Nitrogen adsorption/desorption isotherms at 77 K of the high surface area materials obtained after the heat treatment under flowing ammonia; (a) Si-0.4Py-180-43h, (b) SiAl-180-43h-NH, (c) SiAl-0.27Py-180-43h and (d) Si-150-21d.

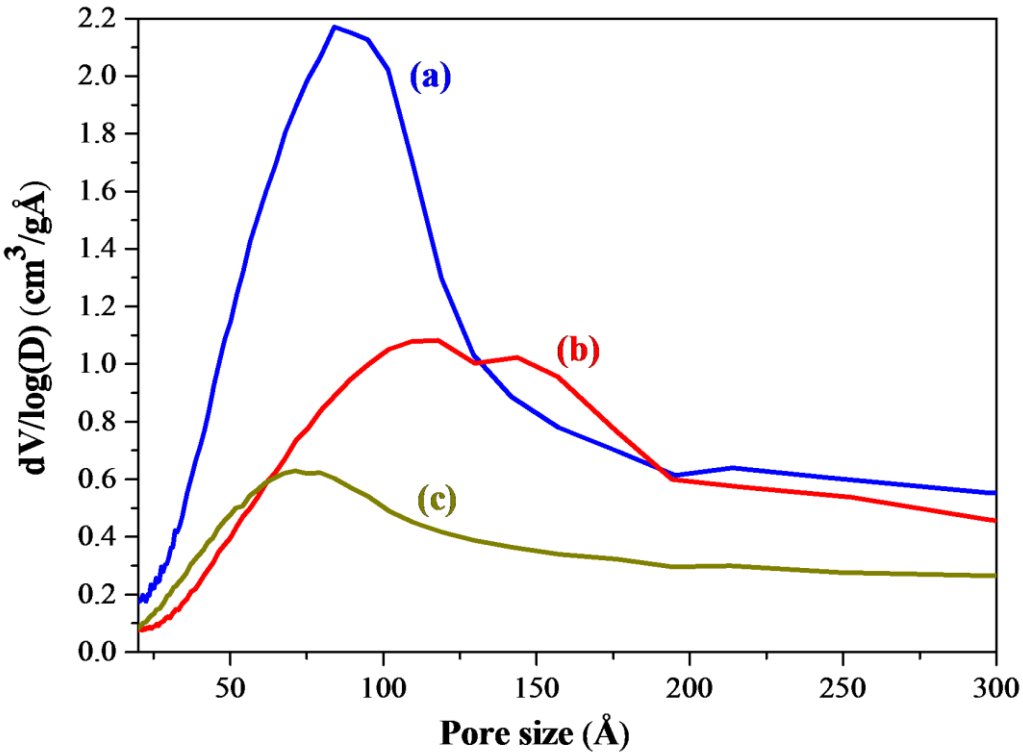

Figure S8. Pore size distribution of the ammonia heat-treated samples; (a) Si-0.4Py-180-43h, (b) SiAl-180-43h-NH and (c) SiAl-0.27Py-180-43h.

Al 2p XPS spectra

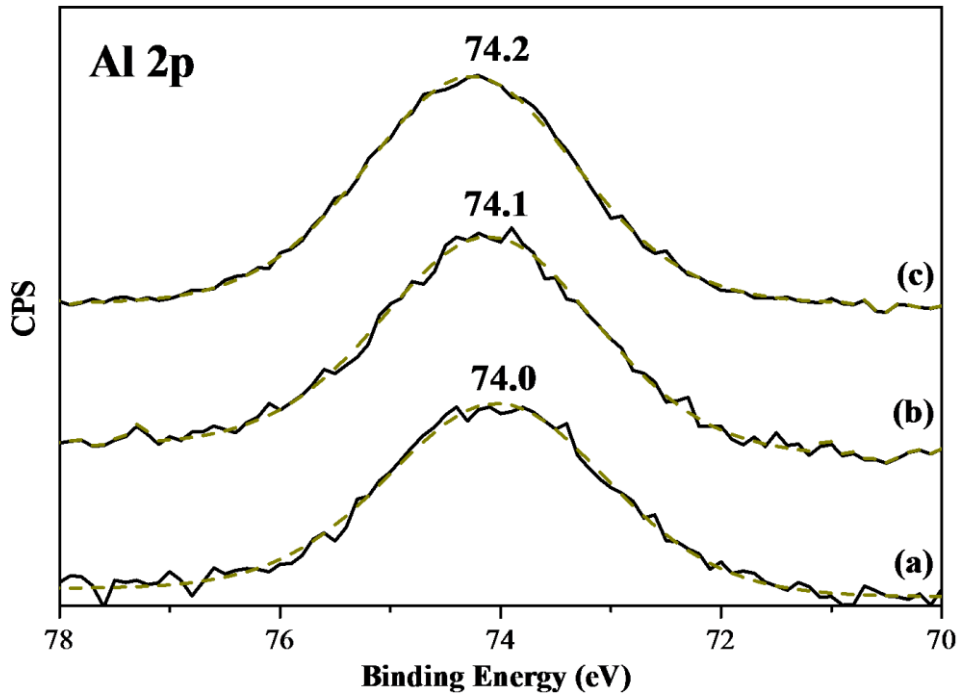

Figure S9. Al 2p XPS spectra of the ammonia heat-treated samples; (a) SiAl-180-43h-NH, (b) SiAl-0.27Py-180-43h-NH and (c) SiAl-0.27Py-180-43h

Catatytic activity

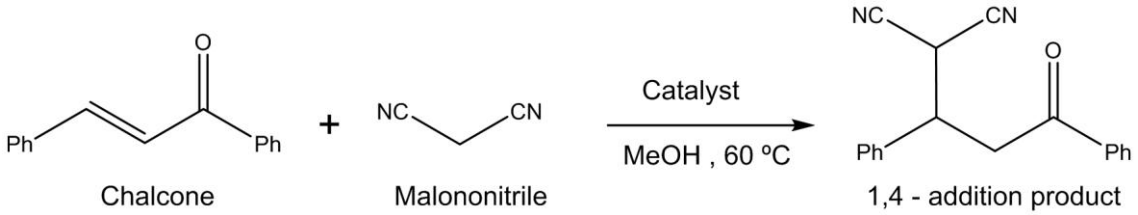

Scheme 1. Michael addition reaction between chalcone and malononitrile.

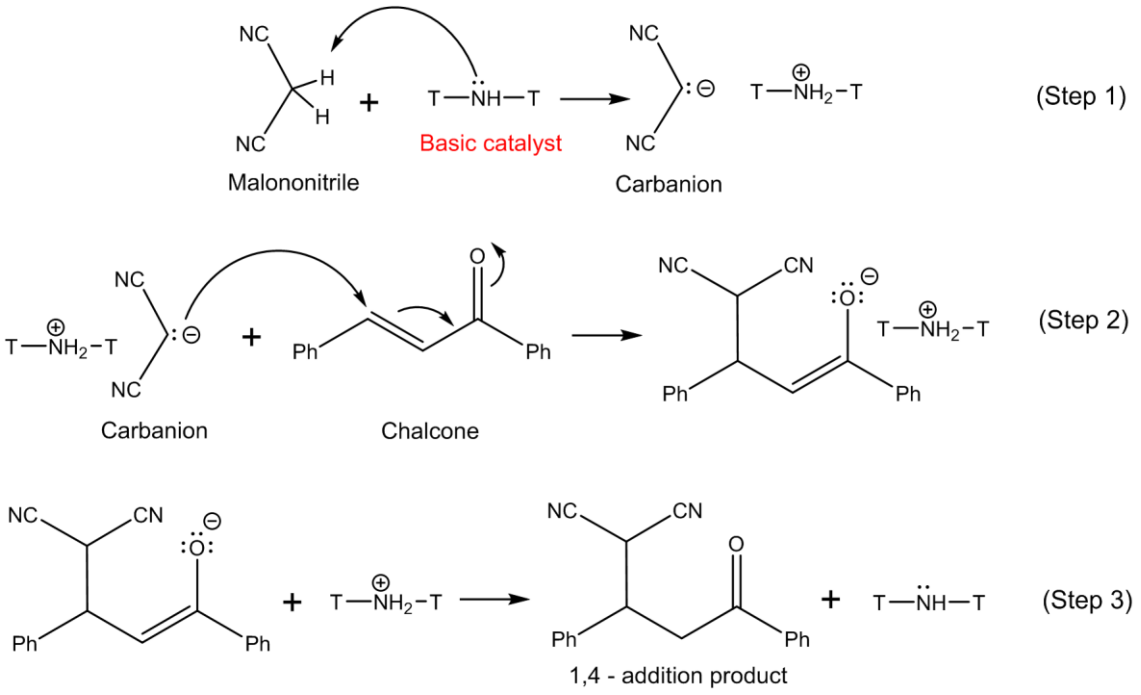

Scheme 2. Michael addition reaction mechanistic.

Table 1. Influence of solvent on the catalytic activity of sample SiAl-180-43h-NH for the Michael addition reaction between chalcone and malononitrile.

Solvent	*Dielectric constant (ε)*	*T[a] / ºC*	*Catalyst/Chalcone (weight ratio)*	*Yield[b] (%)*
Methanol	32.7	60	0.08	98
CH_2Cl_2	8.93	35	0.16	0
THF	7.58	60	0.16	0
$CHCl_3$	5.62	60	0.16	0

[a] Reaction temperature.

[b] Reaction conditions: Chalcone/malononitrile molar ratio: 1, chalcone/solvent weight ratio: 0.05, reaction time: 7 h.

Determination of the basicity by FTIR of adsorbed pyrrole.

The relative strength of basic sites has been determined by measuring the shift of the NH stretching mode of adsorbed pyrrole respect to the molecule in the vapor phase [3].

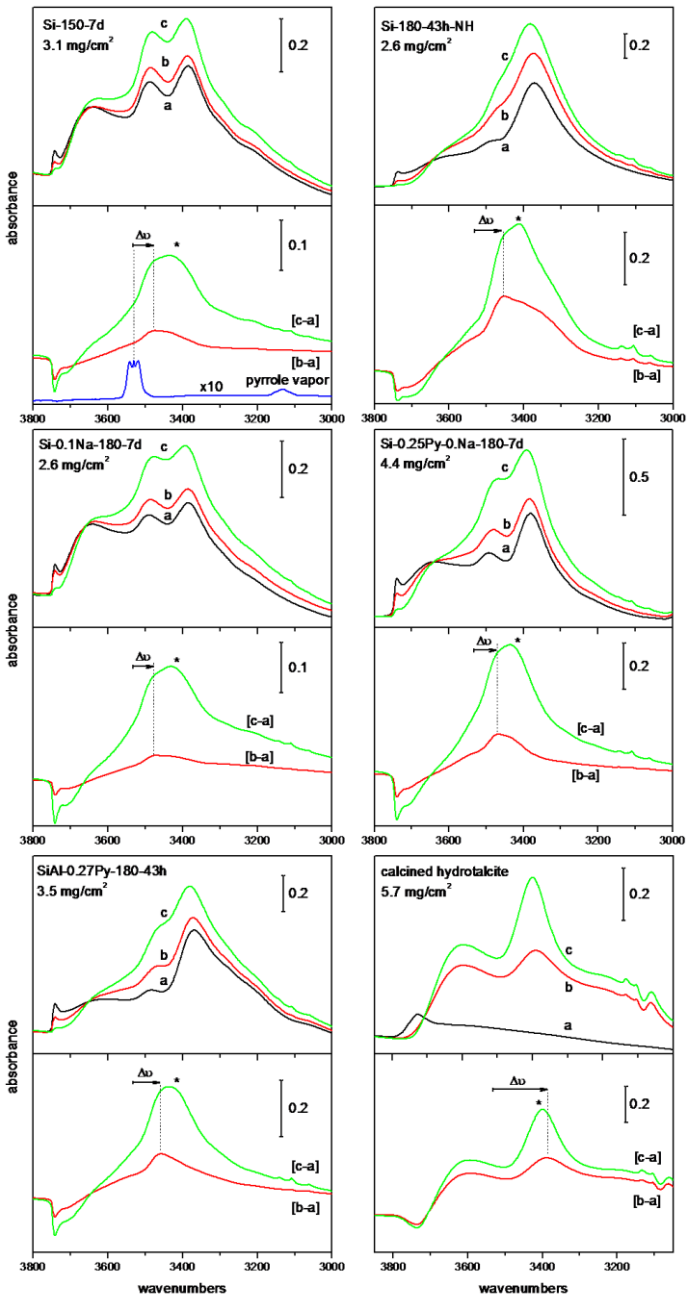

Figure S10. FTIR spectra of Si(Al)-N samples and a calcined Al-Mg hydrotalcite after degassing at 150°C (a) and in contact with pyrrole vapor at 25ºC and equilibrium

pressure of ca. 1 mbar (b) and ca. 10 mbar (c). Difference spectra c-a and b-a are shown to facilitate determination of the shift of the NH stretching band of pyrrole. The spectrum of pyrrole vapor (6 mbar) is also shown for reference (NH stretching band centered at 3530 cm^{-1}). Arrows indicate the shifts of the ν(NH) band of pyrrole due to H-bonding with basic sites. At high equilibrium pressure, the 3410 cm^{-1} band (marked with an asterisk) corresponding to physisorbed pyrrole [3] becomes dominant.

References

[1] W. Yang, Y. Jia, D.-M. Du, Organic & Biomolecular Chemistry. 10 (2012) 332-338.

[2] X. Li, L. Cun, C. Lian, L. Zhong, Y. Chen, J. Liao, J. Zhu, J. Deng, Organic & Biomolecular Chemistry. 6 (2008) 349-353.

[3] B. Camarota, Y. Goto, S. Inagaki, B. Onida, Langmuir. 27 (2011) 1181-1185.

BASICITY AND CATALYTIC ACTIVITY OF POROUS MATERIALS BASED ON A (Si,Al)-N FRAMEWORK

A.I. Saugar[a], C. Márquez-Álvarez[a], I.J. Villar-Garcia[b], T. Welton[c], J. Pérez-Pariente[a,*]

[a] Instituto de Catálisis y Petroleoquímica, CSIC, C/Marie Curie 2, 28049-Cantoblanco, Spain. [b] Department of Materials, Imperial College London. [c] Department of Chemistry, Imperial College London, Exhibition Road, South Kensington SW7 2AZ, United Kingdom.

* Corresponding author: jperez@icp.csic.es

Abstract

Porous materials based on a framework containing T-N linkages, where T represents silicon or silicon and aluminium atoms, have been prepared by the ammonolysis at low temperature of the corresponding silicon and aluminium chlorides in an ionic liquid, both in the presence and in the absence of mineralizing agents such as pyrrolidine, ammonia and sodium amide. IR spectroscopy and XPS data are consistent with these materials having a framework based on T-NH-T groups (T = Si or Al), that contain also a large fraction of T-NH_2 terminal groups. Moreover, XPS evidences the presence of Si-NH-Al groups whenever aluminium is present in the solid. The basic strength of the materials has been determined by pyrrole adsorption, and it has been found that the average basic strength increases with the population of T-NH-T groups and with the aluminium content of the framework. However, this strength is lower than that of a calcined hydrotalcite (Al/(Al+Mg) = 0.33) taken as a reference. These materials are

active and very selective catalysts in the Michael addition reaction between chalcone [and malononitrile (pK_a 11), but turned to be inactive when diethylmalonate having a weaker acidity (pK_a 13.3) is used as donor.

Keywords: Silicon-aluminium imide; Porous materials; Heterogeneous base catalyst; Michael addition; Pyrrole adsorption.

1. Introduction

There is a wide interest towards microporous and mesoporous materials based on corner-sharing TO_4 (T = Si, Al) tetrahedral units, focused on their application in acid-catalyzed reactions. The catalytic properties of these materials are much dependent on the nature of the active centers and on their textural properties. In contrast to the extensive development of those solid acid catalysts, efforts to develop basic microporous and mesoporous materials are significantly lower, even though base-catalyzed reactions play an important role in a number of industrially relevant processes such as the production of fine chemicals.

Due to the lower electronegativity of nitrogen with respect to oxygen, materials based on a nitrogen-containing network would have higher basicity than their oxide counterparts. Silicon diimide, $Si(NH)_2$, which is an amorphous and reactive solid, is isoelectronic and isostructural with SiO_2. Thereby, as silicon dioxide allows the formation or porous solids based on corner-sharing SiO_4 tetrahedral units, silicon diimide would allow the formation of a network built by SiN_4 units.

In heterogeneous catalysis, materials should have a high surface area and pore volume in order to facilitate access of the reactant molecules to the active sites, which in a

silicon-nitrogen based compound would be =NH or even terminal Si-NH_2 groups. In this regard, a limited number of strategies have been developed with the goal of obtaining porous and high-surface area Si-N materials. Pyrolysis of polysilazanes and poly(organosilazanes) results in the formation of microporous silicon imidonitrides, being some of them active in the base-catalyzed Knoevenagel reaction [1-3].

Bradley and co-workers have reported the preparation of a silicon diimide gel containing a significant amount of dimethylamino groups by acid-catalyzed ammonolysis of tris(dimethylamino)silylamine ($[Si(NH_2)(NMe_2)_3]$ (TDSA)) [4]. Pyrolysis of the gel under flowing ammonia at 1000 ºC leads to mesoporous silicon imidonitride with high surface area (466 m^2/g) but with a low amount of Si-NH-Si catalytic active sites [5]. Recently gels prepared from TDSA were used to produce high surface area aerogels by supercritical drying of the gels with ammonia [6].

In the conventional procedures used to prepare silicon nitride ceramics, silicon halides, silicon tetrachloride usually, are reacted with ammonia in an organic solvent to produce the ammonium salt and amorphous silicon diimide, $Si(NH)_2$, which decomposes at higher temperatures to form Si_3N_4 [7] as well as nitridosilicates [8]. Kaskel and co-workers have synthesized high-surface-area mesoporous silicon imidonitride solids by heating the mixture of silicon diimide and ammonium halide in an ammonia flow [9-11].

Until now, the basicity and catalytic activity of the materials obtained from silicon diimide or organosilicon compounds has been hardly investigated as the amount of NH sites in these materials is significantly low, so they do not exhibit a high catalytic activity. With the aim of preparing materials of strong basicity, silicon imidonitride solid obtained from silicon diimide has been used as a support for alkali metals. Potassium-loaded high surface area silicon imidonitride materials were found to be

efficient base catalysts suitable for the side-chain alkylation of toluene [12] and for alkene isomerization reactions [11].

Aiming to increase the intrinsic basicity of these nitrides, aluminium has been incorporated into the Si-N framework. As aluminium atoms are less electronegative than silicon, the Al-N bonds are more polar than Si-N, so the basicity of the nitrogen atoms would be increased.

To generate porous silicon aluminium imide materials, a precursor containing aluminium and silicon ($(C_4H_8O)Al[NHSi(NMe_2)_3]_3$), was prepared was prepared by reacting tris(dimethylamino)silylamidolithium $(Me_2N)_3$-SiNHLi with aluminium trichloride in tetrahydrofuran [13]. The acid-catalyzed ammonolysis reaction of this precursor results in the formation of a silicon aluminium imide gel with a significant amount of dimethylamino groups. Pyrolysis of the gel at 1000 ºC under flowing ammonia leads to an amorphous mesoporous silicon aluminium nitride with a Si:Al molar ratio of 2.9:1 but with a low surface area (190 m^2/g) [14]. Although the heat treatment removes completely the residual dimethylamino groups, it also leads to condensation reactions between the Si-NH and Al-NH functional groups, reducing the amount of catalytic active sites in the material.

Kaskel et al. have synthesized the oxygen-free precursor $[EtAl(\mu\text{-}NHEt)(\mu\text{-}NEt)_2\text{-}Si(NHEt)]_2$, the crystal structure of which contains aluminium and silicon in tetrahedral coordination and bridging and terminal ethylamino groups [15]. When this compound is treated with supercritical ammonia at 150 ºC in a high-pressure autoclave, a xerogel imidonitride with a Al:Si ratio close to 1 and a surface area of 760 m^2/g is obtained [16]. This aluminium-containing silicon imidonitride shows a high catalytic activity in the Michael addition reaction between malononitrile and acrylonitrile, reaching a yield of 96 %. Nevertheless, an extensive study about the correlation between the basic

properties of these silicon aluminium imidonitrides and their catalytic activity has never been reported.

Most of the procedures previously reported to obtain imidonitrides from a silicon diimide or a silicon aluminium imide gel make use of an organic solvent whose main role in the preparation process is to absorb the heat produced by the highly exothermic ammonolysis reaction. In order to design a new synthesis pathway where the solvent would play an active role in the formation of the silicon diimide gel, a novel solvothermal pathway has been recently developed in our group to prepare porous silicon-nitrogen network-based materials from a silicon diimide-type gel obtained by the ammonolysis of silicon tetrachloride using an ionic liquid as solvent [17].

Several studies have demonstrated that some ionic liquids, which are organic salts with high chemical and thermal stability [18], can dissolve high amounts of gaseous ammonia reaching much higher solubilities than the organic solvents currently employed in the ammonolysis reaction [19, 20]. We have demonstrated in our previous report that when the silicon diimide precursor gel is subjected to a thermal treatment in the presence of ammonia dissolved in the ionic liquid, this basic compound can catalyze the condensation process of Si-N moieties improving the textural properties of the resulting silicon-nitrogen network-based materials.

Hydroxyl anions are commonly used to solubilize silicate species in the hydrothermal preparation of silica gels at high pH. In this regard, amide anion (NH_2^-), which is isoelectronic to OH^- anion, could act as a mineralizing agent in the preparation of Si-N based materials. The present paper, reports on the use of $NaNH_2$ as a mineralizing agent in the preparation of silicon-nitrogen based materials by our already reported synthesis technique and its effect in the chemical composition and the textural properties of the resulting materials. We also extend our preparation method to synthesize new porous

silicon-nitrogen based materials containing aluminium in their network, from a silicon aluminium imide gel obtained by the joint ammonolysis reaction of silicon tetrachloride and aluminium chloride using an ionic liquid as solvent.

In order to explore the catalytic properties of the prepared materials, the present work also provides a thorough study about the catalytic activity of the materials in the base-catalyzed Michael addition reaction between chalcone and malononitrile, and the influence of the chemical composition and the textural properties on the catalysts behavior. Moreover, infrared spectroscopy of adsorbed pyrrole has been used to characterize the basic active sites of the catalyst being able to make a correlation between the basic properties and the catalytic activity.

2. Experimental

All the gels were prepared under anaerobic conditions through the use of an air-free system. Silicon diimide gels were prepared according to our previously reported procedure [17] by the reaction of silicon tetrachloride (Sigma-Aldrich, 99 wt%) and gaseous anhydrous ammonia (Air Liquide, H_2O < 400 ppm) using the ionic liquid 1-ethyl-3-methylimidazolium bis(trifluoromethylsulfonyl)imide ($[C_2C_1im][Tf_2N]$) (Sigma-Aldrich, 98 wt%) or the 1-butyl-1-methylpyrrolidinium bis(trifluoromethylsulfonyl)imide ($[C_4C_1pyrr][Tf_2N]$) (Sigma-Aldrich, 98 wt%) as solvent.

The ionic liquid $[C_4C_1pyrr][Tf_2N]$ was only applied when sodium amide was added to the gel to be applied as a mineralizing agent. The silicon-aluminium imide gels were prepared by a modification of our previously reported method [17]. First, 8.65 g of silicon tetrachloride (Sigma-Aldrich, 99 wt%) and 0.68 g of anhydrous aluminium

chloride (Panreac, 98 wt%) were dissolved in 31.7 g of the ionic liquid 1-ethyl-3-methylimidazolium bis(trifluoromethylsulfonyl)imide ($[C_2C_1im][Tf_2N]$) (Sigma-Aldrich, 98 wt%) and reacted with gaseous anhydrous ammonia (Air Liquide, H_2O < 400 ppm) in a vessel kept in an ice bath to avoid the very vigorous course of the reaction.

The resulting silicon diimide and silicon-aluminium imide gels were homogenized inside a nitrogen-filled glove bag and introduced into 60-ml Teflon-lined stainless steel autoclaves which were heated statically at 150 ºC or 180 ºC under autogenous pressure for 43 hours, 7 days or 21 days. In some experiments pyrrolidine (Sigma-Aldrich, ≥99.5 wt%, purified by distillation) and/or sodium amide (Sigma-Aldrich, 95 wt%) were added to the mixture.

For some syntheses, ammonia gas was dissolved in the ionic liquid before the heating process. To dissolve the ammonia, static phase equilibrium cells constructed with Swagelok fittings, one Swagelok ball valve, and glass-lined stainless steel tubing were used. The cells were filled inside the glove bag with the mixture resulting of homogenizing the white gel obtained in the ammonolysis reaction, adding pyrrolidine in some cases. Then, ammonia was dissolved in the ionic liquid by the procedure described in our previous report [17] and the cells were heated as described above.

The obtained products were washed with methanol (Scharlau, 0.028% water as received; it was previously distilled in the presence of activated molecular sieve 3 Å pellets to remove the traces of water) to remove the ammonium chloride, the ionic liquid and the unreacted pyrrolidine and sodium amide if present, and filtered under a nitrogen flow using a stainless steel pressure filter holder. The transfer of the products to the filter holder was performed always in the glove bag, as well as all subsequent manipulations of the washed product. White solids were obtained in all cases. After

washing, the samples were heated under flowing ammonia (100 ml/min) at 600 ºC for 2 h.

In this way, different gels with the molar composition *$SiCl_4$: x $AlCl_3$: y Py: 4 NH_4Cl: (1.5+x) IL: z NH_3: q $NaNH_2$* were prepared, where *x*, *y*, *z* and *q* were varied as stated in Table 1 and *IL* stands for the ionic liquid applied as solvent. All the gels were prepared by using the ionic liquid $[C_2C_1im][Tf_2N]$ except for the gels in which sodium amide was applied as a mineralizing agent where the ionic liquid applied was $[C_4C_1pyrr][Tf_2N]$. Hereafter the samples will be named making reference to the quantity of pyrrolidine, *yPy*, where *y* stands for the Py/Si molar ratio, and to the quantity of sodium amide, *qNa*, where *q* stands for the $NaNH_2$/Si molar ratio, followed by a number indicating the heating temperature and a number indicating the heating time. If ammonia is dissolved in the ionic liquid, the heating time is followed by NH. The samples prepared from a silicon diimide gel were named starting by *Si* while the samples prepared from a silicon-aluminium imide gel were named starting by *SiAl*. As an example, SiAl-0.27Py-180-43h-NH refers to the sample prepared from a silicon-aluminium imide gel with a Py/Si molar ratio of 0.27 heated at 180 ºC for 43 hours with ammonia dissolved in the ionic liquid. The experiments performed are summarized in Table 1. An Al-Mg mixed oxide was also synthesized as reference basic solid material. This sample was obtained by calcination at 550 ºC of a hydrotalcite with Al/(Al+Mg) = 0.33 prepared following a previously reported procedure [21]. The presence of a single phase of high crystallinity was assessed by XRD.

Thermogravimetric analyses of the as-prepared samples were performed in a Perkin-Elmer TGA7 instrument, in an air flow of 40 mL/min, with a heating ramp from 25 to 900 ºC at 20 ºC/min. For the ammonia heat-treated samples, thermogravimetric analysis

were performed in an air flow of 40 mL/min, by using a heating ramp from 25 to 950 ºC at 20 ºC/min and keeping the sample at 950 ºC until constant sample weight.

Chemical CHNS analyses were obtained in a LECO CHNS-932 analyser provided with an AD-4 Perkin-Elmer scale. The silicon and aluminium content of the samples were measured by ICP-AES using an ICP Winlab Optima 3300 DV Perkin-Elmer spectrometer. Samples for ICP-AES analysis were dissolved by alkaline fusion.

Attenuated total reflection Fourier transform infrared (ATR-FTIR) measurements were conducted using a Nicolet Nexus 670 spectrometer provided with a MCT detector and a GladiATR single-bounce monolithic diamond ATR accessory. The spectra were recorded in the 4000-400 cm^{-1} range, at 4 cm^{-1} resolution, by averaging 128 scans.

Nitrogen adsorption isotherms where measured in a Micromeritics ASAP 2420 apparatus at the temperature of liquid nitrogen (-196 ºC). The samples (~ 100 mg) were loaded in the sample tubes in a nitrogen-filled glove bag and degassed in situ at 350 ºC in vacuum for 16 hours prior to analysis. Specific surface areas were determined using the BET method and the external and micropore surface areas were calculated using the t-plot method. The pore volume and the average pore diameter were calculated by applying the BJH protocol to the adsorption branch of the isotherm.

X-ray photoelectron spectroscopy (XPS) analysis was performed using a SPECS GmbH spectrometer equipped with a PHOIBOS 150 9MCD energy analyzer. A non-monochromatic magnesium X-ray source (1253.6 eV) was used with a power of 200 W and voltage of 12 kV. The powder sample was pressed inside a nitrogen-filled glove bag using a hand press and stuck on the sample holder with double-sided adhesive conductive carbon tape. The sample was introduced into the spectrometer without prior thermal treatment. The instrument operated at pressures near 6 x 10^{-9} mbar in the

analysis chamber. Pass energies of 75 and 25 eV were used for acquiring both survey and high-resolution spectra, respectively. The high resolution scans were taken around the emission lines of interest with 0.1 eV steps and 100 ms dwell time per point. SpecsLab Version 2.78 software was used for spectrometer control. The C 1s emission line of adventitious carbon (binding energy of 284.8 eV) was used to calibrate the energy scale of the spectra. The N1s peak was decomposed using the Casa XPS program (Casa Software Ltd) with a Gaussian/Lorentzian (70/30) product function and after subtraction of a Shirley background.

FTIR measurements of adsorbed pyrrole were carried out using a Thermo Nicolet Nexus 670 spectrometer equipped with a MCT detector. Spectra were acquired in the transmission mode, at a resolution of 4 cm^{-1} by averaging 250 scans. Samples were pressed into self-supporting wafers of 2.5-5 mg/cm^2 thickness and placed inside a glass cell provided with KBr windows and greaseless stopcocks. All sample manipulation was done inside a dry nitrogen-filled glove bag to prevent contact with oxygen and moisture. Samples were outgassed at 150 °C for 1 h (pressure less than 10^{-3} mbar) and cooled down to 25 °C and then pyrrole vapor (Aldrich, reagent grade, 98 wt%) was dosed repeatedly to get different equilibrium pressures.

Michael Addition reactions were performed in batch mode using a two-neck round bottom flask (100 mL) immersed in a silicone bath and equipped with a thermometer, a magnetic stirrer and a reflux condenser. In order to avoid the oxidation of the catalysts, the reflux condenser was fitted to a glass silicone-bubbler designed in a way that allows the entry of nitrogen by the top of the condenser and prevents the presence of water and oxygen in the reaction system.

In a typical experiment, 833 mg (4.0 mmol) of trans-chalcone (Sigma-Aldrich, 97 wt%), 264 mg (4.0 mmol) of malononitrile (Sigma-Aldrich, ≥99 wt%) and 150 mg of

anhydrous toluene (Sigma-Aldrich, 99.8 wt%) as internal standard were dissolved in dry methanol (chalcone/methanol weight ratio of 0.05). An aliquot of this solution was taken to determine the composition of the reaction mixture at zero time before adding the solution over the catalyst (catalyst/chalcone weight ratio of 0.04), which was previously introduced in the round bottom flask inside a nitrogen-filled glove bag.

All the test reactions were performed at 60 ºC under magnetic stirring and the progress of the reaction was monitored by withdrawing small aliquots (0.1 cm^3) using a syringe at defined time intervals. The samples were diluted with 0.2 cm^3 of chloroform, filtered and analyzed by gas chromatography using a Varian 430-GC gas chromatograph equipped with a flame ionization detector (FID) and a (95%)-dimethyl-(5%)-diphenylpolysiloxane DB – 5ms capillary column (15 m × 0.25mm ID × 0.25 μm). Under the same reaction conditions, a blank experiment (in the absence of catalyst) was performed resulting in a yield of 0% after 7 h.

To isolate the product from the reaction mixture, the catalyst was filtered and the resulting filtrate was cooled leading to the precipitation of the product. The resulting solid was extracted by filtration and purified by washing with cold methanol and hexane several times. The product 2-(3-oxo-1,3-diphenylpropyl)malononitrile was identified by ^{1}H-NMR spectroscopy (Bruker Avance III-HD NANOBAY 300 MHz). The spectrum (Figure S1 of the Supporting Information) agrees with those reported in literature [22, 23]. ^{1}H-NMR (300 MHz, $CDCl_3$) δ: 7.98-7.95 (m, 2H, ArH), 7.65-7.60 (m, 1H, ArH), 7.54-7.38 (m, 7H, ArH), 4.64 (d, J = 5.1 Hz, 1H, CN-CH), 3.96 (dt, J = 8.1, 5.4 Hz, 1H, Ar-CH), 3.76 – 3.60 (m, 2H, CH_2).

3. Results and discussion

Several silicon diimide and silicon-aluminium imide-type gels have been prepared as summarized in Table 1. The silicon diimide gels were obtained by the ammonolysis reaction of silicon tetrachloride using an ionic liquid (*IL*) as solvent, according to reaction (1), resulting in a white gel of silicon diimide, ammonium chloride and the ionic liquid.

$$SiCl_4 + 6\ NH_3\,(g) \xrightarrow{IL} Si(NH)_2 + 4\ NH_4Cl \qquad (1)$$

For the preparation of the silicon-aluminium imide gels, the silicon tetrachloride was subjected to a joint ammonolysis with anhydrous aluminium chloride, using the ionic liquid $[C_2C_1im][Tf_2N]$ as solvent. In this case, a gel consisting in silicon-aluminium imide ($T(NH)_x$ where T = Si, Al), ammonium chloride and the ionic liquid was obtained.

All the gels were prepared by using the ionic liquid 1-ethyl-3-methylimidazolium bis(trifluoromethylsulfonyl)imide ($[C_2C_1im][Tf_2N]$) ((Figure S2 (a) of the Supporting Information) except for the gels in which sodium amide was applied as a mineralizing agent. This imidazolium-based ionic liquid incorporates a hydrogen substituent at the C2 position which can be easily deprotonated under basic conditions leading to N-heterocyclic carbenes [24]. Therefore, it is necessary to use a different ionic liquid when sodium amide is applied in order to avoid the reaction between this compound and the ionic liquid. Although substitution of the C2 position of the imidazolium cation should prevent side reactions with base compounds, we found that the C2 methyl substituted 1-ethyl-2,3-dimethylimidazolium [Edmim] cation is not completely inert under basic conditions. When the ionic liquid $[Edmim][Tf_2N]$ was kept under stirring at room

temperature during 10 minutes in the presence of an excess of sodium amide ($NaNH_2$/[Edmim][Tf_2N] molar ratio of 2), the [Edmim] cation decomposed completely. This decomposition was confirmed by comparing the ^1H NMR spectrum of the reaction mixture with the spectrum of the pure ionic liquid (Figures S3 and S4 of the Supporting Information). As the substitution of the C2 position did not increase the chemical stability of the imidazolium-based ionic liquid under basic conditions, we focused our attention on the ionic liquids based on a N,N'-dialkylpyrrolidinium cation. This cation, having only one nitrogen atom in a five-member ring structure, should exhibit a lower acidity. When the ionic liquid 1-butyl-1-methylpyrrolidinium bis(trifluoromethylsulfonyl)imide ([C_4C_1pyrr][Tf_2N]) ((Figure S2 (b) of the Supporting Information) is heated at 180 ºC under vigorous stirring for 1 hour in the presence of an excess of sodium amide ($NaNH_2$/[C_4C_1pyrr][Tf_2N]) molar ratio of 2), the [C_4C_1pyrr] cation does not seem to react with the sodium amide as the ^1H NMR spectrum of the reaction mixture shows all the signals corresponding to the pure ionic liquid (Figure S5 of the Supporting Information). Due to the high chemical stability of the pyrrolidinium-based ionic liquid under basic conditions at the temperature required to process the materials (180 ºC), the solvent used when the sodium amide was applied as a mineralizing agent was the ionic liquid 1-butyl-1-methylpyrrolidinium bis(trifluoromethylsulfonyl)imide ([C_4C_1pyrr][Tf_2N]). The experimental procedure of the ionic liquids synthesis and of the study of their chemical stability can be found in the Supporting Information.

3.1. Characterization of the as-prepared samples.

The ATR-FTIR spectra of the as-prepared samples obtained after the solvothermal treatment of the different all-silicon diimide gels (Figure 1) indicate the effective formation of the Si-N network by the presence of various bands attributed to ν(Si-N) modes (905 cm^{-1}, 1083 cm^{-1} and 820 cm^{-1}) [6]. In all the cases, bands corresponding to the $\nu_a(CF_3)$, ν(C-ethyl), $\nu_s(SO_2)$, ν_a(SNS) and ν_s(SNS)/ν(CS)/γ(CH) modes of the $[Tf_2N]^-$ anion [25] appear, evidencing that the ionic liquid is present in all the materials. As the samples were washed with an abundant amount of methanol, this suggests that the ionic liquid is strongly retained in the material. As we have already observed elsewhere [17], changes in the spectral features of the samples take place as a function of the chemical composition and thermal treatment of the gels. Thus, the spectrum of sample Si-150-21d shows similar intensity in the three regions corresponding to ν(Si-N) bands (820, 905 and 1083 cm^{-1}), while samples prepared with other chemical compositions or subjected to different thermal treatment of the gel show a significantly higher absorbance of the 905 cm^{-1} band. This variation might be associated with changes in the polymerization degree of the silicon diimide gel. The mineralizing role of basic compounds as pyrrolidine and ammonia, i.e., its promotion of the condensation of the silicon diimide gel, which has already been observed in the samples studied in our previous report, is also observed in the samples studied in this work. The addition of these compounds seems to catalyze the condensation process of Si-N moieties; the samples Si-0.4Py-180-43h and Si-180-43h-NH, which were prepared in the presence of pyrrolidine and ammonia, respectively, show a strong 905 cm^{-1} band but much weaker 820 and 1085 cm^{-1} bands than the samples obtained in the absence of these compounds, the band at 820 cm^{-1} being hardly observed. On the other hand, the addition of sodium amide doesn't result in any significant change in the polymerization degree and in fact, when pyrrolidine is applied along with sodium amide, the promotion of the

condensation is disfavored since the band at 905 cm^{-1} shows notably lower intensity in the sample Si-0.25Py-0.1Na-180-7d, prepared in the presence of both pyrrolidine and sodium amide, than in the sample prepared under the same experimental conditions but in the absence of any basic compound (Si-180-7d). This observation evidences the complexity of the chemical process that leads to these diimide gels.

The heating temperature also seems to affect the polymerization process as the samples treated at 180 ºC show a relatively stronger 905 cm^{-1} band compared with the ones subjected to a solvothermal treatment at 150 ºC for the same heating time. Moreover, a long heating time of 21 days leads to a decrease in the condensation process, which is more significant when the samples are treated at 150 ºC.

The formation of the Si-N network and the presence of the ionic liquid in the samples are also proven from the ATR-FTIR spectra of the as-prepared samples obtained after the solvothermal treatment of the different silicon-aluminium imide gels (Figure 2). In this case, the effect of ammonia and pyrrolidine on the degree of condensation of the Si(Al)-N network is not so pronounced as in the samples obtained from pure silicon gels. Moreover, the presence of both mineralizing agents in the same gel results in a reduction of the polymerization degree of the silicon-aluminium imide gel since the intensity of the 905 cm^{-1} band is higher in the sample heated under presure of ammonia but in the absence of pyrrolidine as compared to the sample obtained in the presence of both mineralizing agents.

The chemical CHNS analysis results (Table 2) indicate that the as-prepared samples contain a high proportion of ionic liquid as there is a significant amount of sulfur in all of them, which can only come from the anion $[Tf_2N]^-$ of the ionic liquid. This suggests that the ionic liquid might play a structure-forming role during the polymerization process, as will be discussed below. We have already discussed elsewhere [17] that,

based on the amount of carbon present in the samples in relation to the sulfur content, two different anions ($[Tf_2N]^-$ and Cl^-) would compensate the charge of the ionic liquid cations trapped in the solid. Taking this assumption into account, it is possible to determine the total organic content from the chemical analysis. Table 3 shows the results obtained for some selected samples, which are in reasonable agreement with the organic content determined as the total weight loss observed by TG analysis (Supplementary Information, S6). It is also interesting to notice the high proportion of ionic liquid occluded as compared with the amount of silicon and aluminium present in the material. The calculated ionic liquid/Si+Al molar ratio varied from 0.13 to 0.24 depending on the chemical composition and thermal treatment of the gels (Table 3), and it is mainly affected by the heating time, as it increases from 7 to 21 days. This increase of the amount of the ionic liquid occluded is in agreement with the decrease in the condensation process obserbed in the ATR-FTIR spectra of the as-prepared samples since the lower the polymerization, the greater the amount of ionic liquid occluded in the materials. On the other hand, the content of nitrogen measured by the method described in the experimental section is not reliable for these materials, for it was found that it greatly underestimated the amount of nitrogen of a silicon nitride reference sample. Therefore, it should be taken into account that nitrogen content values included in Table 2 might significantly underestimate the actual composition of the samples.

Chemical analysis of the samples obtained from the silicon-aluminium imide gels, indicate the presence of aluminium in the as-prepared samples (Table 2). Although the Si/Al molar ratio of the sample SiAl-180-43h-NH, which was heated under presure of ammonia in the absence of pyrrolidine, is close to that of the starting gel, this value is different for samples synthesized in the presence of pyrrolidine. The use of pyrrolidine

seems to increase the aluminium incorporation, but when ammonia and pyrrolidine are applied together, gels poorer in aluminium are obtained.

3.2. Characterization of the ammonia heat-treated samples.

The occluded organic material was nearly completely removed by heating the as-prepared samples under flowing ammonia at 600 ºC for 2 h, according to the residual carbon and sulfur content of the samples, which are below 1 wt% and 0.02 respectively in most cases (Table 4). The resulting ammonia heat-treated materials were analyzed by nitrogen adsorption-desorption at 77 K in order to determine their textural properties (Table 5). All the samples present a high surface area in the range 267-693 m^2/g and their isotherms show a notable hysteresis loop (Figure S7 of the Supporting Information). Their pore size distributions, evaluated using the BJH method, are relatively narrow and centered in the pore size range of the mesoporous materials (Figure S8 of the Supporting Information). However, there is a significant fraction of the total surface area that corresponds to micropores. The capability of several ionic liquids to act as structure-directing agents in the formation of open-framework structures has already been studied [26, 27], as in the synthesis of zeolite-type materials [28]. Therefore, it can be deduced that the ionic liquid used is this work is able to act as a pore-forming compound in the formation of the T-N (T = Si, Al) network.

The different surface area, pore volume and pore size that the materials exhibit, reveal that the templating action of the ionic liquid is very dependent upon the specific chemical composition and thermal treatment of the synthesis gel. It can be noticed that, in the purely siliceous materials, the surface area increases with the heating temperature for a given synthesis time, but the micropore surface follows the opposite trend, and it

also decreases with the heating time. On the other hand, the samples prepared by using pyrrolidine or ammonia as the only mineralizing agent are the ones with the highest surface area, above 600 m^2/g, and pore volume. Moreover, applying sodium amide, either alone or together with pyrrolidine, does not seem to have any benefit from the point of view of the textural properties, as both surface area and pore volume are even smaller than those of the sample obtained under the same experimental conditions but in the absence of this compound.

In the case of the aluminium-containing materials, heating the synthesis mixture having both pyrrolidine and ammonia together seems to be more effective in increasing the surface area than using either reagents separately. Nevertheless, the effect in the textural properties of the aluminium-containing materials caused by these base compounds is not as prominent as in the purely siliceous samples since the surface area of the sample SiAl-180-43h-NH, prepared in the presence of ammonia, is not as high as the one exhibited by the purely siliceous sample prepared under the same experimental conditions. Moreover, the Al-materials do not practically contain micropores as compared to the purely siliceous samples.

As it was mentioned above, direct determination of the nitrogen content of the samples by CHNS analysis gave unreliable results. Therefore, the nitrogen content of the ammonia heat-treated materials was estimated taking into account the content of silicon, aluminium, sulfur, hydrogen and carbon as determined from chemical analysis. As is shown in Table 4, a N/(Si+Al) molar ratio higher than 2 is obtained for all the samples, being significantly higher than in some mesoporous materials prepared by a different synthesis route but subjected to a heat treatment under flowing ammonia at the same temperature [10].

The ATR-FTIR spectra of the ammonia heat-treated samples (Figure 3) show the bands corresponding to various skeletal ν(Si-N) modes of the Si-N groups of the network and a band at 1209 cm^{-1} which correspond to a δ(NH) mode [10].

The stability of the ammonia heat-treated samples in air was studied in our previous work by recording an ATR-FTIR spectrum of one sample after being exposed to air for 1, 24 and 72 hours [17]. An air-exposure of 1 hour did not result in any perceptible change in the FTIR spectrum. However, prolonged exposure led to the appearance of characteristic Si-O vibration bands, which are the consequence of bulk partial oxidation and/or hydrolysis of the sample due to exposure to oxygen and water vapor. Here, in order to explore which one of these compounds is responsible for the modification of the samples, we have studied the stability of sample Si-0.4Py-180-43h under two different conditions. To evaluate its resistance to the combined oxidation by oxygen and hydrolysis by ambient water, we have recorded an ATR-FTIR spectrum of the sample after being exposed to air for 24 hours. To study its oxidation due only to oxygen, the sample was exposed to air using a system provided with a drying tube with 3 Å molecular sieve to remove the ambient water. Figure 4 shows that the exposure to air under anhydrous conditions leads to the appearance of characteristic Si-O vibration bands at ca. 1200, 1060, 950 and 800 cm^{-1}, attributed to υ_{as}(Si-O-Si), υ(Si-O), δ(Si-OH) and υ_s'(Si-O-Si), respectively [29-31]. These bands show higher intensity (especially the band at 1060 cm^{-1}) when the sample is exposed to both oxygen and ambient water. This means that not only the oxygen but also the ambient water lead to the decomposition of the material.

The chemical environments of nitrogen, silicon and aluminium on the materials surface were investigated by XPS. The N 1s, Si 2p and Al 2p core-level spectra of some selected ammonia heat-treated samples are shown in Figures 5, 6 and S9, respectively.

Analysis of the asymmetric N 1s band (Figure 5) reveals two components attributed to two different bonding states of nitrogen atoms (Table 6). The first component at high binding energy (400 - 399 eV) corresponds to T-NH_2 terminal groups on the materials surface, while the lower binding energy component is attributed to T-NH-T groups. In the samples based on a Si-N network, this last component is located between 398 and 398.3 eV [32]. However, when aluminium atoms are incorporated to the network, the position of this band shifts towards lower binding energies (~ 397.6 eV) [33]. Aluminium atoms, being less electronegative than silicon, cause an increase of the electron density on the nitrogen atoms resulting in a small decrease in the binding energy of the N 1s peak. Hence, the electron donor ability of the nitrogen atoms bonded to aluminium atoms will be higher than that for the purely siliceous materials. As it will be discussed below, this higher electron donor ability will result in an increase of the basic strength of the active sites of these materials. It can be noticed that the contribution of the first component, which is due to the presence of T-NH_2 terminal groups, is significantly smaller in the samples prepared by heating the synthesis mixture under pressure of ammonia (Si-180-43h-NH, SiAl-180-43h-NH and SiAl-0.27Py-180-43h-NH) and in that prepared having both pyrrolidine and sodium amide together (Si-0.25Py-0.1Na-180-7d). It can be concluded that the relative proportion of the two N 1s components depends on the chemical composition of the synthesis gel. On the other hand, the abundance of terminal –NH_2 groups, which in some samples account for nearly 50% of the total N atoms, is in agreement with the N/T ratio being higher than 2, as it was discussed above.

On the other hand, Si 2p XPS spectra (Figure 6) show only one symmetric peak evidencing a quite homogeneous chemical environment for the silicon atoms of the surface. The binding energy values for the Si 2p peak of the purely siliceous materials

are close to 103 eV (Table 7). Taking into account that a binding energy of 101.7 eV has been assigned to the Si 2p core-level of a Si-NNNN configuration of Si_3N_4 [34] and that the BE for silicon dioxide (SiO_2) is 103.9 eV [35], the Si 2p peaks of the ammonia heat-treated samples can be attributed to silicon atoms in a polysilazane-type environment ($Si(NH)_x$). It can be noticed that in the samples with a high contribution of the N 1s component due to T–NH–T groups (Si-180-43h-NH and Si-0.25Py-0.1Na-180-7d), a slight shift of the Si 2p peak towards lower binding energy (102.7 eV) takes place due to the lower electronegativity of the T–NH–T group as compared to the T–NH_2 terminal groups. When aluminium atoms are present in the samples, a more remarkable shift of the Si 2p peak towards lower binding energies takes place. As has been discussed for the N 1s spectra, aluminium atoms, being less electronegative than silicon, cause an increase of the electron density on the silicon atoms, resulting in a significant decrease in the Si 2p binding energy, as happens in the case of the sialon-type materials [33, 36]. This change in the Si 2p peak position is an undeniable proof of the presence of Al atoms bonded to Si atoms through –(NH)- groups on the materials surface.

The formation of an $Al(NH)_x$ environment was also confirmed by the analysis of the Al 2p spectra which show only one symmetric peak located at ~ 74.0 eV (Supplementary Information, Figure S9 and Table 7). As several XPS studies performed on aluminium nitride (AlN) films, have shown an Al 2p peak located between 73.7 and 73.3 eV [37, 38] while a binding energy of 75.9 eV has been assigned to aluminium bound to oxygen in γ-Al_2O_3 [39], the Al 2p peak of the materials studied in this work is assigned to aluminium in an intermediate electron-withdrawing environment such as aluminium bound to –(NH)- groups ($Al(NH)_x$).

Table 7 also shows the Si/Al molar ratio on the materials' surfaces determined by XPS, which is is close to that of the bulk composition determined by ICP analysis.

3.3. Catatytic activity

The properties of the ammonia heat-treated materials as solid base catalysts have been evaluated by using the Michael addition reaction between chalcone and malononitrile as a probe reaction (Scheme 1 of the Supporting Information).

As the desired 1,4 – addition product was the only product detected in any of the reactions studied, the evolution of the Michael addition reaction is given by the yield of this product. Figure 7 shows the evolution with time of the yield of the 1,4 – addition product for the ammonia heat-treated catalysts using a catalyst/chalcone weight ratio of 0.04. All the catalysts show high catalytic activity, reaching a yield of at least 80% in some cases, while a mesoporous silica MCM-41 used for comparison purposes, which would be an oxygen-based analogue of the Si-N based materials, showed no catalytic activity at the same reaction conditions. This result reveals that the incorporation of nitrogen in a silicon-based network results in the generation of basic active sites.

The comparison between the catalytic activity of the different catalysts would show the influence of the surface area and the chemical composition of the materials. At short reaction times ($t < 1$ h), the reaction yield increases very fast, and a smooth increase of yield as a function of time is observed as the reaction is prolonged beyond 1 or 2 hours. The largest differences in activity mainly take place at the first stages of the reaction ($t < 1$ h), which can mainly be due to differences in the surface area of the materials but also to differences in the intrinsic catalytic activity of the active sites. Figure 8, which represents the reaction yield versus the specific surface area of the catalysts for a specific reaction time ($t = 15$ min), shows that in the case of the purely siliceous

materials there is a trend for the reaction yield to increase with the specific surface area, with the exception of sample Si-180-43h-NH which was prepared in the presence of ammonia. This sample exhibits higher catalytic activity than other catalysts with similar surface area. This effect can be due to the high proportion of Si-NH-Si groups on the material surface as compared with the remaining Si-N based catalysts, according to XPS results discussed above. In these groups, the electron donor ability of the nitrogen atoms would be higher than for the Si-NH_2 terminal groups, which should result in a higher basic strength of the active sites.

These conclusions are supported by additional characterization results obtained by FTIR analysis of samples kept in a vacuum cell under controlled atmosphere and using pyrrole as a probe to evaluate the relative strength of the basic sites. Spectra corresponding to sample Si-150-7d have been plotted in Figure 9 as a representative example, together with the spectrum of pyrrole vapor used as reference (spectra of other samples have been included in the supplementary information, Figure S10). The spectra of samples previously degassed at 150°C show a strong band at ca. 3380 cm^{-1} that can be assigned to the N-H stretching mode of Si-NH-Si groups and two bands at 3490 and 3640 cm^{-1} (the later one being notably broader) that are attributed to the symmetric and asymmetric H-N-H stretching modes of Si-NH_2 species (supplementary information, Figure S10). Additionally, weak bands can be observed at 3740 cm^{-1} and at ca. 3700 cm^{-1} (broad shoulder), corresponding to isolated and perturbed silanol species, which reveals that samples are slightly oxidized. The relative intensities of the Si-NH-Si and Si-NH_2 stretching bands evidence that most of the nitrogen atoms in sample Si-180-43h-NH are present as bridging Si-NH-Si species, that the fraction of terminal Si-NH_2 groups is slightly higher in sample Si-0.25Py-0.1Na-180-7d and that it increases notably for samples Si-150-7d and Si-0.1Na-180-7d, in agreement with the relative proportions

of the two components observed in the N1s core-level spectra (Table 6). The relative strength of basic sites present in these samples was evaluated by adsorption of pyrrole, for it is known that the interaction of the NH group of pyrrole with an electron donor site produces a bathochromic shift of its stretching vibration band with respect to the molecule in the vapor phase, and the magnitude of this shift can be used as a measure of the strength of the basic site [40]. The FTIR spectra recorded after dosing of pyrrole vapor into the cell showed the development of bands that overlap with those of the NH and NH_2 groups of the samples (supplementary information, Figure S10). The difference spectra obtained by subtracting the spectrum of the corresponding degassed sample show that the band corresponding to the ν(NH) mode of adsorbed pyrrole interacting with basic sites appears at wavenumber values in the range 3450-3470 cm^{-1}, and that its exact position varies from one sample to another. In addition, an overlapping band that grows as the equilibrium pressure increases can be observed at 3410 cm^{-1}, which is assigned to physisorbed pyrrole [40]. The calculated shifts for the ν(NH) band of pyrrole adsorbed on basic site with respect to free pyrrole are collected in Table 8. The results show that the largest shift is obtained for sample Si-180-43h-NH (-78 cm^{-1}), proving that this sample possess the strongest basicity among the Si-N samples. The data also confirm that the overall basic strength of the catalysts decreases as the ratio of bridging Si-NH-Si to terminal Si-NH_2 groups decreases, in agreement with the expected higher electron donor ability of the nitrogen atom in Si-NH-Si moieties. The variation in the magnitude of the shift of the ν(NH) band of pyrrole suggests that there are significant differences in basic strength among the samples. For comparison purposes, adsorption of pyrrole was also carried out on a strong basic solid material, an Al-Mg mixed oxide obtained by calcination of a hydrotalcite material with Mg/Al ratio of 2. For this sample, adsorption of pyrrole gave rise to the development of

a strong band at 3388 cm^{-1}, indicating a -142 cm^{-1} shift of the ν(NH) band of pyrrole (supplementary information, Figure S10), in agreement with previous results obtained with similar samples [41]. This shift is notably larger than the maximum value obtained for the Si-N materials (-78 cm^{-1}), which suggests that these materials exhibit moderate basic strength.

Figure 8 shows that the active sites of two of the aluminium-containing samples exhibit a higher intrinsic catalytic activity as compared with the Si-N based materials. In this case, the relative proportion of the T-NH-T groups is not the only factor influencing the catalytic activity of the catalysts. The incorporation of aluminium atoms, which are less electronegative than silicon, causes an increase of the electron density on the nitrogen atoms bound to aluminium atoms resulting in an enhancement of the intrinsic catalytic activity of the active sites. Indeed, the calculated shift of the NH stretching of pyrrole adsorbed on sample SiAl-0.27Py-180-43h (Table 8) is higher than the one expected for Si-N samples with similar molar ratio of bridging T-NH-T to terminal T-NH_2 sites (as determined by XPS: Table 6). Nevertheless, this shift is slightly smaller than that obtained for the Si-N with the highest content of Si-NH-Si groups, which indicates that the basic strength of sample SiAl-0.27Py-180-43h is close but slightly lower than that of sample Si-180-43h-NH.

Comparing the two aluminium-containing samples, sample SiAl-0.27Py-180-43h exhibits a higher catalytic activity in spite of its lower surface area and its higher proportion of T-NH_2 terminal groups. As the Si/Al molar ratio of this sample is significantly lower than that of the remaining aluminium-containing samples, it can be concluded that an increase of the aluminium content leads to the formation of active sites with higher overall intrinsic activity. In this regard, the calculated reaction yield/S_{BET} ratio for a specific reaction time (t = 15 min) has been plotted in Figure 10 as

a function of the Al/Si molar ratio for three of the catalysts. It can be seen that the intrinsic catalytic activity of a purely siliceous catalyst like sample Si-180-7d is considerably lower than that of the aluminium-containing samples, and the activity of the latter increases with their aluminium content.

Sample SiAl-180-43h-NH was selected to investigate the influence of the solvent on the reaction yield. Table 1 of the Supporting Information shows the activity of this catalyst for the Michael addition reaction between chalcone and malononitrile in different solvents. As we previously discussed, when the reaction is conducted in methanol for a catalyst/chalcone weight ratio of 0.08 the reaction yield is ~ 98 %. However, when THF, CH_2Cl_2 or $CHCl_3$ (all of them previously dried) is used as solvent, the Michael addition reaction between chalcone and malononitrile does not take place even if the catalyst/chalcone ratio is increased to 0.16. Several reports have shown this great influence of the solvent nature on the catalytic behavior. For example, no 1,4 – addition product formation was observed in aprotic solvents when using different chiral amines as basic catalysts, whereas the reaction proceeds very well in methanol [42]. Moreover, some reports indicate that the use of an aprotic solvent leads to a decrease in the yield of the 1,4 – addition product [22, 43]. According to the classical mechanism of the Michael addition reaction, the abstraction of a proton from the donor by the basic sites (T-NH-T) of the catalyst generates a carbanion which can be stabilized by the cationic charge created in the lattice (Scheme 2 of the Supporting Information, step 1). The carbanion then reacts in a 1,4-conjugate addition to the chalcone (step 2). The resulting anion would be protonated giving the final product and regenerating the active site (step 3). Based on this mechanism we hypothesize that methanol, being a polar protic solvent, can stabilize the charged intermediates by hydrogen bonding and promote rapid proton

transfer [44]. In aprotic and less polar solvents, the formation of the intermediates is not so favored.

As mentioned above, the initial step of the Michael addition reaction is deprotonation of the donor to form a carbanion. To carry out this step, the catalysts must have a pK_a for their conjugate acid in the same range as that of the Michael donor. The lower the pK_a value of the donor, the easier it is to abstract a proton, so the basic strength of the catalysts could be estimated by varying the pKa of the donors. When malononitrile (pK_a 11) is the donor, the Michael addition to chalcone takes place with a high yield (~ 98 %.) over SiAl-180-43h-NH in methanol. On the contrary, when using diethylmalonate (pK_a 13.3), the reaction does not occur even if the catalyst/chalcone ratio is increased to 0.16. Since malononitrile is a weak acid compared with other Michael donors [45], such as cyanoacetamide (pK_a 2.96), it can be estimated that the strength of the basic sites on SiAl-180-43h-NH is considerably high, although it is not high enough to deprotonate an acid as weak as the diethylmalonate. Therefore, the basic strength of these N-containing materials should be in the range $11 < pK_a < 13.3$. To compare the catalytic activity of the catalysts with well-known basic catalysts, Michael addition reaction was performed at the same conditions over the sodium form of zeolite (Aldrich 13X zeolite powder) and an Al-Mg mixed oxide (obtained by calcination of a hydrotalcite material with Mg/Al ratio of 2). Figure 11 and Table 9 shows the yield of the 1,4 – addition product for these catalysts and for SiAl-0.27Py-180-43h, Si-180-21d and Si-180-43h-NH after 15 min and 7 hours of reaction. It can be noticed that at the first stages of the reaction (t = 15 min), the catalysts prepared in this work show lower catalytic activity than the sodium zeolite and the calcined hydrotalcite, the latter of which gave the highest yield. However, when the reaction time comes to 7 hours, the yield is almost the same for the five materials (Table 9). Considering the calculated reaction yield/S_{BET} ratio of the

materials, it can be observed that the intrinsic catalytic activity of the Al-Mg mixed oxide is notably higher than that of the other materials (Table 9), in agreement with its higher basic strength estimated by FTIR of adsorbed pyrrole and with previous catalytic studies [46]. However, despite having lower aluminium content, the SiAl-0.27Py-180-43h catalyst exhibits an intrinsic catalytic activity which is quite close at least, if not higher, than that of the sodium zeolite.

As we mentioned above, the ammonia heat-treated samples undergo oxidation and hydrolysis when exposed to the air, leading to the appearance of Si-O groups and to the consequent reduction of the number of T-NH active sites. To study the influence of this alteration of the material upon the reaction yield, we have performed the Michael addition reaction over the Si-0.4Py-180-43h sample before and after being exposed to air for 15 days. This prolonged air exposure did not result in any significant change of the FTIR spectrum with respect to the one recorded after 24 hours air-exposure (shown in Figure 4). Figure 12, which represents the reaction yield versus time, shows that the catalytic activity is reduced significantly when the sample is oxidized reaching a yield of ~ 33% after 7 hours of reaction, while the fresh sample reached a yield close to 70%. This result reveals that air-exposure leads to a significant reduction of the number of T-NH active sites but not to the complete oxidation of the sample. Although the bands corresponding to the T-NH groups are not clearly observed in the FTIR spectrum of the oxidized sample, they might be obscured due to overlapping with the wide Si-O bands as the material should have some T-NH active groups which have resisted the oxidation and are active to catalyze the reaction.

Conclusions

All-silicon and silicon-aluminium porous materials containing a framework formed by T-NH-T linkages can be easily prepared by the reaction between ammonia and silicon and aluminium chlorides in an ionic liquid under controlled reaction conditions. The ionic liquid occluded in the as-made materials can be removed by heating in an ammonia flow at 600 ºC, leaving materials with a high surface area and porosity. It has been found that the textural properties of the resulting solids are very much dependent upon the specific synthesis conditions and the chemical composition of the gel, and in particular of the aluminium content of the framework. In this latter case, when aluminium is present in the solid, mesoporous materials containing no micropores have been obtained.

Beside the presence of T-NH-T units, a large amount of terminal T-NH_2 groups are also evidenced by IR and XPS. These groups can be considered as defects that interrupted the framework very much in the same way as Si-OH are commonly found in silicon and oxygen-based mesoporous materials. The relative content of these defects is also strongly related to the specific synthesis conditions and chemical composition of the gels.

These nitrogen-containing materials exhibit basic properties owing to the presence of two types of N-groups, the bridging –NH- units and the T-NH_2 terminal groups. The overall basic strength of these materials has been shown by pyrrole adsorption to increase with the fraction of T-NH-T groups and the aluminium content of the framework. Moreover, this basic strength is lower than that of a calcined hydrotalcite (Al/(Al+Mg) = 0.33). However, these materials are active catalysts in the Michael addition reaction between chalcone and malononitrile (pK_a 11) carried out in methanol, although they turned to be inactive when diethylmalonate having a weaker acidity (pK_a 13.3) is used as the donor. Therefore, the basic sites of these materials should have pK_a

values within that range. It is also noteworthy that no products other than that resulting from the Michael addition are detected. The reaction is also very sensitive to the nature of the solvent, for it does not proceed in dichloromethane, chloroform and tetrahydrofuran.

Acknowledgments

A. Saugar, C. Márquez-Álvarez and J. Pérez-Pariente acknowledge the Spanish Ministry of Economy and Competitiveness for the funding through Project MAT2012-31127. A. Saugar also acknowledges this Ministry for a research grant to stay at the Prof. Welton laboratory at Imperial College.

References

[1] J.S. Bradley, O. Vollmer, R. Rovai, U. Specht, F. Lefebvre, Advanced Materials. 10 (1998) 938-942.

[2] O. Vollmer, F. Lefebvre, J.S. Bradley, Journal of Molecular Catalysis A: Chemical. 146 (1999) 87-96.

[3] H.N. Han, D.A. Lindquist, J.S. Haggerty, D. Seyferth, Chemistry of Materials. 4 (1992) 705-711.

[4] R. Rovai, C.W. Lehmann, J.S. Bradley, Angewandte Chemie International Edition. 38 (1999) 2036-2038.

[5] F. Cheng, S. Clark, S.M. Kelly, J.S. Bradley, F. Lefebvre, Journal of the American Ceramic Society. 87 (2004) 1413-1417.

[6] V. Rocher, S.M. Kelly, A.L. Hector, Microporous and Mesoporous Materials. 156 (2012) 196-201.

[7] K.S. Mazdiyasni, C.M. Cooke, Journal of the American Ceramic Society. 56 (1973) 628-633.

[8] W. Schnick, H. Huppertz, Chemistry – A European Journal. 3 (1997) 679-683.

[9] S. Kaskel, D. Farrusseng, K. Schlichte, Chemical Communications. (2000) 2481-2482.

[10] S. Kaskel, K. Schlichte, B. Zibrowius, Physical Chemistry Chemical Physics. 4 (2002) 1675-1681.

[11] S. Kaskel, Journal of Catalysis. 201 (2001) 270-274.

[12] D. Farrusseng, K. Schlichte, B. Spliethoff, A. Wingen, S. Kaskel, J.S. Bradley, F. Schüth, Angewandte Chemie International Edition. 40 (2001) 4204-4207.

[13] J.S. Bradley, F. Cheng, S.J. Archibald, R. Supplit, R. Rovai, C.W. Lehmann, C. Kruger, F. Lefebvre, Dalton Transactions. (2003) 1846-1851.

[14] F. Cheng, S.M. Kelly, F. Lefebvre, S. Clark, R. Supplit, J.S. Bradley, Journal of Materials Chemistry. 15 (2005) 772-777.

[15] S. Kaskel, Christian W. Lehmann, G. Chaplais, K. Schlichte, M. Khanna, European Journal of Inorganic Chemistry. 2003 (2003) 1193-1196.

[16] S. Kaskel, G. Chaplais, K. Schlichte, Chemistry of Materials. 17 (2005) 181-185.

[17] A.I. Saugar, A. Mayoral, J. Pérez-Pariente, Microporous and Mesoporous Materials. 186 (2014) 146-154.

[18] S. Sowmiah, V. Srinivasadesikan, M.C. Tseng, Y.H. Chu, Molecules (Basel, Switzerland). 14 (2009) 3780-3813.

[19] A. Yokozeki, M.B. Shiflett, Industrial & Engineering Chemistry Research. 46 (2007) 1605-1610.

[20] G. Li, Q. Zhou, X. Zhang, LeiWang, S. Zhang, J. Li, Fluid Phase Equilibria. 297 (2010) 34-39.

[21] S. Miyata, Clays and Clay Minerals. 28 (1980) 50-56.

[22] W. Yang, Y. Jia, D.-M. Du, Organic & Biomolecular Chemistry. 10 (2012) 332-338.

[23] X. Li, L. Cun, C. Lian, L. Zhong, Y. Chen, J. Liao, J. Zhu, J. Deng, Organic & Biomolecular Chemistry. 6 (2008) 349-353.

[24] S. Chowdhury, R.S. Mohan, J.L. Scott, Tetrahedron. 63 (2007) 2363-2389.

[25] O. Höfft, S. Bahr, V. Kempter, Langmuir. 24 (2008) 11562-11566.

[26] Z. Ma, J. Yu, S. Dai, Advanced Materials. 22 (2010) 261-285.

[27] S. Dai, Y.H. Ju, H.J. Gao, J.S. Lin, S.J. Pennycook, C.E. Barnes, Chemical Communications. (2000) 243-244.

[28] E.R. Cooper, C.D. Andrews, P.S. Wheatley, P.B. Webb, P. Wormald, R.E. Morris, Nature. 430 (2004) 1012-1016.

[29] P.N. Sen, M. Thorpe, Physical review. B, Solid state. 15 (1977) 4030-4038.

[30] R.B. Laughlin, J. Joannopoulos, Physical review. B, Solid state. 16 (1977) 2942-2952.

[31] P. McMillan, The American mineralogist. 69 (1984) 622-644.

[32] J.L. Bischoff, F. Lutz, D. Bolmont, L. Kubler, Surface Science. 251–252 (1991) 170-174.

[33] T. Hagio, A. Takase, S. Umebayashi, J Mater Sci Lett. 11 (1992) 878-880.

[34] T.T.T. Hien, C. Ishizaki, K. Ishizaki, Nippon Seramikkusu Kyokai Gakujutsu Ronbunshi/Journal of the Ceramic Society of Japan. 113 (2005) 647-653.

[35] D.F. Mitchell, K.B. Clark, J.A. Bardwell, W.N. Lennard, G.R. Massoumi, I.V. Mitchell, Surface and Interface Analysis. 21 (1994) 44-50.

[36] C. Qin, G. Wen, X. Wang, L. Song, X. Huang, Journal of Materials Chemistry. 21 (2011) 5985-5991.

[37] L. Rosenberger, R. Baird, E. McCullen, G. Auner, G. Shreve, Surface and Interface Analysis. 40 (2008) 1254-1261.

[38] D. Manova, V. Dimitrova, W. Fukarek, D. Karpuzov, Surface and Coatings Technology. 106 (1998) 205-208.

[39] B. Ealet, M.H. Elyakhloufi, E. Gillet, M. Ricci, Thin Solid Films. 250 (1994) 92-100.

[40] B. Camarota, Y. Goto, S. Inagaki, B. Onida, Langmuir. 27 (2011) 1181-1185.

[41] D. Tichit, M.N. Bennani, F. Figueras, J.R. Ruiz, Langmuir. 14 (1998) 2086-2091.

[42] S. Colonna, H. Hiemstra, H. Wynberg, Journal of the Chemical Society, Chemical Communications. (1978) 238-239.

[43] H. Keipour, M.A. Khalilzadeh, A. Hosseini, A. Pilevar, D. Zareyee, Chinese Chemical Letters. 23 (2012) 537-540.

[44] B.D. Mather, K. Viswanathan, K.M. Miller, T.E. Long, Progress in Polymer Science. 31 (2006) 487-531.

[45] B.M. Choudary, M. Lakshmi Kantam, C.R. Venkat Reddy, K. Koteswara Rao, F. Figueras, Journal of Molecular Catalysis A: Chemical. 146 (1999) 279-284.

[46] A. Corma, V. Fornés, R.M. Martín-Aranda, F. Rey, Journal of Catalysis. 134 (1992) 58-65.

TABLES

Table 1. Experimental conditions used for the preparation of silicon- and silicon-aluminium imidonitride materials from gels with the following molar composition: *$SiCl_4$: x $AlCl_3$ y Py: 4 NH_4Cl: (1.5+x) IL: z NH_3: q $NaNH_2$*, where *Py* stands for pyrrolidine applied as a potential structure directing agent, *z* stands for the quantity of ammonia dissolved in the gel before the heating process and *q* stands for the sodium amide applied as a potential mineralizing agent. *IL* refers to the ionic liquid applied as solvent (*$[C_2C_1im][Tf_2N]$* or *$[C_4C_1pyrr][Tf_2N]$*).

Sample	*x*	*y*	*z*	*q*	T^a / °C	t^b
Si-150-7d	0	0	0	0	150	7 days
Si-150-21d	0	0	0	0	150	21 days
Si-180-7d	0	0	0	0	180	7 days
Si-180-21d	0	0	0	0	180	21 days
Si-0.4Py-180-43h	0	0.4	0	0	180	43 hours
Si-180-43h-NH	0	0	3.0	0	180	43 hours
Si-0.1Na-180-7d[c]	0	0	0	0.1	180	7 days
Si-0.25Py-0.1Na-180-7d[c]	0	0.25	0	0.1	180	7 days
SiAl-0.27Py-180-43h	0.1	0.27	0	0	180	43 hours
SiAl-180-43h-NH	0.1	0	3.6	0	180	43 hours
SiAl-0.27Py-180-43h-NH	0.1	0.27	3.6	0	180	43 hours

[a] Heating temperature.

[b] Heating time.

[c] *IL*: *$[C_4C_1pyrr][Tf_2N]$*.

Table 2. Elemental composition of the as-prepared samples determined by CHNS chemical analysis and ICP-OES (Si and Al).

As-prepared sample	*Chemical CHNS analysis*				*ICP*		
	C (wt%)	*H (wt%)*	*N (wt%)*	*S (wt%)*	*Si (wt%)*	*Al (wt%)*	*Si/Al*[a]
Si-150-7d	15.80	5.00	13.64	1.00	38.1	-	-
Si-150-21d	20.33	6.10	8.83	0.80	40.5	-	-
Si-180-7d	14.20	4.69	15.88	1.12	36.6	-	-
Si-180-21d	16.94	4.94	13.33	1.35	30.6	-	-
Si-0.4Py-180-43h	9.12	3.67	19.25	1.86	29.5	-	-
Si-180-43h-NH	11.90	4.20	16.85	1.03	31.6	-	-
Si-0.1Na-180-7d	19.16	6.41	11.76	0.88	32.3	-	-
Si-0.25Py-0.1Na-180-7d	18.26	6.01	12.55	0.81	35.1	-	-
SiAl-180-43h-NH	11.26	4.46	15.57	0.89	30.9	2.9	10.2
SiAl-0.27Py-180-43h-NH	13.26	4.8	14.24	0.68	29.6	2.3	12.4
SiAl-0.27Py-180-43h	15.95	4.99	12.43	1.13	26.0	3.1	8.1

[a] Molar ratio between the silicon and the aluminium content.

Table 3. Organic content of selected as-prepared samples determined from CHNS and ICP-OES analyses and from TG results.

As-prepared sample	*Chemical CHNS and ICP analyses*			*TG*
	$Cat^+[Tf2N]^-$ (wt%)	*Cat^+Cl^- (wt%)*	*Org/(Si+Al)*[a]	*Organic*[b] *(wt%)*
Si-150-7d	6.11	29.08	0.16	30.91
Si-150-21d	4.89	38.90	0.19	42.96
Si-180-7d	6.84	25.46	0.15	29.45
Si-180-21d	8.25	30.33	0.21	40.85
Si-180-43h-NH	6.29	21.06	0.14	26.21
Si-0.1Na-180-7d	5.80	28.49	0.15	37.08
SiAl-180-43h-NH	5.44	20.18	0.13	25.37

Cat^+: $[C_2C_1im]^+$or $[C_4C_1pyrr]^+$.

[a] Molar ratio between the organic species (Cat+[Tf2N]- and Cat+Cl-) content estimated from the CHNS analysis and the silicon and aluminium content of the material determined by ICP-OES.

[b] Weight loss in the TG analysis performed in an air flow from 25 to 900ºC.

Table 4. Elemental composition of the ammonia heat-treated samples determined by CHNS chemical analysis and ICP-OES (Si and Al).

Ammonia heat-treated sample	*Chemical CHNS analysis*				*ICP-OES*			
	C (wt%)	*H (wt%)*	*N (wt%)*	*S (wt%)*	*Si (wt%)*	*Al (wt%)*	*N/(Si+Al)*[a]	*Si/Al*[b]
Si-150-7d	1.06	1.16	7.32	0.02	48.5	-	2.04	-
Si-150-21d	0.47	1.52	4.61	0.01	38.3	-	3.10	-
Si-180-7d	0.53	1.40	14.1	0.00	44.1	-	2.45	-
Si-180-21d	0.77	1.60	9.51	0.02	39.4	-	2.96	-
Si-0.4Py-180-43h	1.77	1.75	14.05	0.01	36.9	-	3.24	-
Si-180-43h-NH	0.42	1.76	16.88	0.02	43.5	-	2.50	-
Si-0.1Na-180-7d	0.67	1.13	10.43	0.02	42.2	-	2.66	-
Si-0.25Py-0.1Na-180-7d	0.93	1.05	10.67	0.03	42.2	-	2.80	-
SiAl-180-43h-NH	0.51	1.44	11.37	0.01	38.1	3.6	2.70	10.2
SiAl-0.27Py-180-43h-NH	0.43	1.34	11.24	0.01	39.7	3.0	2.59	12.7
SiAl-0.27Py-180-43h	0.42	1.28	8.06	0.01	37.4	5.2	2.61	6.91

[a] Nitrogen to silicon (or silicon plus aluminium) molar ratio. Nitrogen content estimated taking into account the content of silicon, aluminium, sulfur, hydrogen and carbon determined by chemical analysis.

[b] Molar ratio between the silicon content and the aluminium content.

Table 5. Specific surface area, external surface, micropore area, pore volume and average pore diameter of the ammonia heat-treated samples.

Ammonia heat-treated sample	S_{BET} (m^2/g)	S_{ext} [a] (m^2/g)	S_{micro} [b] (m^2/g)	V_p [c] (cm^3/g)	Average pore diameter (nm)
Si-150-7d	267	202	65	0.57	9.0
Si-150-21d	306	119	187	0.44	9.4
Si-180-7d	626	569	57	1.25	7.2
Si-180-21d	537	440	97	1.04	7.5
Si-0.4Py-180-43h	693	653	40	1.54	7.9
Si-180-43h-NH	630	574	56	1.44	8.2
Si-0.1Na-180-7d	460	410	50	0.87	7.4
Si-0.25Py-0.1Na-180-7d	497	465	32	1.11	8.0
SiAl-0.27Py-180-43h	267	267	0	0.60	7.7
SiAl-180-43h-NH	325	319	6	0.90	9.7
SiAl-0.27Py-180-43h-NH	448	444	4	1.25	8.7

[a] Non-micropore (external and mesopore) surface area.

[b] Micropore surface area.

[c] Pore volume.

Table 6. Binding energy (B.E.) and relative contribution of N1s components of the XPS spectra.

Ammonia heat-treated sample	*Component 1*		*Component 2*	
	B.E. (eV)	*%*	*B.E. (eV)*	*%*
Si-150-7d	399.7	63	398.3	37
Si-180-7d	399.4	59	398.0	41
Si-180-21d	399.8	54.6	398.3	45.4
Si-0.4Py-180-43h	400.0	51.5	398.1	48.5
Si-0.1Na-180-7d	399.8	48	398.2	52
Si-0.25Py-0.1Na-180-7d	398.8	22.6	397.8	77.4
Si-180-43h-NH	398.9	20.3	398.0	79.7
SiAl-0.27Py-180-43h	399.4	31.4	397.7	68.6
SiAl-0.27Py-180-43h-NH	399.4	18.8	397.6	81.2
SiAl-180-43h-NH	399.1	14.3	397.4	85.7

Table 7. Binding energy (B.E.) of Si 2p and Al 2p bands of the XPS spectra and molar ratio between silicon and aluminium on the materials surface determined by XPS.

Sample	*B.E (eV)*		*Si/Al*
	Al 2p	*Si 2p*	
Si-150-7d	-	103.4	-
Si-180-7d	-	103.4	-
Si-180-21d	-	103.4	-
Si-0.4Py-180-43h	-	103.3	-
Si-0.1Na-180-7d	-	103.2	-
Si-0.25Py-0.1Na-180-7d	-	102.7	-
Si-180-43h-NH	-	102.7	-
SiAl-0.27Py-180-43h	74.2	102.3	7.8
SiAl-0.27Py-180-43h-NH	74.1	102.3	11.8
SiAl-180-43h-NH	74.0	102.0	11.1

Table 8. Shift of the N-H stretching mode of pyrrole upon adsorption on Si(Al)-N materials and an Al-Mg mixed oxide (calcined hydrotalcite).

Sample	$\Delta\nu\ (cm^{-1})$
Si-150-7d	-57
Si-0.1Na-180-7d	-58
Si-0.25Py-0.1Na-180-7d	-63
Si-180-43h-NH	-78
SiAl-0.27Py-180-43h	-73
Calcined hydrotalcite	-142

Table 9. Activity of Si(Al)-N materials and reference basic solid catalysts for the Michael addition reaction between chalcone and malononitrile.

Sample	*Physicochemical properties*		*t = 15 min*		*t = 7 hours*	
	$S_{BET}\ (m^2/g)$	*Si/Al*[a]	*Yield*[b] *(%)*	$Yield/S_{BET}$	*Yield*[b] *(%)*	$Yield/S_{BET}$
Si-180-21d	537	-	19	0.03	81	0.15
Si-180-43h-NH	630	-	39	0.06	83	0.13
SiAl-0.27Py-180-43h	266	6.91	37	0.14	89	0.33
Sodium zeolite	681	1.2	43	0.06	85	0.12
Calcined hydrotalcite	202	-	50	0.24	86	0.42

[a] Silicon to aluminium molar ratio determined by ICP.

[b] Reaction conditions: Chalcone/malononitrile molar ratio: 1, catalyst/chalcone weight ratio: 0.04; chalcone/solvent weight ratio: 0.05, reaction temperature: 60 ºC.

Figure Captions.

Fig. 1. ATR-FTIR spectra of the as-prepared samples obtained from silicon diimide-type gels; (a) Si-150-21d, (b) Si-180-21d, (c) Si-0.25Py-0.1Na-180-7d, (d) Si-150-7d, (e) Si-180-7d, (f) Si-0.1Na-180-7d, (g) Si-0.4Py-180-43h and (h) Si-180-43h-NH.

Fig. 2. ATR-FTIR spectra of the as-prepared samples obtained from silicon-aluminium imide-type gels; (a) SiAl-0.27Py-180-43h, (b) SiAl-0.27Py-180-43h-NH and (c) SiAl-180-43h-NH.

Fig. 3. ATR-FTIR spectra of the ammonia heat-treated samples; (a) SiAl-0.27Py-180-43h-NH, (b) Si-150-21d, (c) SiAl-180-43h-NH and (d) Si-180-7d.

Fig. 4. FTIR spectra of the ammonia heat-treated sample Si-0.4Py-180-43h before and after being exposed to air for 24h in the presence and in the absence of ambient water.

Fig. 5. N 1s XPS spectra of the some selected ammonia heat-treated samples.

Fig. 6. Si 2p XPS spectra of some selected ammonia heat-treated samples; (a) SiAl-180-43h-NH, (b) SiAl-0.27Py-180-43h-NH, (c) Si-180-43h-NH and (d) Si-0.4Py-180-43h.

Fig. 7. Yield of the 1,4 – addition product vs reaction time of the ammonia heat-treated catalysts. Reaction conditions: reaction temp: 60 ºC, chalcone/malononitrile molar ratio: 1, catalyst/chalcone weight ratio: 0.04, chalcone/methanol weight ratio: 0.05.

Fig. 8. Influence of the specific surface area of the catalyst on the yield of the 1,4 – addition product for the Si-N based materials (full symbols) and for the aluminium-

containing materials (open symbols) after 15 min of reaction. Reaction conditions: reaction temp: 60 ºC, chalcone/malononitrile molar ratio: 1, catalyst/chalcone weight ratio: 0.04, chalcone/methanol weigth ratio: 0.05.

Fig. 9. FTIR spectra of sample Si-150-7d (3.1 mg/cm^2 thickness) after degassing at 150°C (a) and in contact with pyrrole vapor at 25ºC and equilibrium pressure of ca. 1 mbar (b) and ca. 10 mbar (c). Difference spectra c-a and b-a are shown to facilitate determination of the shift of the NH stretching band of pyrrole. The spectrum of pyrrole vapor (6 mbar) is also shown for reference (NH stretching band centered at 3530 cm^{-1}). The arrow indicates the shifts of the ν(NH) band of pyrrole due to H-bonding with basic sites. At high equilibrium pressure, the 3410 cm^{-1} band (marked with an asterisk) corresponding to physisorbed pyrrole [40] becomes dominant.

Fig. 10. Calculated reaction yield/S_{BET} ratio for t = 15 min vs Al/Si molar ratio for the Si-N based materials (full symbols) and for the aluminium-containing materials (open symbols). Reaction conditions: reaction temp: 60 ºC, chalcone/malononitrile molar ratio: 1, catalyst/chalcone weight ratio: 0.04, chalcone/methanol weigth ratio: 0.05.

Fig. 11. Yield of the 1,4 – addition product vs reaction time of SiAl-0.27Py-180-43h, Si-180-43h-NH and two reference basic catalysts; sodium zeolite and calcined hydrotalcite. Data corresponding to the first hour of reaction are shown in the right figure for clarity. Lines are guide for the eyes. Reaction conditions: reaction temp: 60 ºC, chalcone/malononitrile molar ratio: 1, catalyst/chalcone weight ratio: 0.04, chalcone/methanol weigth ratio: 0.05.

Fig. 12. Yield of the 1,4 – addition product vs reaction time of SiAl-0.4Py-180-43h before and after being exposed to ambient air for 15 days (lines are guide for the eyes). Reaction conditions: reaction temp: 60 ºC, chalcone/malononitrile molar ratio: 1, catalyst/chalcone weight ratio: 0.04, chalcone/methanol weigth ratio: 0.05.

FIGURES

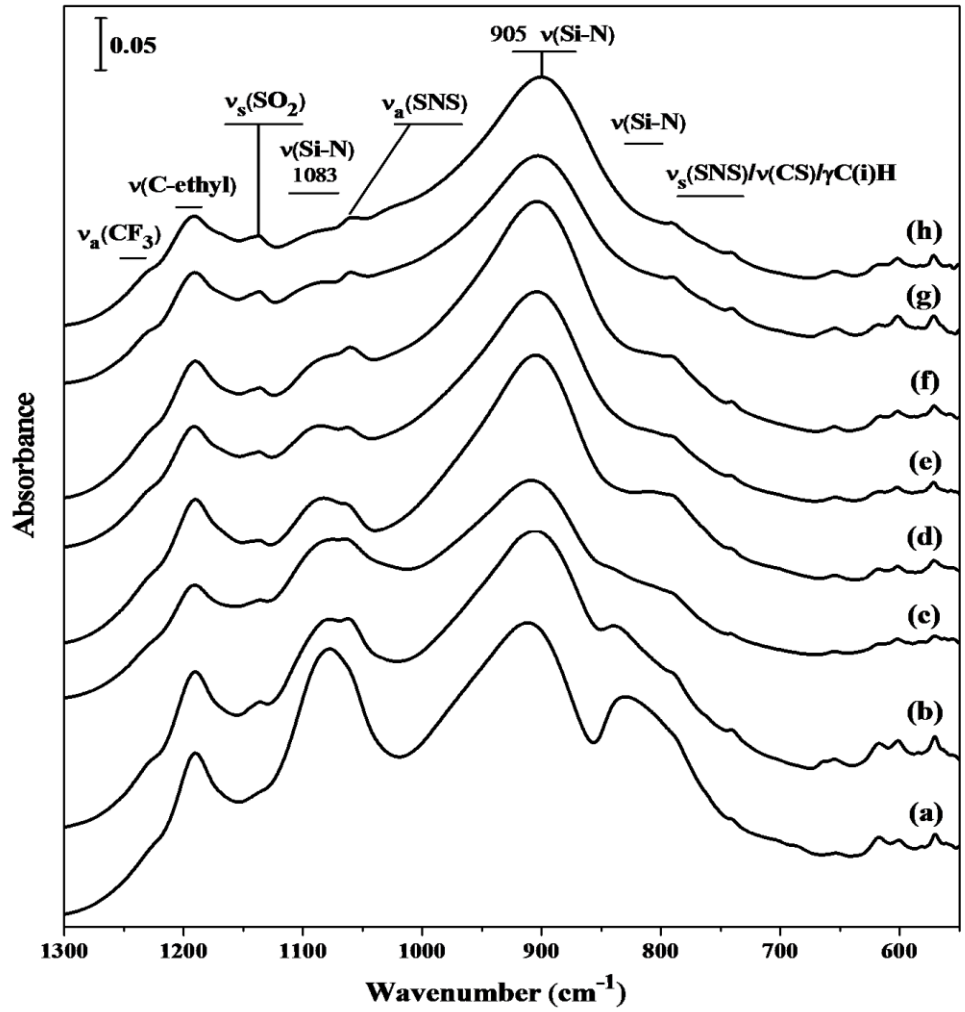

Fig. 1.

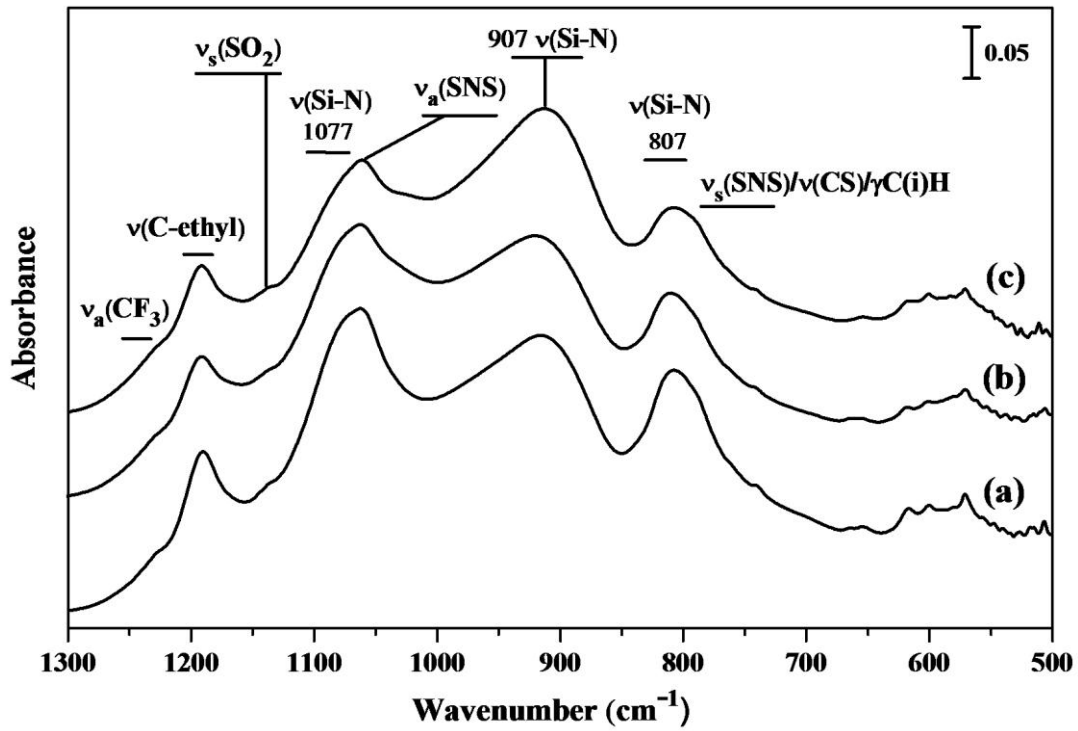
νs(SO2)
907 ν(Si-N)
0.05
ν(Si-N)
1077
νa(SNS)
ν(Si-N)
807
νs(SNS)/ν(CS)/γC(i)H
ν(C-ethyl)
νa(CF3)
(c)
(b)
(a)
Absorbance
1300
1200
1100
1000
900
800
700
600
500
Wavenumber (cm-1)

Fig. 2.

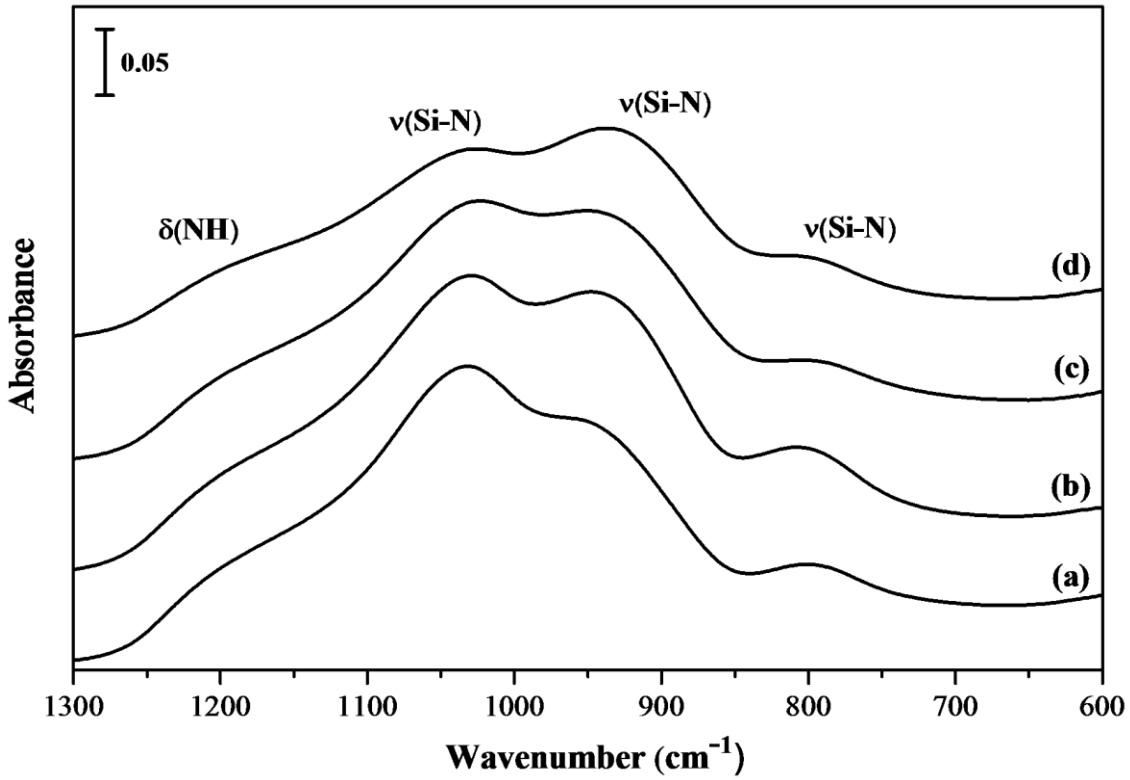
0.05
ν(Si-N)
ν(Si-N)
δ(NH)
ν(Si-N)
(d)
(c)
(b)
(a)
Absorbance
1300
1200
1100
1000
900
800
700
600
Wavenumber (cm-1)

Fig. 3.

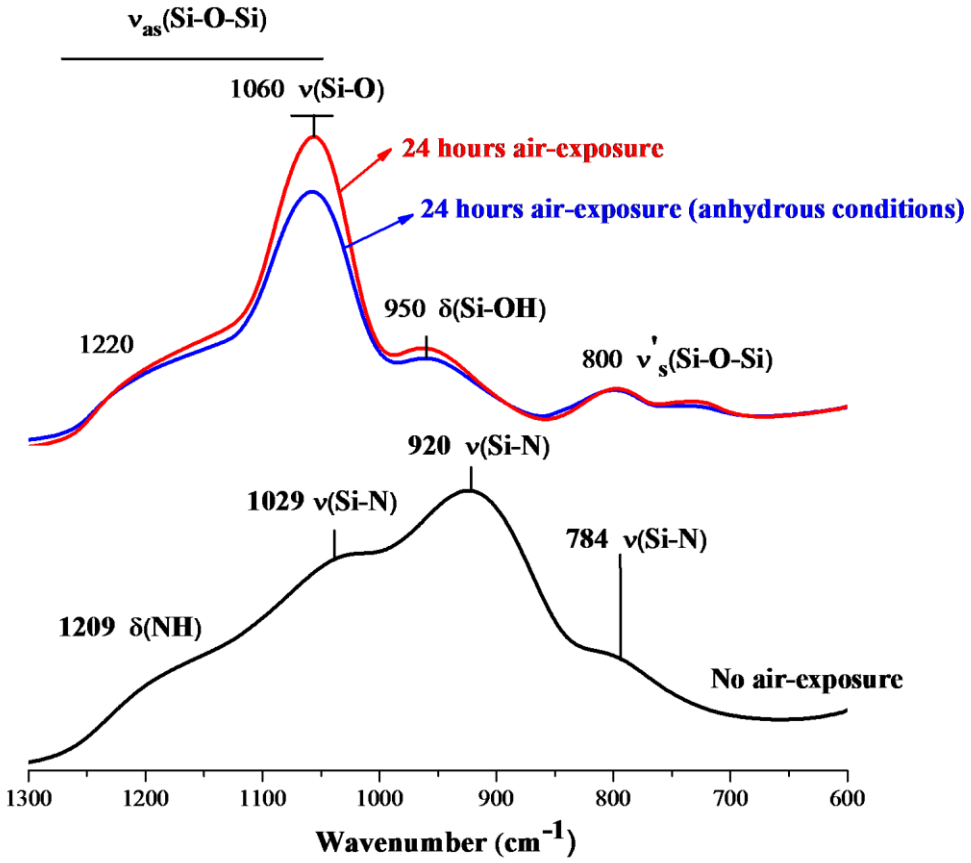
ν_{as}(Si-O-Si)
1060 ν(Si-O)
24 hours air-exposure
24 hours air-exposure (anhydrous conditions)
950 δ(Si-OH)
1220
800 ν'_s(Si-O-Si)
920 ν(Si-N)
1029 ν(Si-N)
784 ν(Si-N)
1209 δ(NH)
No air-exposure
1300
1200
1100
1000
900
800
700
600
Wavenumber (cm^{-1})

Fig. 4.

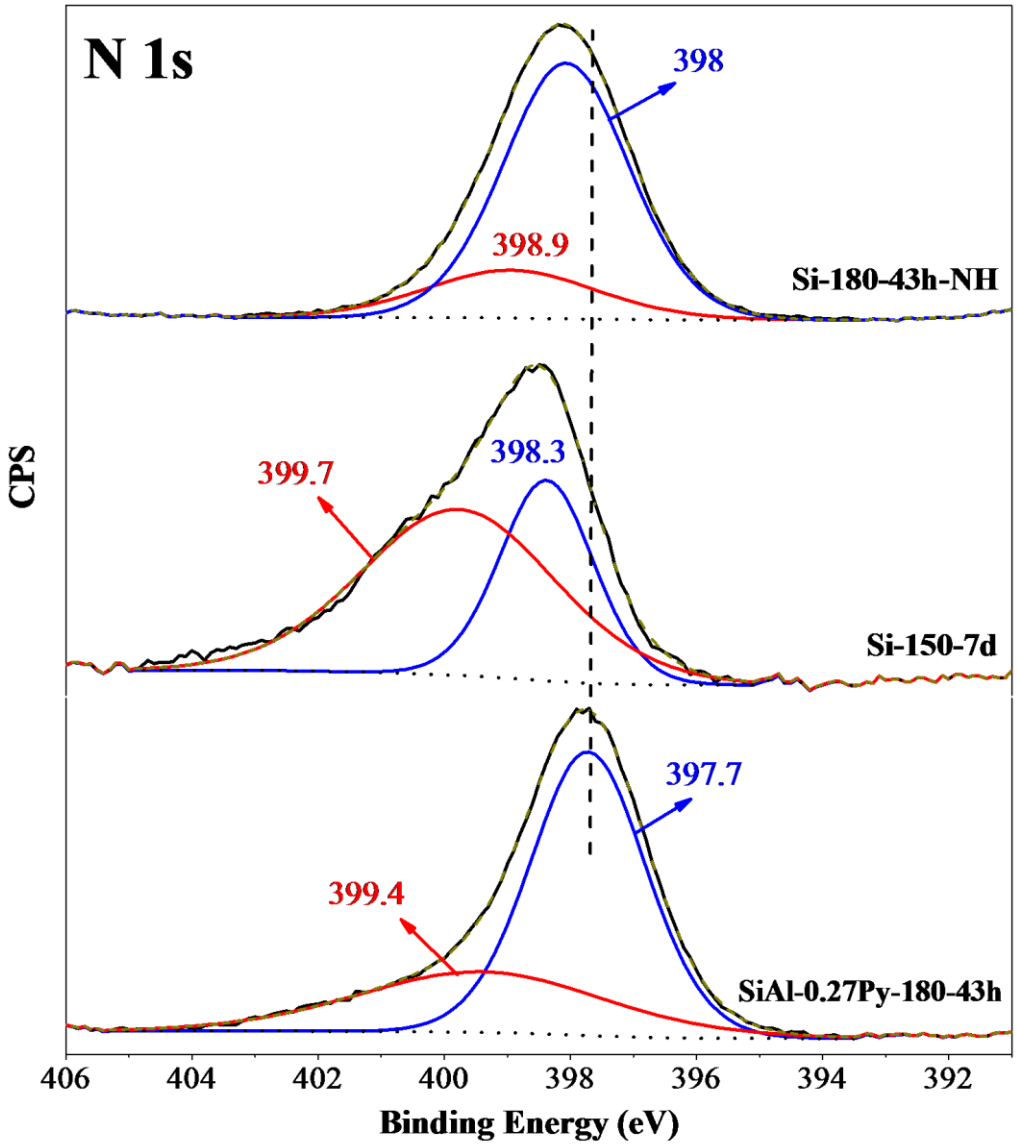
N 1s
398
398.9
Si-180-43h-NH
399.7
398.3
Si-150-7d
397.7
399.4
SiAl-0.27Py-180-43h
CPS
406
404
402
400
398
396
394
392
Binding Energy (eV)

Fig. 5.

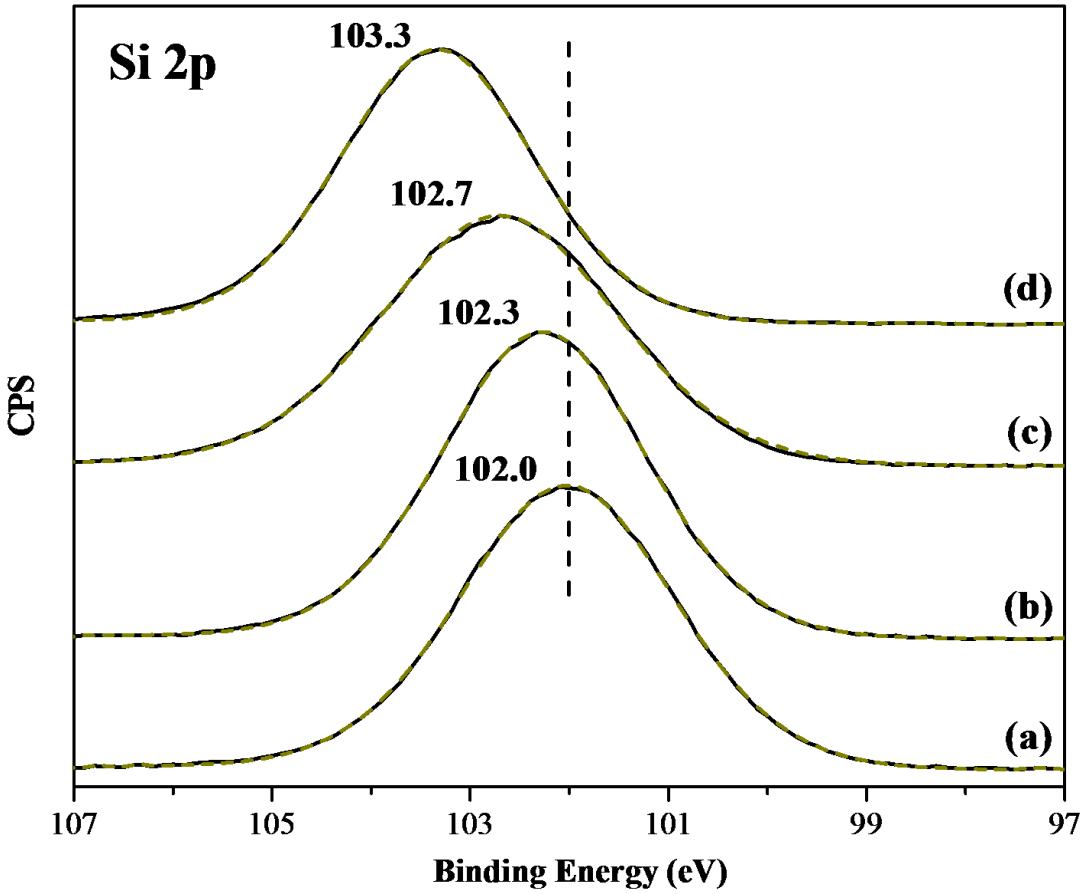
Si 2p
103.3
102.7
102.3
102.0
(d)
(c)
(b)
(a)
CPS
107
105
103
101
99
97
Binding Energy (eV)

Fig. 6.

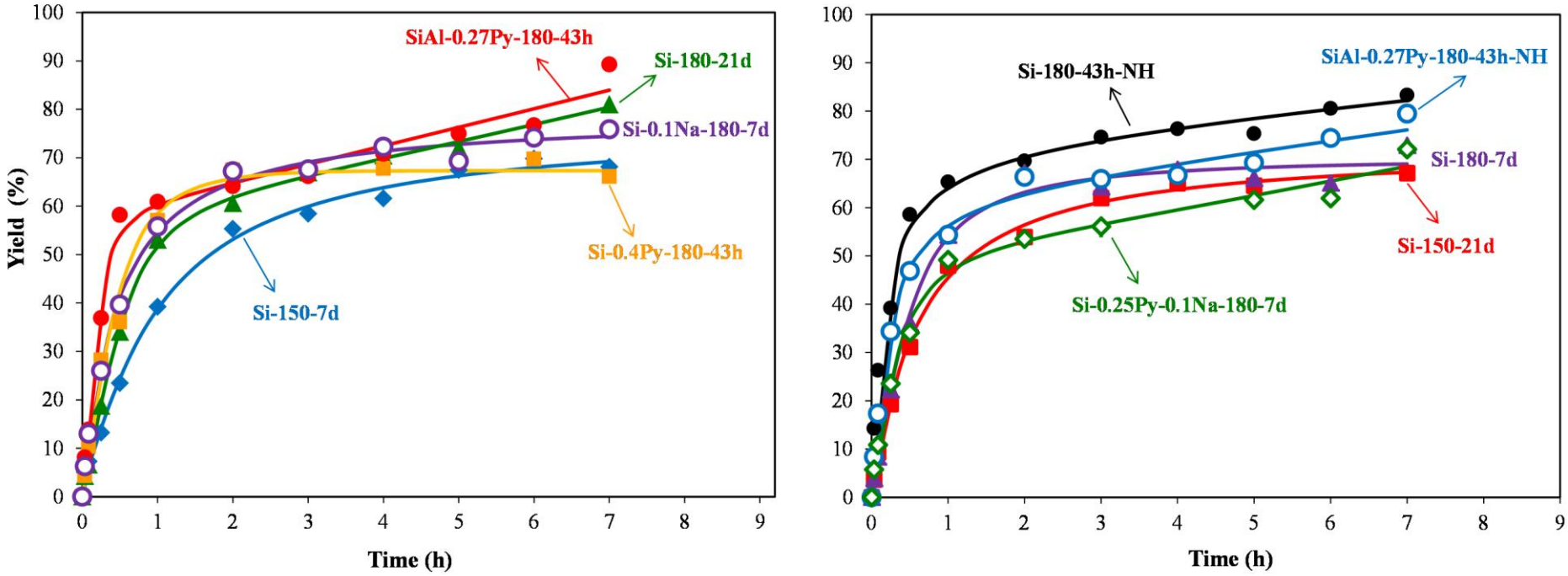
Yield (%)
Time (h)
SiAl-0.27Py-180-43h
Si-180-21d
Si-0.1Na-180-7d
Si-0.4Py-180-43h
Si-150-7d
Si-180-43h-NH
SiAl-0.27Py-180-43h-NH
Si-180-7d
Si-150-21d
Si-0.25Py-0.1Na-180-7d

Fig. 7.

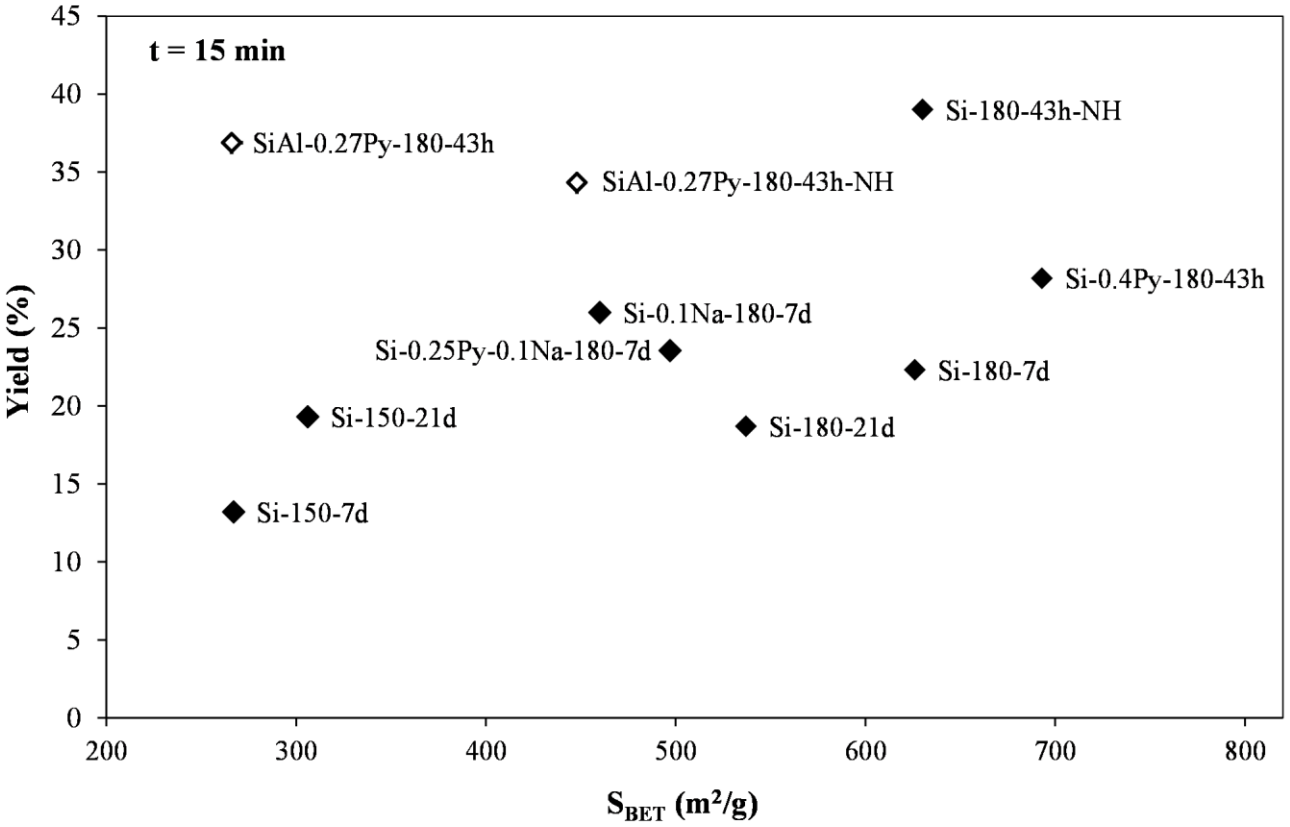
t = 15 min
Si-180-43h-NH
SiAl-0.27Py-180-43h
SiAl-0.27Py-180-43h-NH
Si-0.4Py-180-43h
Si-0.1Na-180-7d
Si-0.25Py-0.1Na-180-7d
Si-180-7d
Si-150-21d
Si-180-21d
Si-150-7d
Yield (%)
S_{BET} (m^2/g)
0
5
10
15
20
25
30
35
40
45
200
300
400
500
600
700
800

Fig. 8.

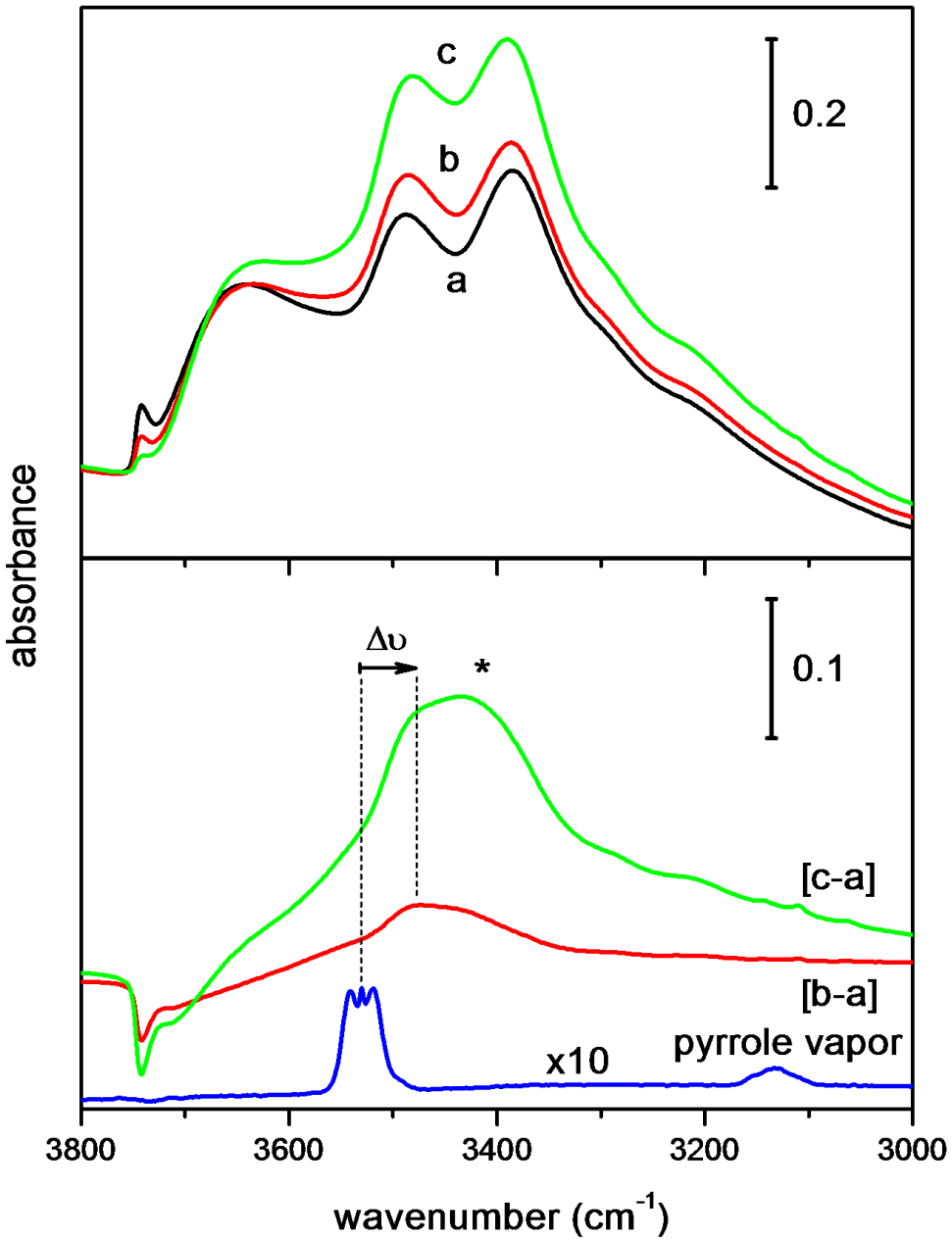
c
b
a
0.2
absorbance
Δυ
*
0.1
[c-a]
[b-a]
pyrrole vapor
x10
3800
3600
3400
3200
3000
wavenumber (cm-1)

Fig 9.

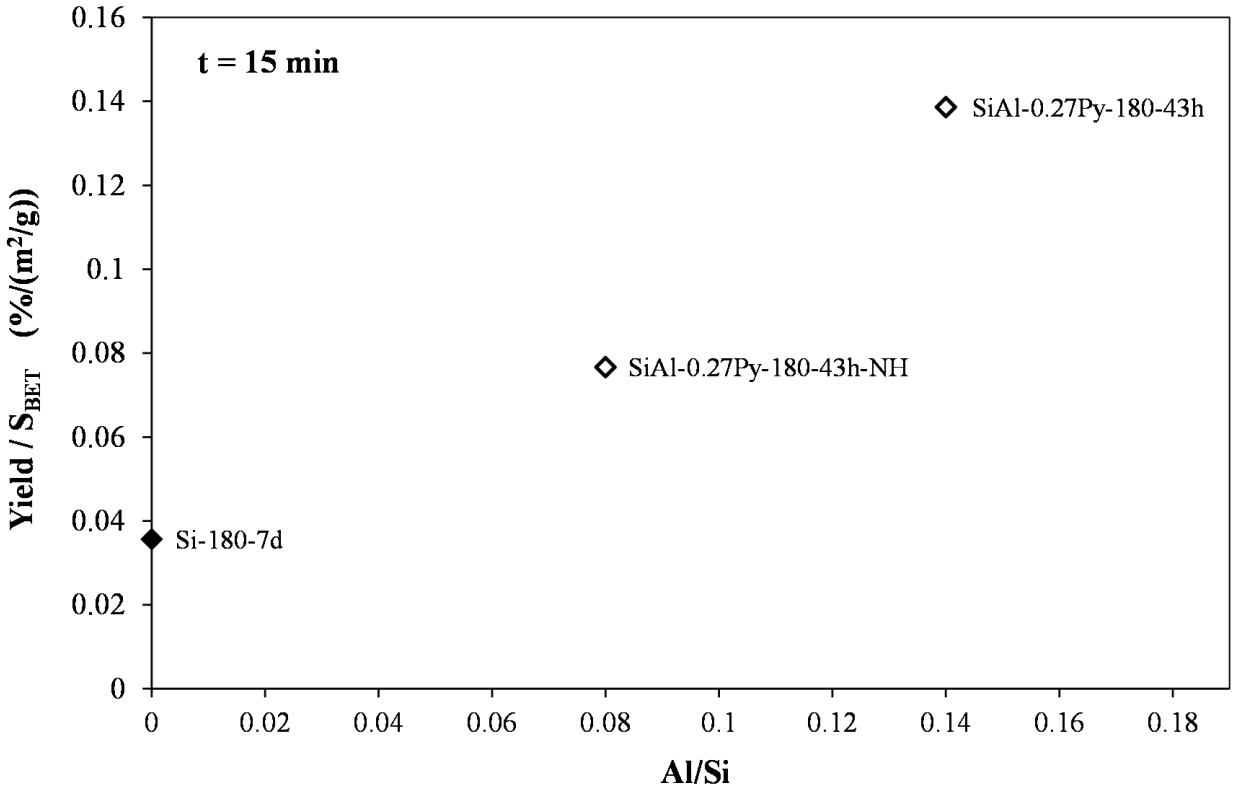
t = 15 min
SiAl-0.27Py-180-43h
SiAl-0.27Py-180-43h-NH
Si-180-7d
Yield / S_{BET} (%/(m²/g))
Al/Si
0.16
0.14
0.12
0.1
0.08
0.06
0.04
0.02
0
0
0.02
0.04
0.06
0.08
0.1
0.12
0.14
0.16
0.18

Fig. 10.

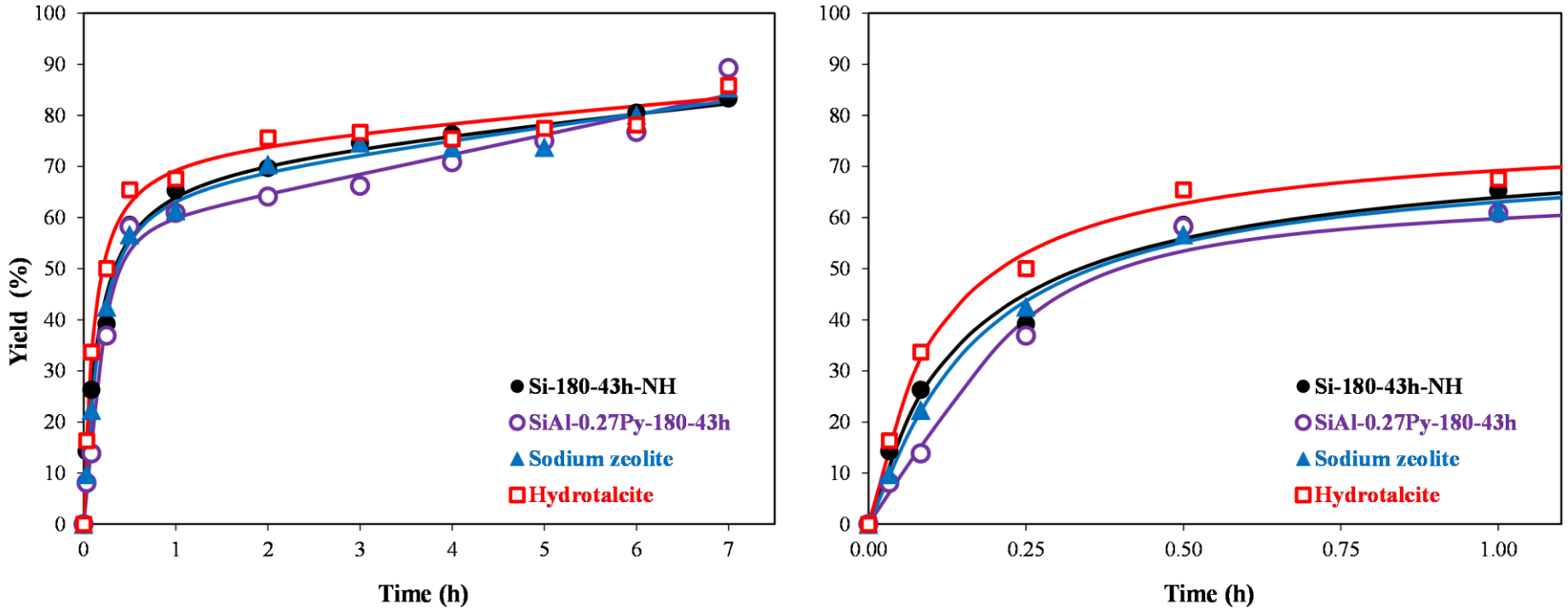
Yield (%)
Time (h)
Si-180-43h-NH
SiAl-0.27Py-180-43h
Sodium zeolite
Hydrotalcite
Time (h)
Si-180-43h-NH
SiAl-0.27Py-180-43h
Sodium zeolite
Hydrotalcite

Fig. 11.

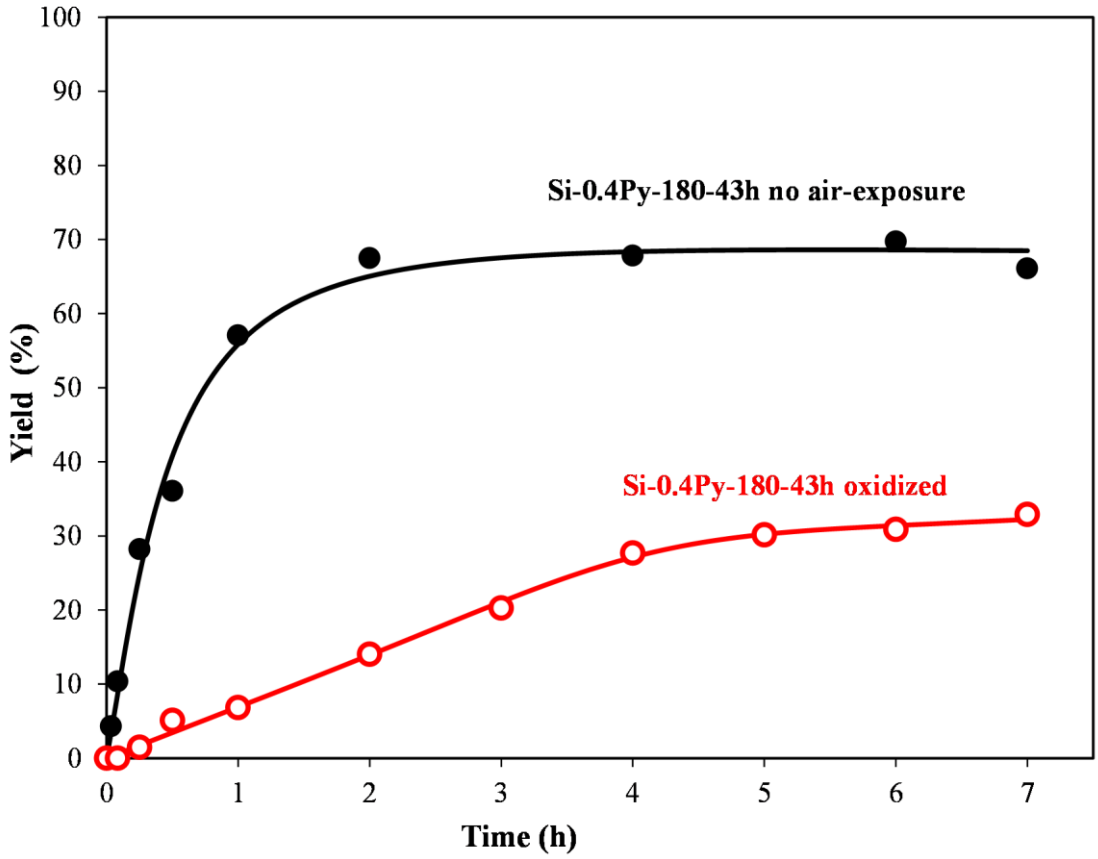
Si-0.4Py-180-43h no air-exposure
Si-0.4Py-180-43h oxidized
Yield (%)
Time (h)
100
90
80
70
60
50
40
30
20
10
0
0
1
2
3
4
5
6
7

Fig. 12.

Supporting Information

Basicity and catalytic activity of porous materials based on a (Si,Al)-N framework

A.I. Saugar [a], C. Márquez-Álvarez [a], I.J. Villar-Garcia [b], T. Welton [b], J. Pérez-Pariente [a]

[a] Instituto de Catálisis y Petroleoquímica, CSIC, C/Marie Curie 2, 28049-Cantoblanco, Spain. [b] Department of Chemistry, Imperial College London, Exhibition Road, South Kensington SW7 2AZ, United Kingdom.

Identification of 2-(3-Oxo-1,3-diphenylpropyl)malononitrile

The identification of the product obtained in the Michael addition reaction was carried out by ^{1}H NMR spectroscopy, using a Bruker Avance III-HD 300 MHz NanoBay equipment operating at 300 MHz.

Figure S1 shows the ^{1}H NMR spectrum of the isolated product of the reaction mixture dissolved in deuterated chloroform. The chemical shifts of the spectrum signals correspond to those reported in literature for the 2-(3-oxo-1,3-diphenylpropyl)malononitrile addition product [1, 2]. ^{1}H-NMR (300 MHz, $CDCl_3$) δ: 7.98-7.95 (m, 2H, ArH), 7.65-7.60 (m, 1H, ArH), 7.54-7.38 (m, 7H, ArH), 4.64 (d, J = 5.1 Hz, 1H, CN-CH), 3.96 (dt, J = 8.1, 5.4 Hz, 1H, Ar-CH), 3.76 – 3.60 (m, 2H, CH_2).

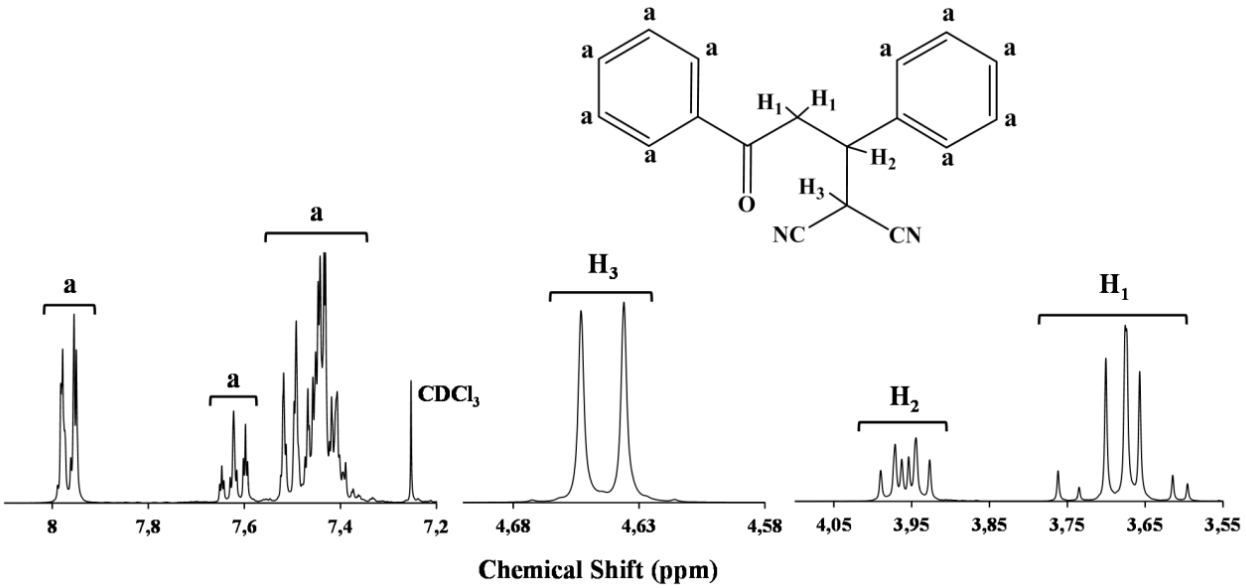

Figure S1. ^{1}H-NMR (300 MHz, $CDCl_3$) spectrum of the product 2-(3-oxo-1,3 diphenylpropyl)malono-nitrile obtained in the Michael addition reaction.

Synthesis of the ionic liquid compounds.

All the gels were prepared by using the ionic liquids 1-ethyl-3-methylimidazolium bis(trifluoromethylsulfonyl)imide ($[C_2C_1im][Tf_2N]$) (Figure S2 (a)) and 1-butyl-1-methylpyrrolidinium bis(trifluoromethylsulfonyl)imide, $[C_4C_1pyrr][Tf_2N]$ (Figure S2 (b)).

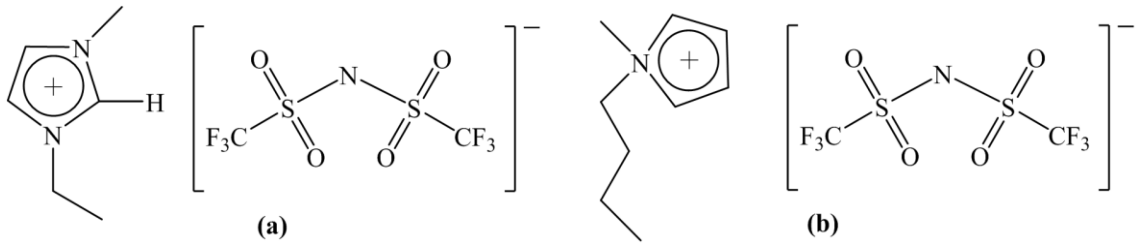

Figure S2. Molecular structure of the ionic liquid (a) 1-ethyl-3-methylimidazolium bis(trifluoromethylsulfonyl)imide ($[C_2C_1im][Tf_2N]$) and (b) 1-butyl-1-methylpyrrolidinium bis(trifluoromethylsulfonyl)imide ($[C_4C_1pyrr][Tf_2N]$).

The ionic liquids 1-ethyl-2,3-dimethylimidazolium bis(trifluoromethylsulfonyl)imide, [Edmim][Tf_2N] and 1-butyl-1-methylpyrrolidinium bis(trifluoromethylsulfonyl)imide, [C_4C_1pyrr][Tf_2N] were synthesized from the corresponding bromide salts. Bromoethane and bromobutane were previously distilled over phosphorous pentoxide and N-methylpyrrolidine was distilled over calcium hydride. All other reagents were purchased from commercial sources and used without further purification.

NMR spectra were recorded on a Bruker AVANCE III 600 MHz equipment operating at 400 MHz for ^{1}H NMR and 100 MHz for ^{13}C NMR at room temperature.

Synthesis of 1-ethyl-2,3-dimethylimidazolium bromide [Edmim][Br].

Into a round bottom flask equipped with a septum, a magnetic stirrer and a reflux condenser, 0.22 mol of 1,3-dimethylimidazole and 75 ml of dry ethyl acetate were placed under nitrogen atmosphere. An excess of 1-bromoethane (0.67 mol) was added drop wise by a dropping funnel with pressure compensation. The reaction mixture was vigorously stirred and heated at 35 °C for 20 h. The mixture was allowed to cool to room temperature and the resulting residue was filtered and dried under vacuum. The recrystallization of the residue was done by solving the compound in a small quantity of acetonitrile and by adding a small amount of ethyl acetate to the solution. This solution was cooled in a freezer, and white crystals of the ionic liquid were formed. After filtration, the remaining solvent was removed by evaporation on a rotavap under reduced pressure giving the 1-ethyl-2,3-dimethylimidazolium bromide as white crystals. ^{1}H-NMR (400 MHz, $CDCl_3$) δ: 7.42 (d, 1H), 7.37 (d, 1H), 3.98 (q, 2H), 3.65 (s, 3H), 2.47 (s, 3H), 1.17 (t, 3H). ^{13}C-NMR (100 MHz, $CDCl_3$) δ: 143.1, 122.7, 120.5, 43.8, 35.8, 15.1, 10.6.

Synthesis of 1-ethyl-2,3-dimethylimidazolium bis(trifluoromethylsulfonyl)imide [Edmim][Tf_2N].

Into a round bottom flask cooled in a water bath, 31.6 mmol of 1-ethyl-2,3-dimethylimidazolium bromide were dissolved in water (30 ml). A solution of $LiNTf_2$ (37.9 mmol) in water (100 ml) was added drop wise by a dropping funnel with pressure compensation to the vigorously stirred mixture. After the reaction mixture had been stirred for 48 h, the mixture was extracted with dicloromethane. The organic phase was washed with water (2 × 30 ml) and the solvent was removed by evaporation on a rotavap under reduced pressure. The resulting residue was dried under vacuum giving the 1-ethyl-2,3-dimethylimidazolium bis(trifluoromethylsulfonyl)imide. The corresponding ^{1}H-NMR spectrum is shown in Figure S3. ^{1}H-NMR (400 MHz, $(CD_3)_2SO$) δ: 7.66 (d, 1H), 7.62 (d, 1H), 4.15 (q, 2H), 3.75 (s, 3H), 2.59 (s, 3H), 1.35 (t, 3H). ^{13}C-NMR (100 MHz, $(CD_3)_2SO$) δ: 143.3, 121.5, 119.3, 119.1 (q, J = 320.7 Hz), 42.6, 33.6, 13.3, 7.79.

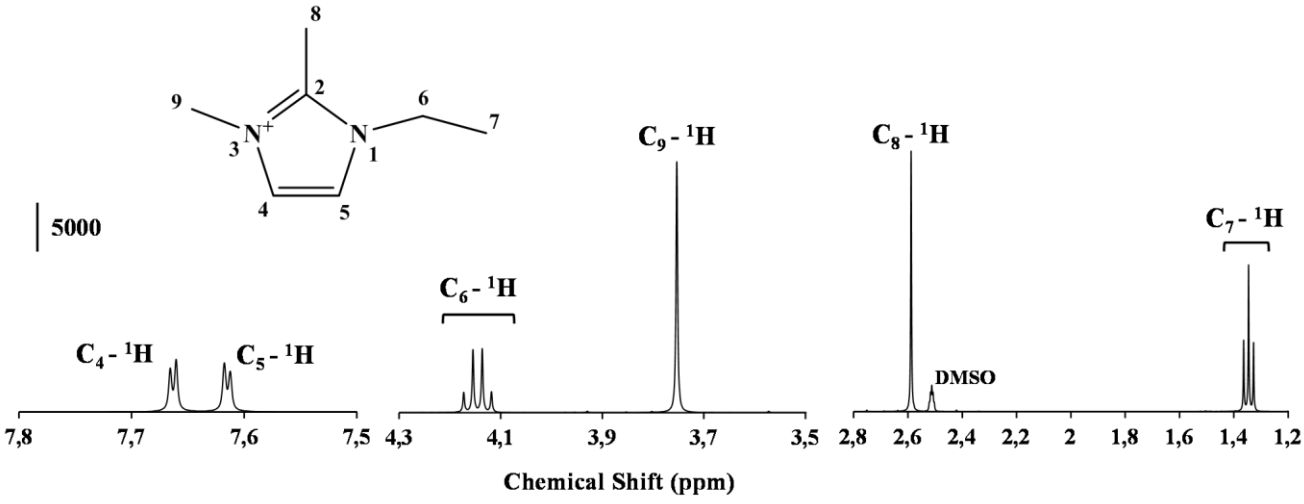

Figure S3. ^{1}H-NMR (400 MHz, $(CD_3)_2SO$) spectrum of the 1-ethyl-2,3-dimethylimidazolium cation $[Edmim]^+$.

Synthesis of 1-butyl-1-methylpyrrolidinium bromide [C_4C_1pyrr][Br].

Into a round bottom flask equipped with a septum, a magnetic stirrer and a reflux condenser, 0.22 mol of N-methylpyrrolidine and 75 ml of dry ethyl acetate were placed under nitrogen atmosphere. An excess of 1-bromobutane (0.67 mol) was added drop wise by a dropping funnel with pressure compensation. The reaction mixture was vigorously stirred and heated at 45 °C for 20 h. The mixture was allowed to cool to room temperature and the resulting residue was filtered and dried under vacuum. The residue was purified by recrystallization, using the same procedure as described for *[Edmim][Br]*, giving the 1-butyl-1-methylpyrrolidinium bromide. ^{1}H-NMR (400 MHz, $(CD_3)_2SO$ capillary) δ: 0.38 (t, 3H), 0.80 (sxt, 2H), 1.16-1.22 (m, 2H), 1.57-1.68 (m, 4H), 2.59 (s, 3H), 2.93-2.98 (m, 2H), 3.03-3.11 (m, 4H). ^{13}C-NMR (100 MHz, $(CD_3)_2SO$ capillary) δ:62.32, 62.58, 46.73, 23.90, 19.99, 17.98, 11.31.

Synthesis of 1-butyl-1-methylpyrrolidinium bis(trifluoromethylsulfonyl)imide [C_4C_1pyrr][Tf_2N].

Into a round bottom flask cooled in a water bath, 33 mmol of 1-butyl-1-methylpyrrolidinium bromide were dissolved in water. A solution of $LiNTf_2$ (39.5 mmol) in water (100 ml) was added drop wise by a dropping funnel with pressure compensation to the vigorously stirred mixture. After the reaction mixture had been stirred for 48 h, the mixture was extracted with dicloromethane. The organic phase was washed with water (2 × 30 ml) and the solvent was removed by evaporation on a rotavap under reduced pressure. The resulting residue was dried under vacuum giving the 1-butyl-1-methylpyrrolidinium bis(trifluoromethylsulfonyl)imide. The corresponding ^{1}H-NMR spectrum it is shown in Figure S5 a). ^{1}H-NMR (400 MHz,

$(CD_3)_2SO$) δ: 3.55-3.35 (m, 4H), 3.35-3.25 (m, 2H), 2.98 (s, 3H), 2.19-2.00 (m, 4H), 1.79-1.61 (m, 2H), 1.33 (sxt, 2H), 0.94 (t, 3H). ^{13}C-NMR (100 MHz, $(CD_3)_2SO$) δ: 119.9 (q, J = 321.8 Hz), 63.8, 63.4, 47.9, 25.37, 21.51, 19.73, 13.82.

Study of the chemical stability of the ionic liquids under basic conditions

The chemical stability of the ionic liquids [Edmim][Tf_2N] and [C_4C_1pyrr][Tf_2N] was studied by using the previously synthesized ionic liquids compounds. Sodium amide was purchased from Sigma-Aldrich as a toluene suspension which was previously filtered via cannula filtration giving a white powder.

Chemical stability of [Edmim][Tf_2N]

I Into a round bottom flask equipped with a septum, a magnetic stirrer and a thermometer, 1.44 mmol of [Edmim][Tf_2N] and an excess of sodium amide (2.88 mmol) were placed under nitrogen atmosphere. After the reaction mixture was stirred for 10 minutes at room temperature, a small aliquot was withdrawn using a syringe and dissolved in deuterated dimethylsulfoxide. The corresponding ^{1}H-NMR spectrum is shown in Figure S4 b).

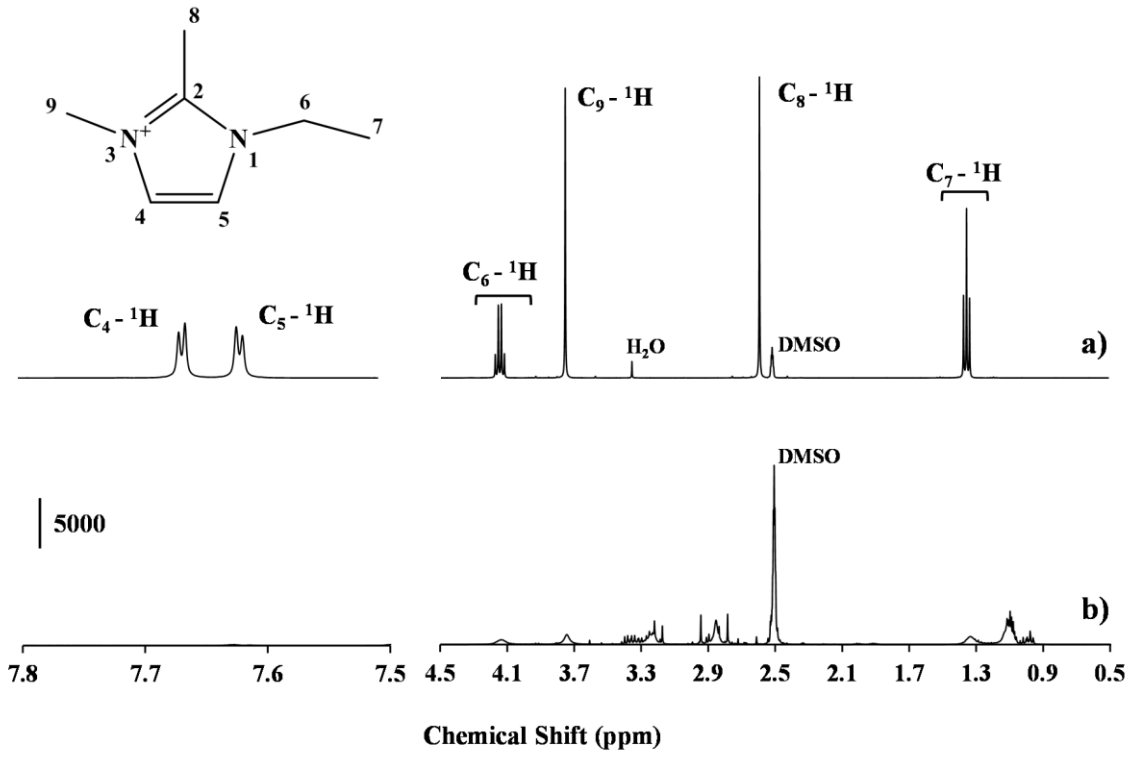

Figure S4. ^{1}H-NMR (400 MHz, $(CD_3)_2SO$) spectrum of a) the 1-ethyl-2,3-dimethylimidazolium cation $[Edmim]^+$ and b) the mixture obtained after stirring the ionic liquid $[Edmim][Tf_2N]$ at room temperature during 10 minutes in the presence of an excess of sodium amide ($NaNH_2$/$[Edmim][Tf_2N]$ molar ratio of 2).

Chemical stability of $[C_4C_1pyrr][Tf_2N]$.

Using the same experimental set up as described for the chemical stability study of $[Edmim][Tf_2N]$, 1.44 mmol of $[C_4C_1pyrr][Tf_2N]$ and an excess of sodium amide (2.88 mmol) were heated at 180 ºC under vigorous stirring for 1 hour. A small aliquot of the reaction mixture was withdrawn using a syringe and dissolved in deuterated dimethylsulfoxide. The corresponding ^{1}H-NMR spectrum it is shown in Figure S5 b).

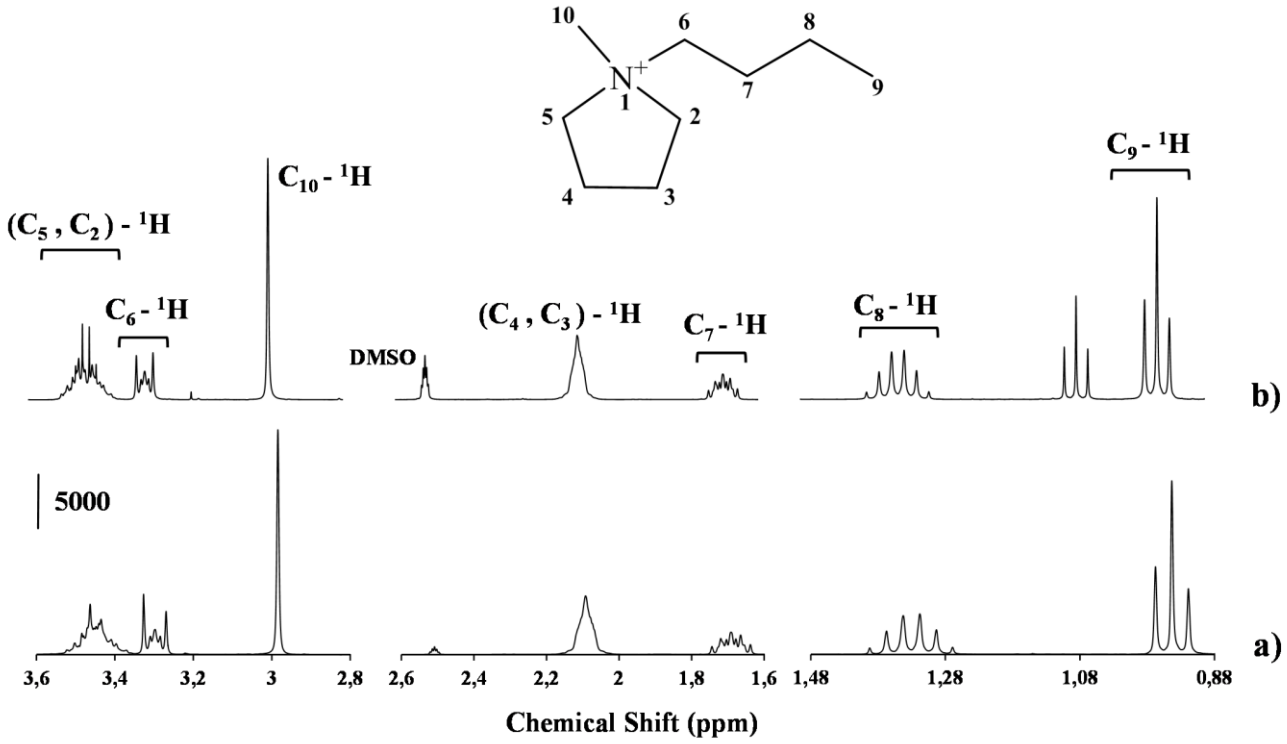

Figure S5. ^{1}H-NMR (400 MHz, $(CD_3)_2SO$) spectrum of a) the 1-butyl-1-methylpyrrolidinium cation $[C_4C_1pyrr]^+$ and b) the mixture obtaining after heating the ionic liquid $[C_4C_1pyrr][Tf_2N]$ at 180 ºC under vigorous stirring for 1 hour in the presence of an excess of sodium amide ($NaNH_2$/$[C_4C_1pyrr][Tf_2N]$) molar ratio of 2).

Thermogravimetric analyses of the as-prepared samples

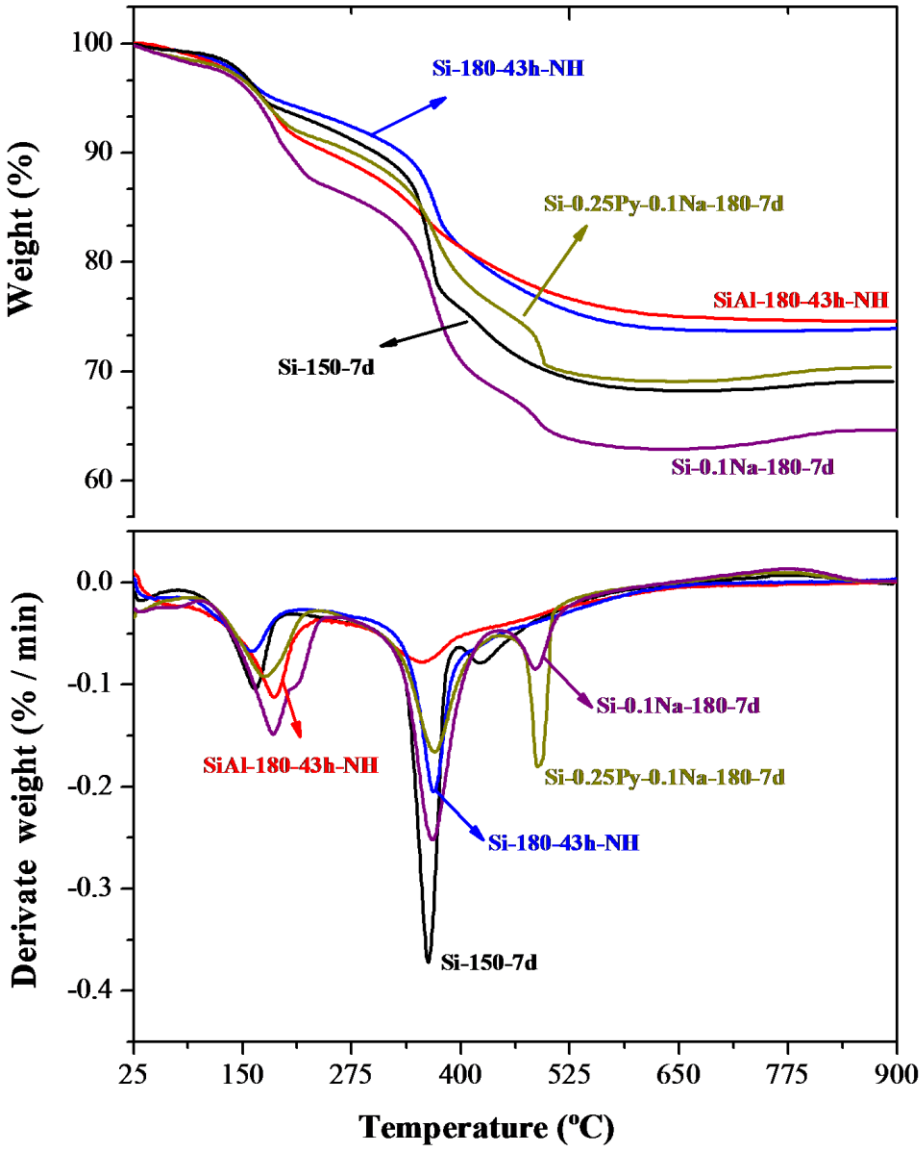

Figure S6. Thermogravimetry plots (top) and derivative of the TG curves (bottom) of some selected as-prepared samples.

Nitrogen adsorption-desorption measurements.

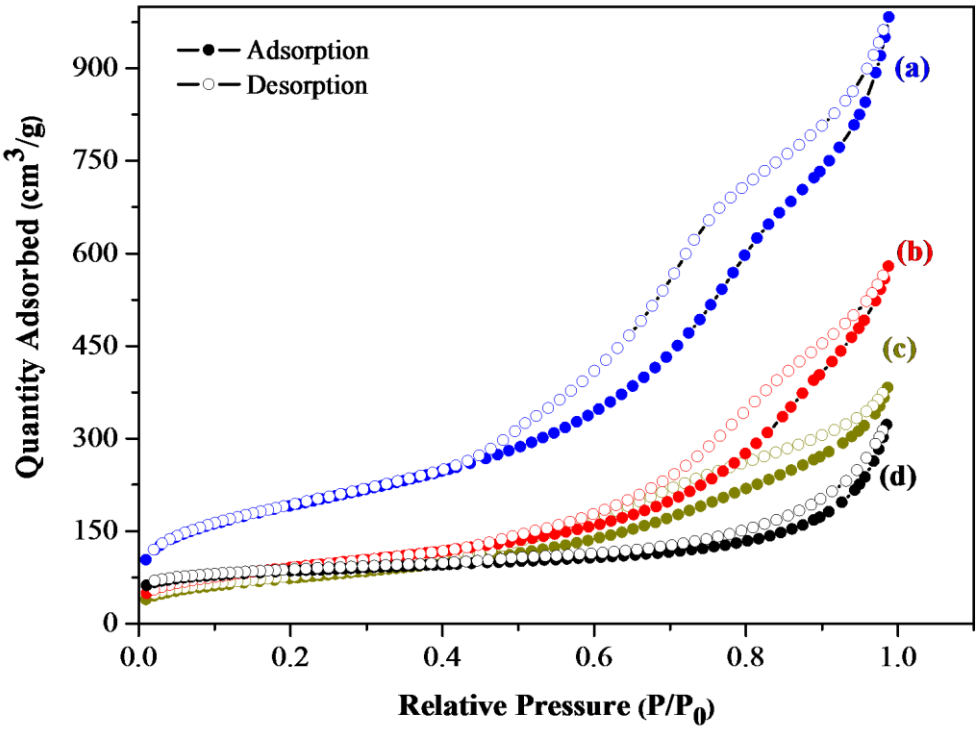

Figure S7. Nitrogen adsorption/desorption isotherms at 77 K of the high surface area materials obtained after the heat treatment under flowing ammonia; (a) Si-0.4Py-180-43h, (b) SiAl-180-43h-NH, (c) SiAl-0.27Py-180-43h and (d) Si-150-21d.

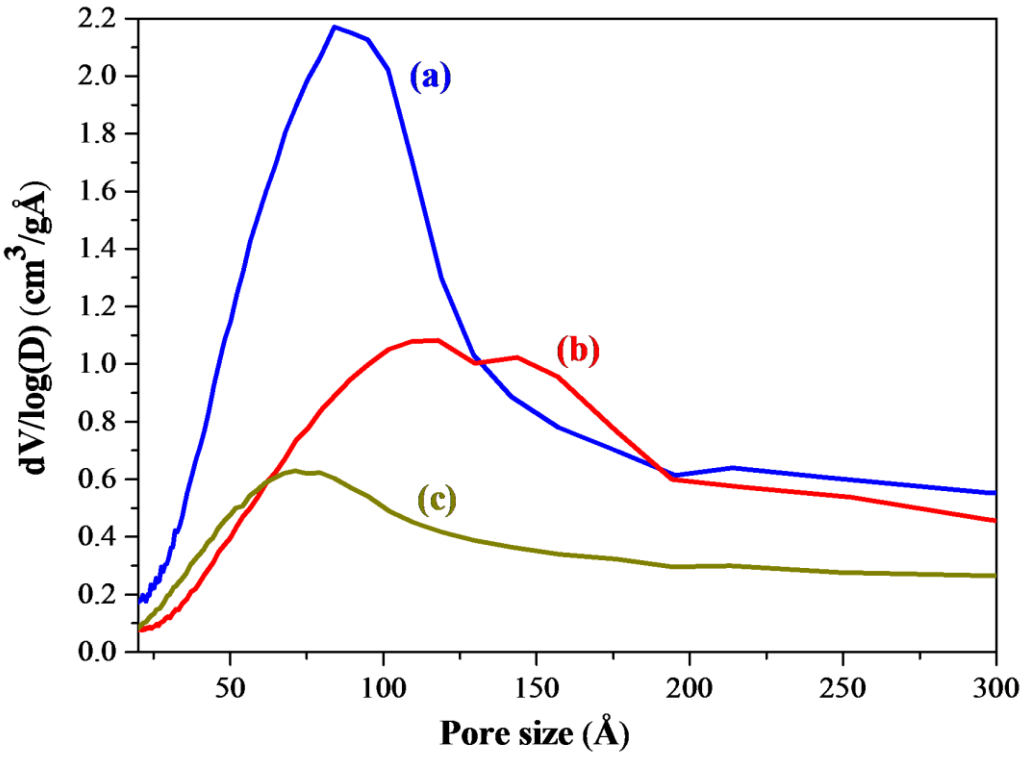

Figure S8. Pore size distribution of the ammonia heat-treated samples; (a) Si-0.4Py-180-43h, (b) SiAl-180-43h-NH and (c) SiAl-0.27Py-180-43h.

Al 2p XPS spectra

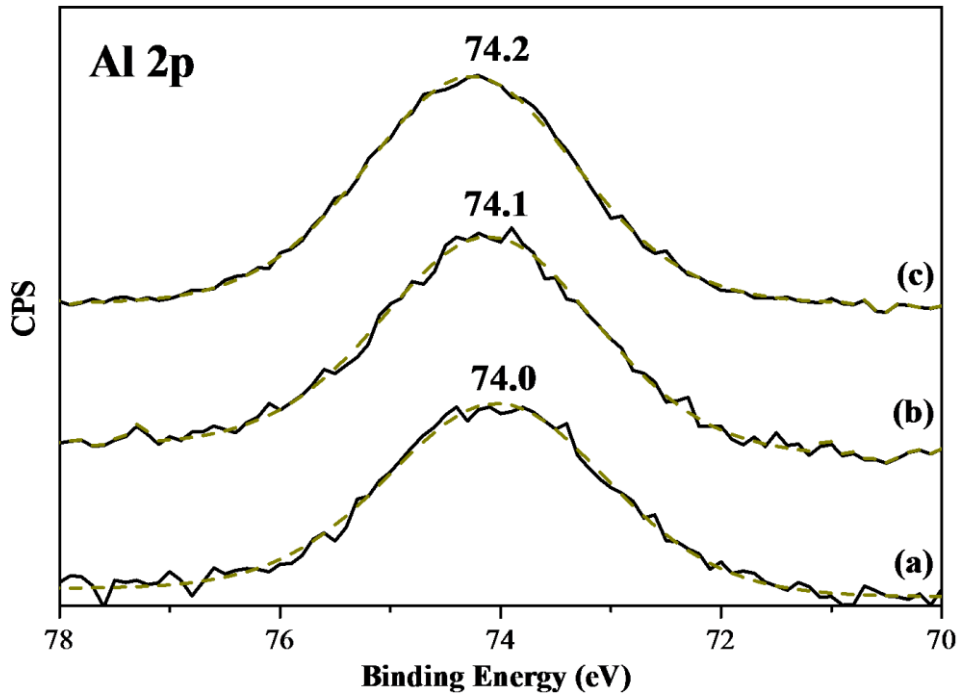

Figure S9. Al 2p XPS spectra of the ammonia heat-treated samples; (a) SiAl-180-43h-NH, (b) SiAl-0.27Py-180-43h-NH and (c) SiAl-0.27Py-180-43h

Catatytic activity

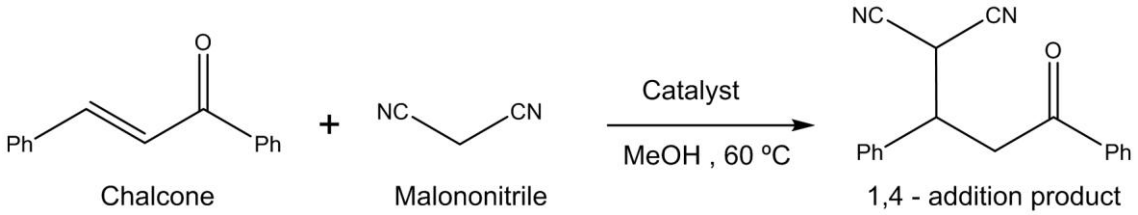

Scheme 1. Michael addition reaction between chalcone and malononitrile.

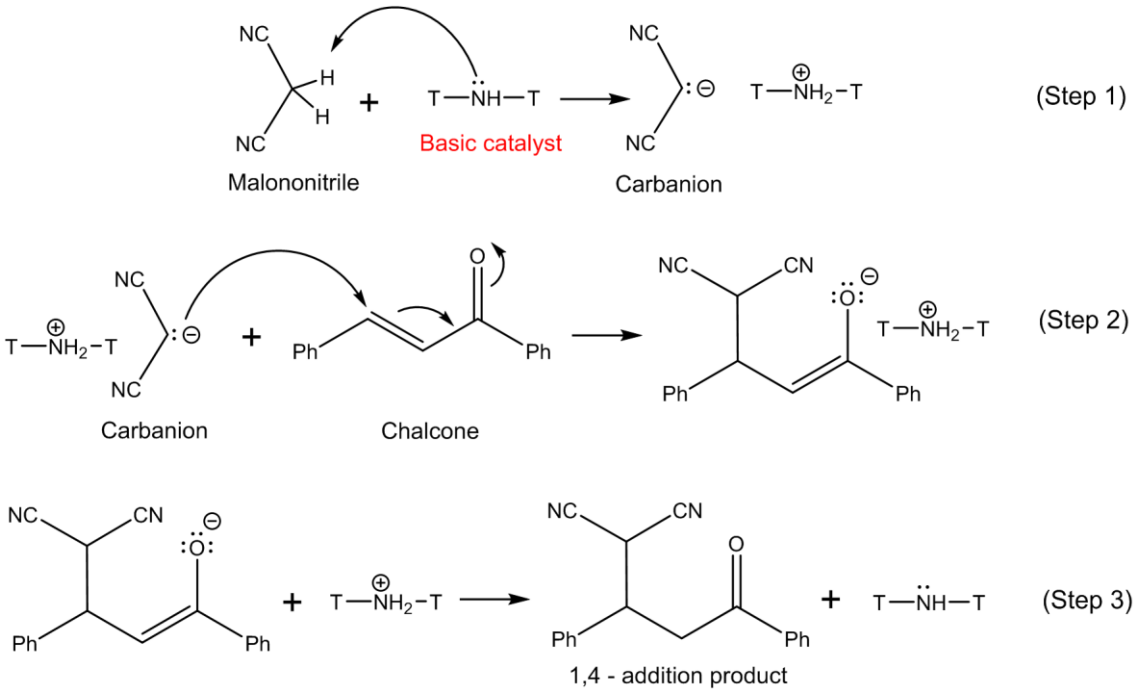

Scheme 2. Michael addition reaction mechanistic.

Table 1. Influence of solvent on the catalytic activity of sample SiAl-180-43h-NH for the Michael addition reaction between chalcone and malononitrile.

Solvent	*Dielectric constant (ε)*	*T^a / ºC*	*Catalyst/Chalcone (weight ratio)*	*Yield[b] (%)*
Methanol	32.7	60	0.08	98
CH_2Cl_2	8.93	35	0.16	0
THF	7.58	60	0.16	0
$CHCl_3$	5.62	60	0.16	0

[a] Reaction temperature.

[b] Reaction conditions: Chalcone/malononitrile molar ratio: 1, chalcone/solvent weight ratio: 0.05, reaction time: 7 h.

Determination of the basicity by FTIR of adsorbed pyrrole.

The relative strength of basic sites has been determined by measuring the shift of the NH stretching mode of adsorbed pyrrole respect to the molecule in the vapor phase [3].

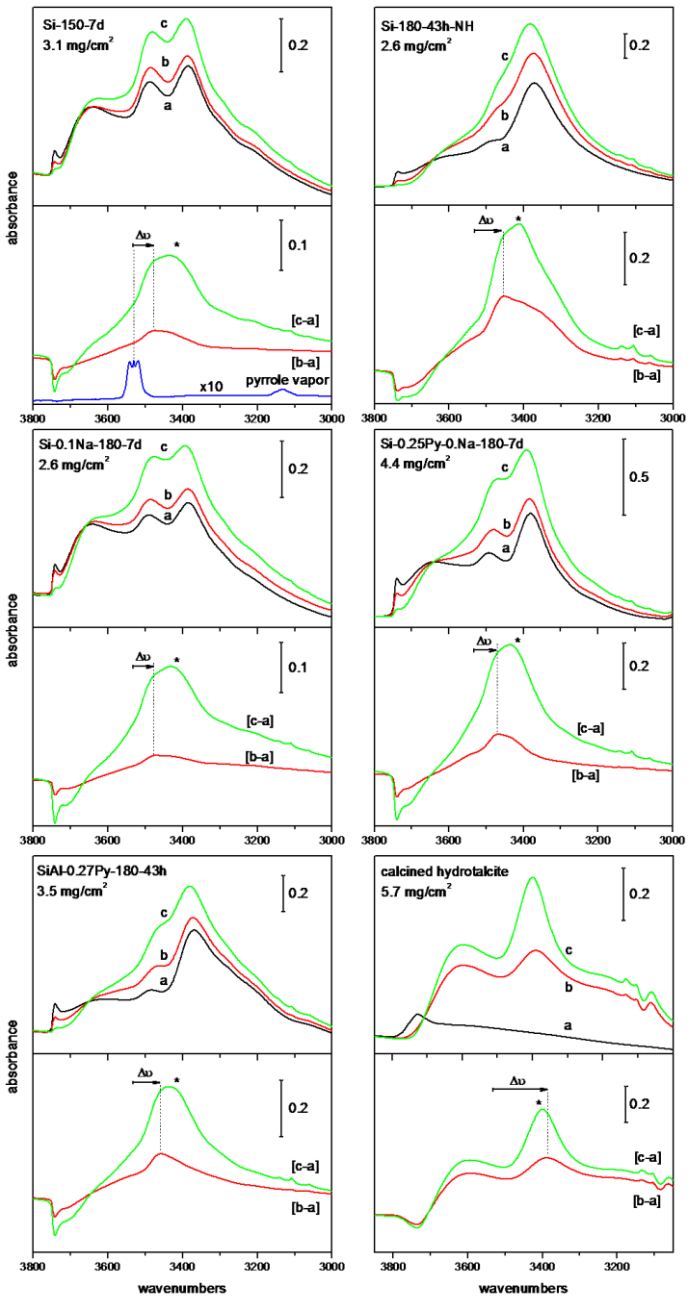

Figure S10. FTIR spectra of Si(Al)-N samples and a calcined Al-Mg hydrotalcite after degassing at 150°C (a) and in contact with pyrrole vapor at 25ºC and equilibrium

pressure of ca. 1 mbar (b) and ca. 10 mbar (c). Difference spectra c-a and b-a are shown to facilitate determination of the shift of the NH stretching band of pyrrole. The spectrum of pyrrole vapor (6 mbar) is also shown for reference (NH stretching band centered at 3530 cm^{-1}). Arrows indicate the shifts of the ν(NH) band of pyrrole due to H-bonding with basic sites. At high equilibrium pressure, the 3410 cm^{-1} band (marked with an asterisk) corresponding to physisorbed pyrrole [3] becomes dominant.

References

[1] W. Yang, Y. Jia, D.-M. Du, Organic & Biomolecular Chemistry. 10 (2012) 332-338.

[2] X. Li, L. Cun, C. Lian, L. Zhong, Y. Chen, J. Liao, J. Zhu, J. Deng, Organic & Biomolecular Chemistry. 6 (2008) 349-353.

[3] B. Camarota, Y. Goto, S. Inagaki, B. Onida, Langmuir. 27 (2011) 1181-1185.

fig_1.tif

Click here to download high resolution image

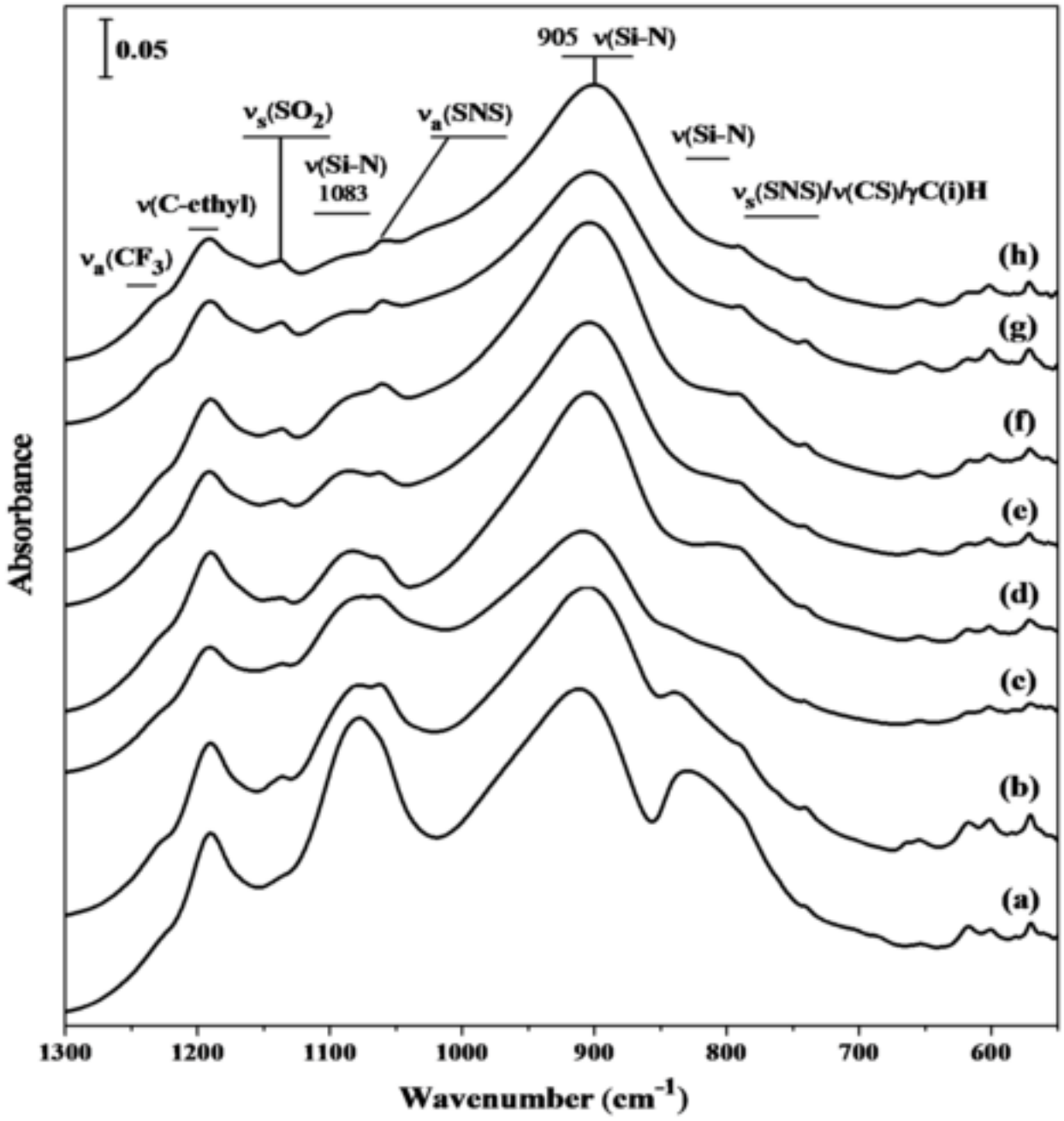

fig_2.tif

Click here to download high resolution image

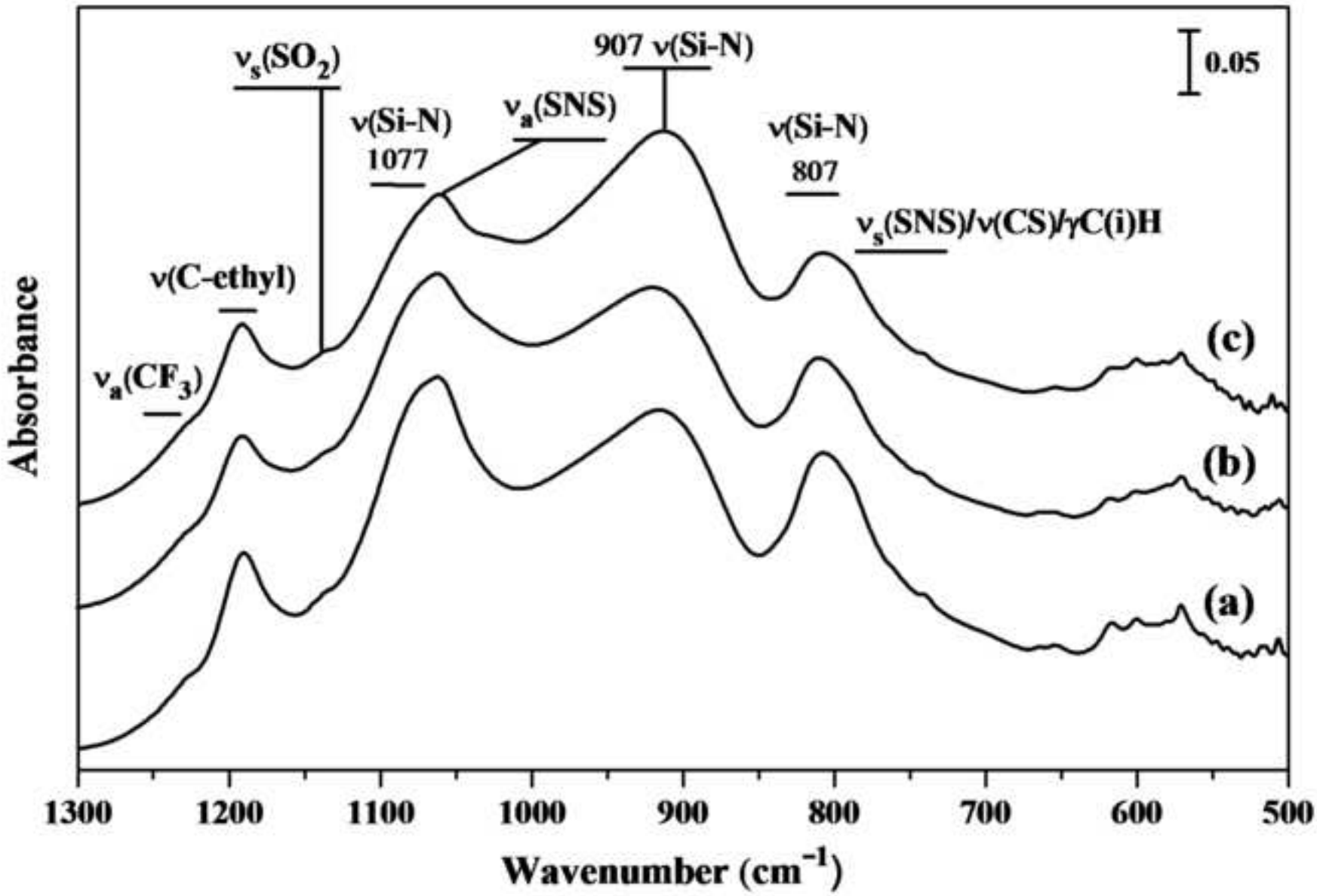

fig_3.tif
Click here to download high resolution image

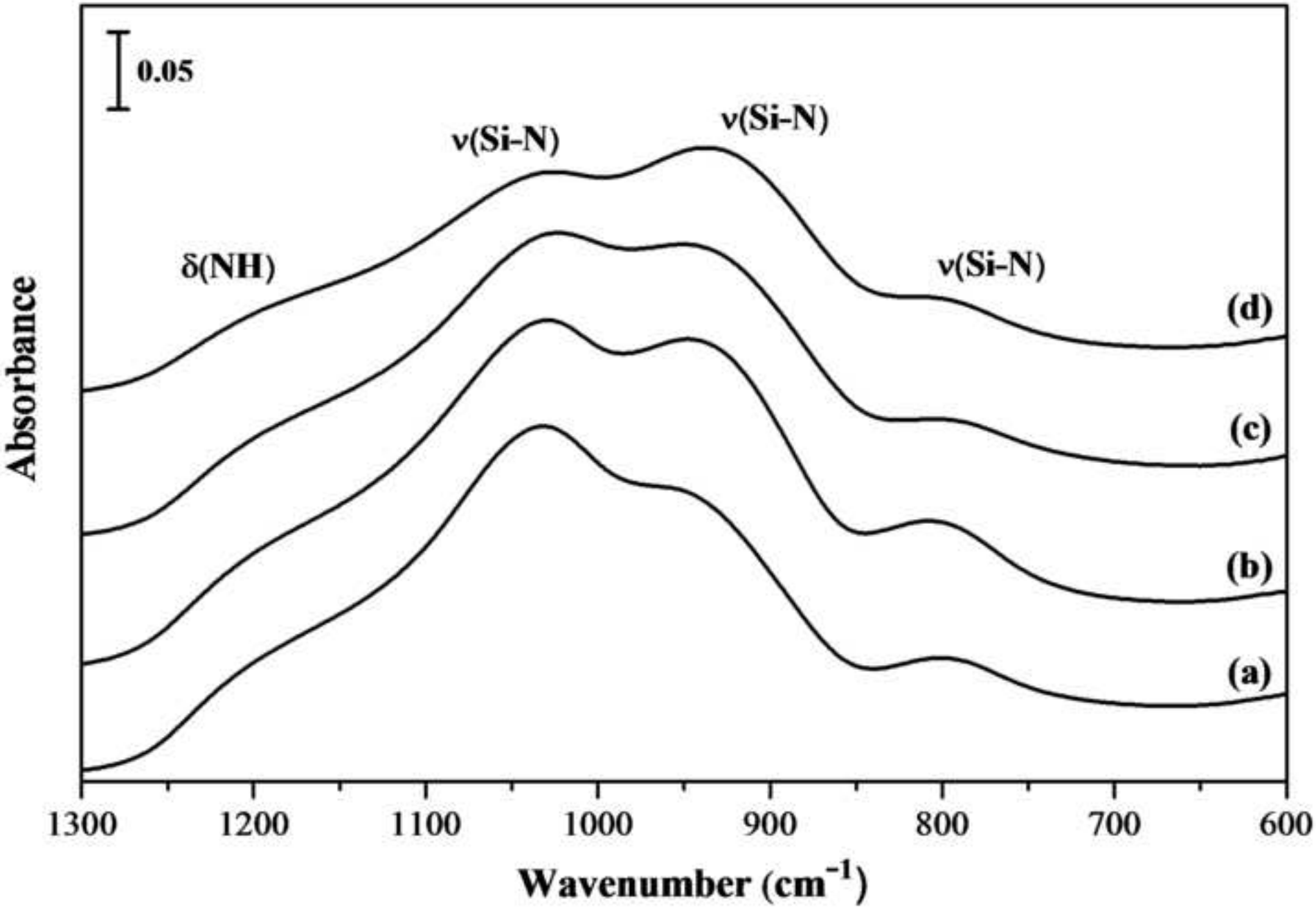

fig_4.tif
Click here to download high resolution image

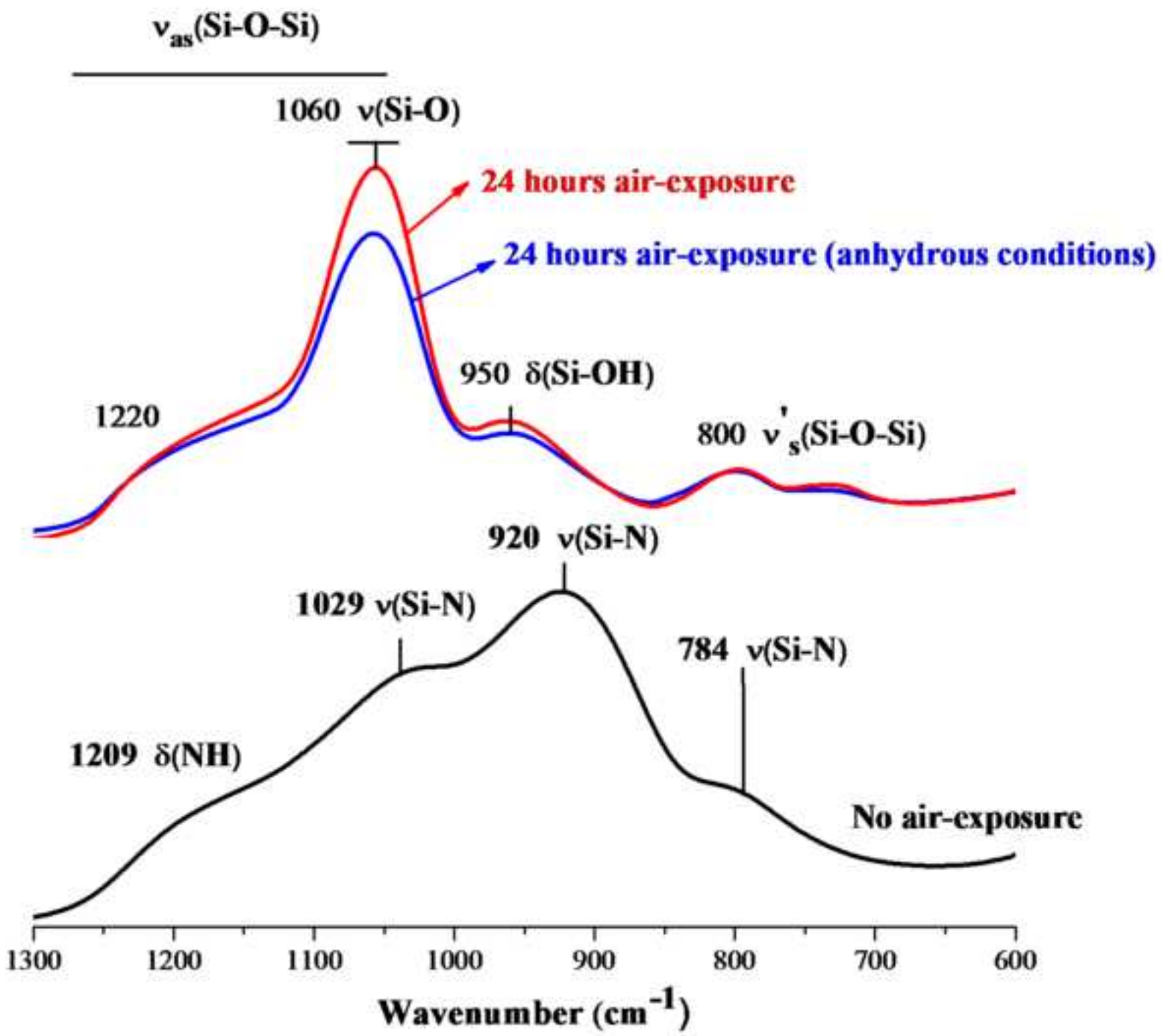

fig_5.tif
Click here to download high resolution image

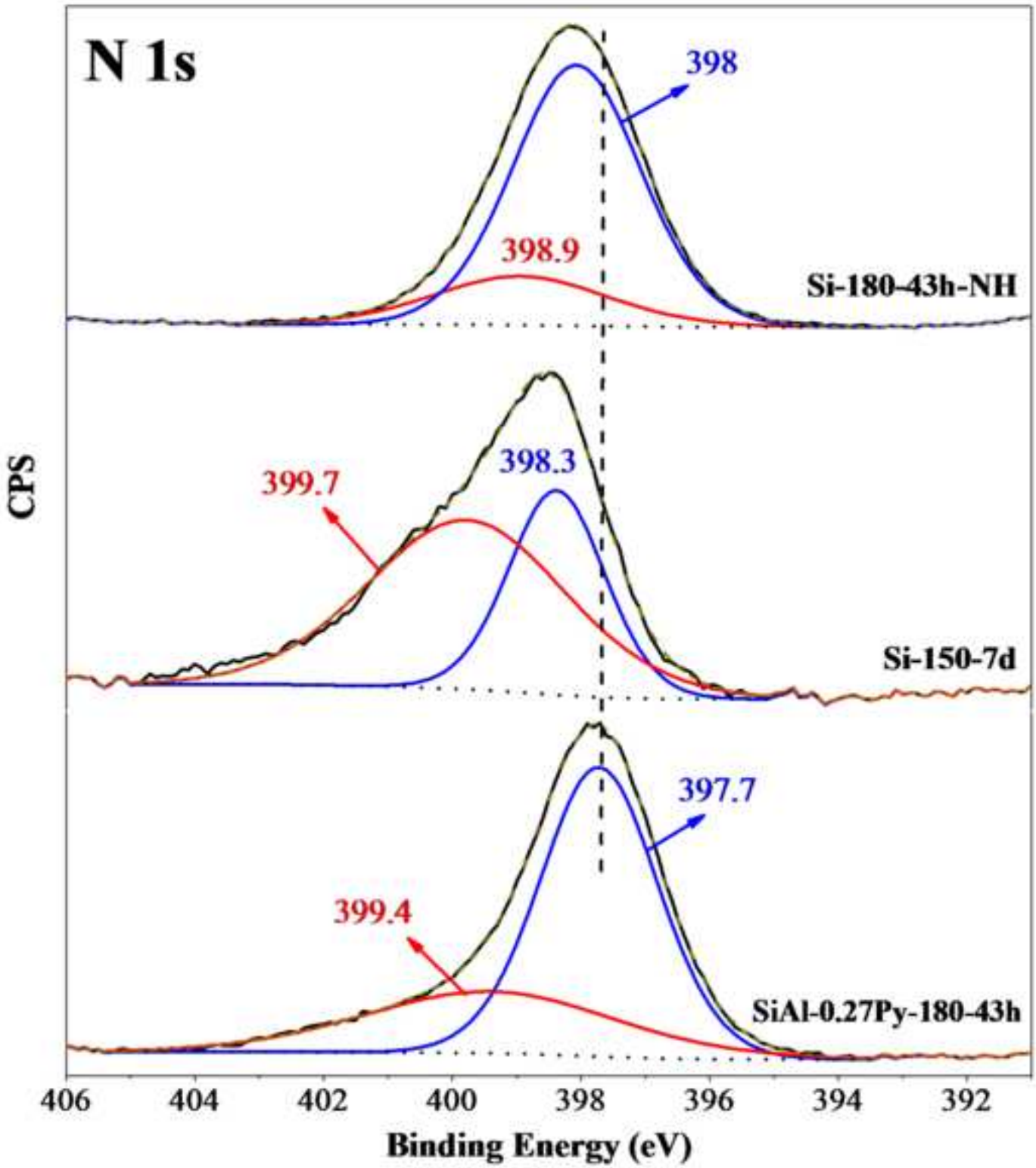

fig_6.tif
Click here to download high resolution image

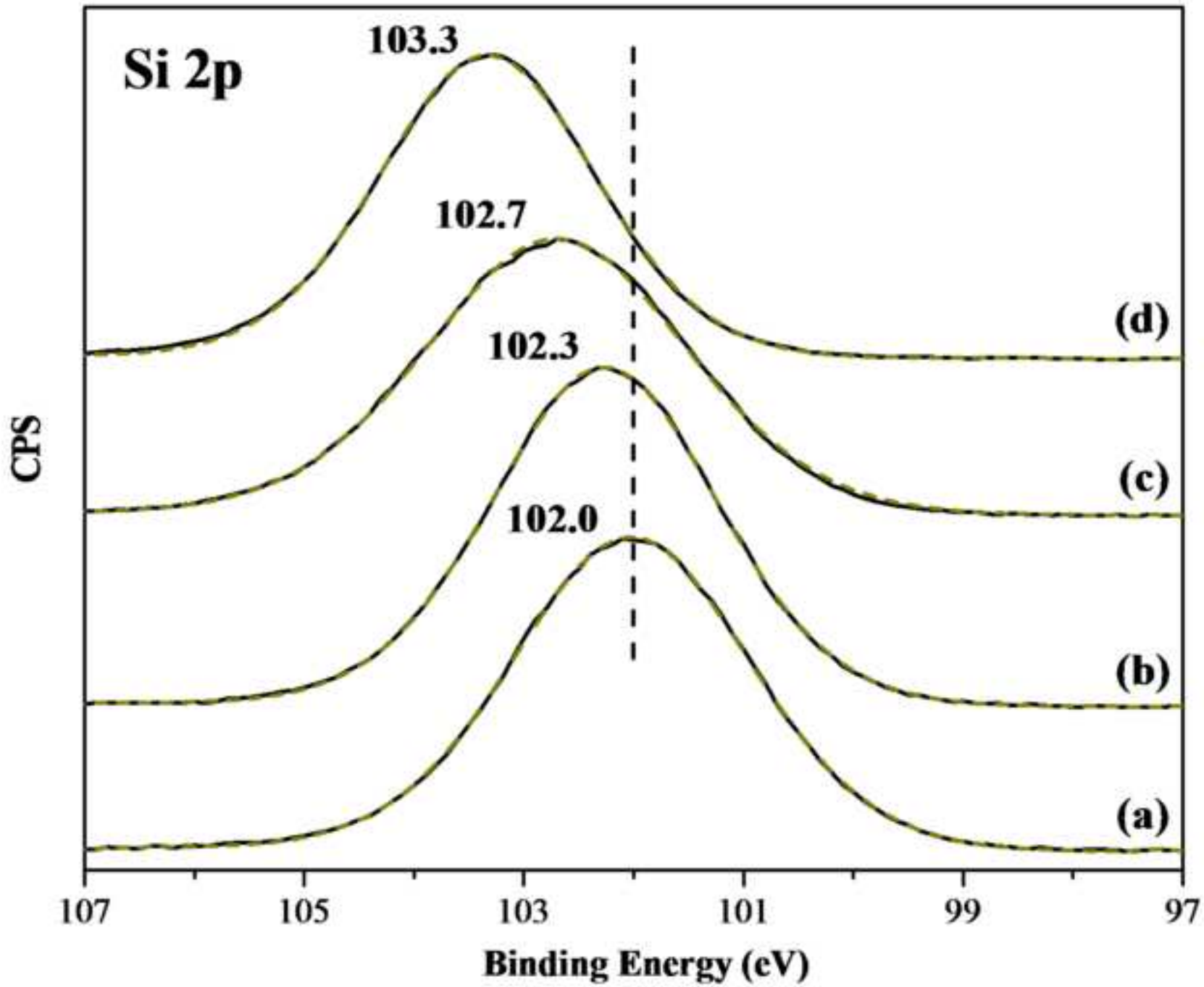

fig_7.tif
Click here to download high resolution image

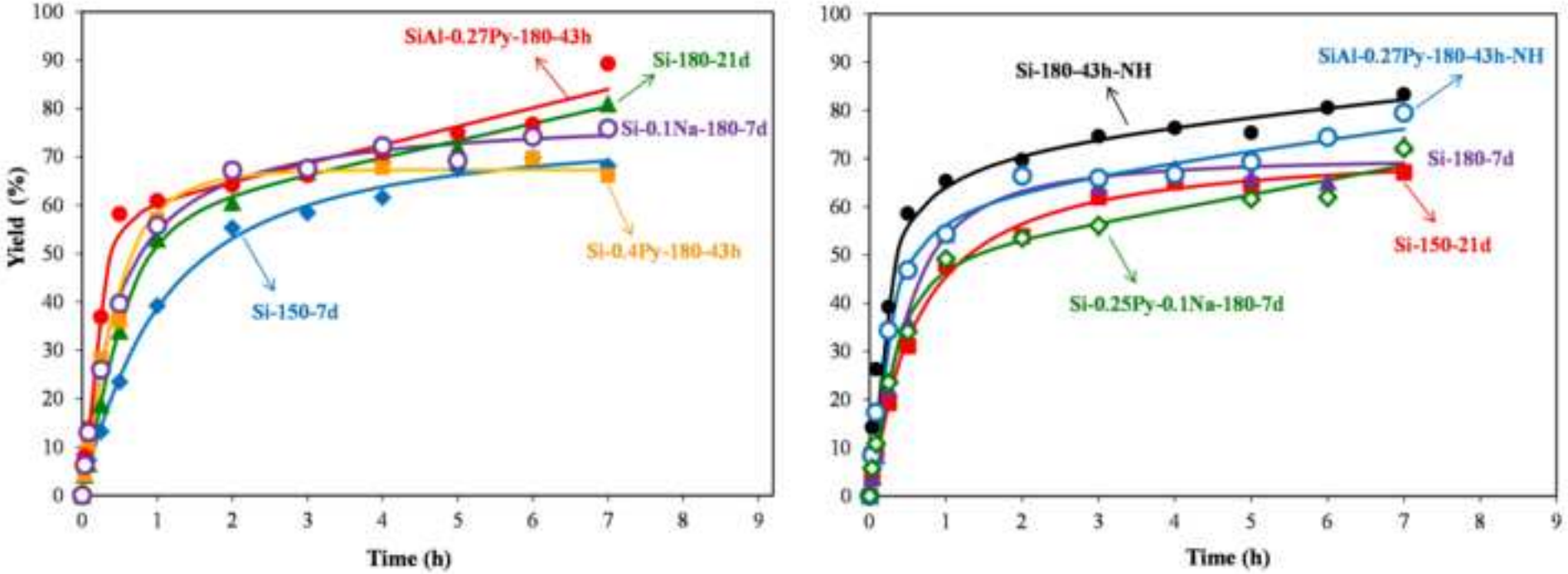

fig_8.tif
Click here to download high resolution image

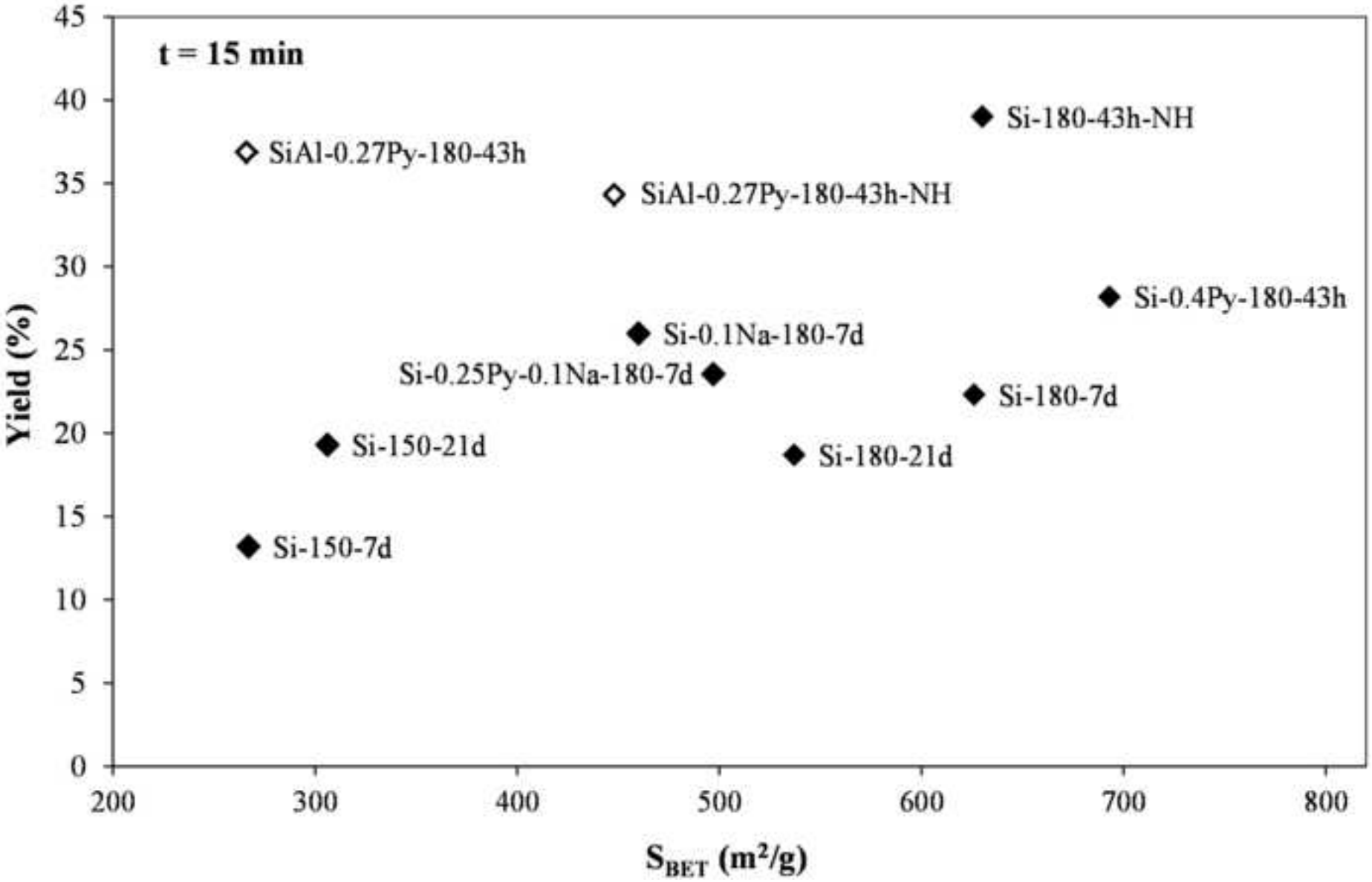

fig_9.tif
Click here to download high resolution image

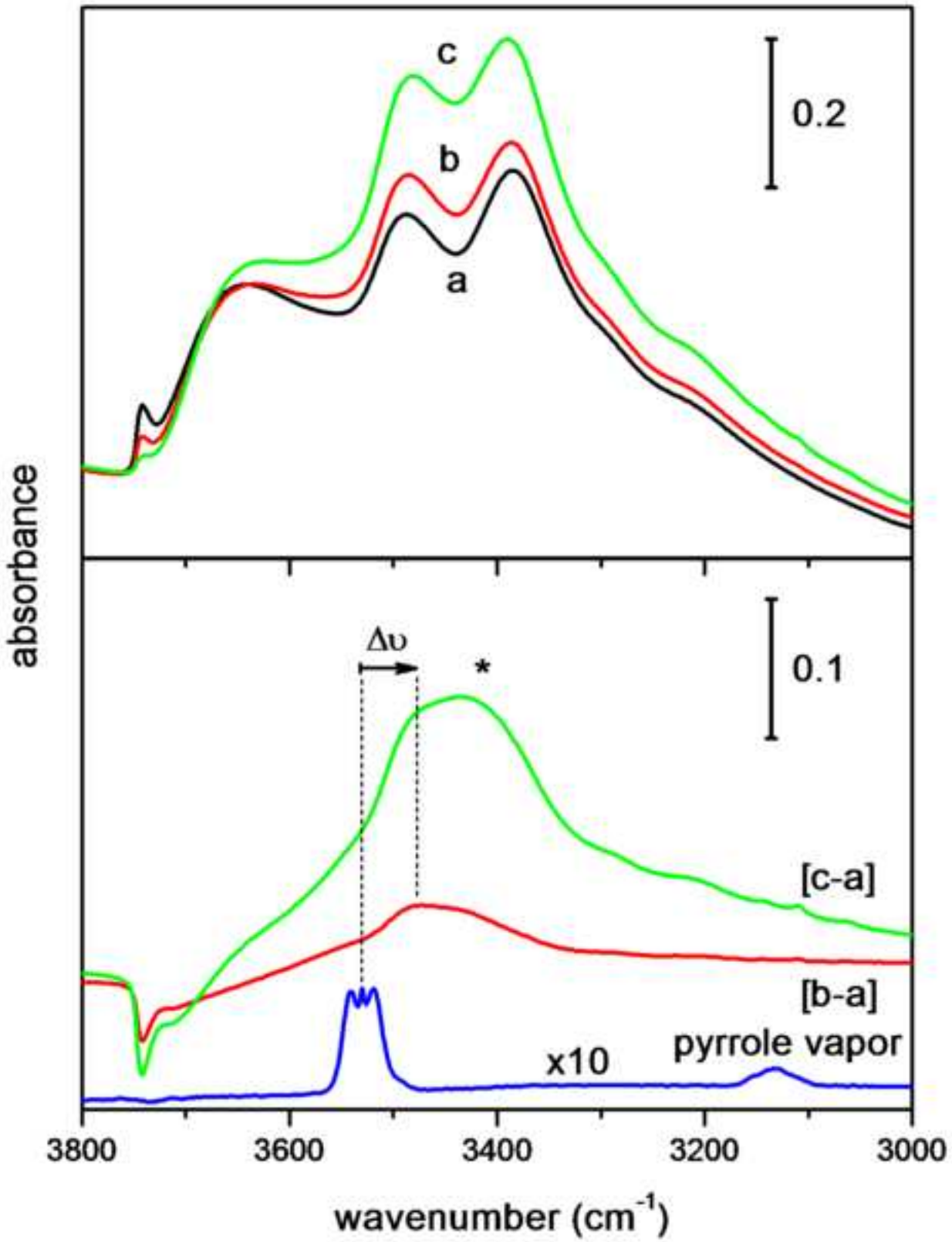

fig_10.tif
Click here to download high resolution image

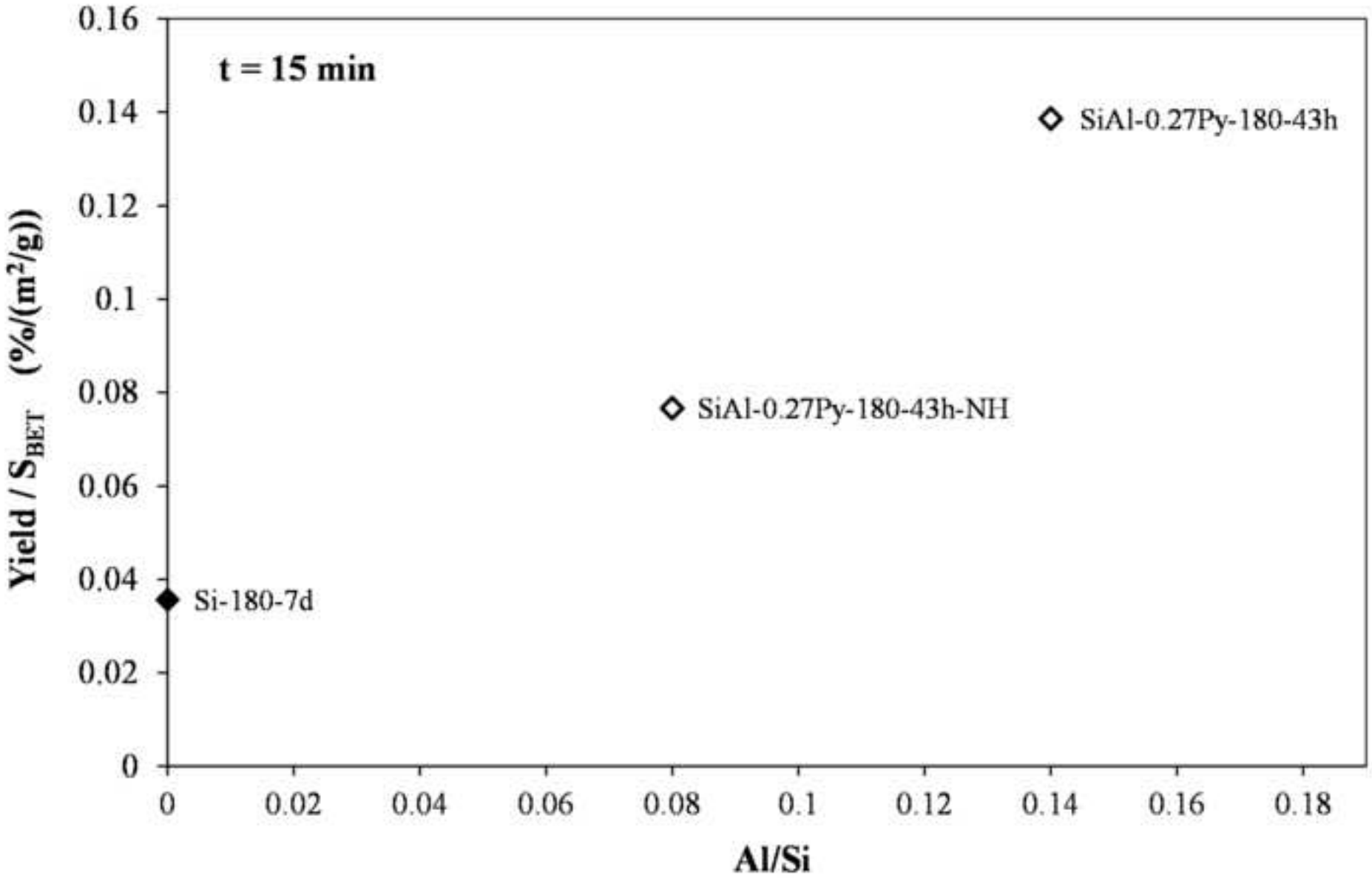

fig_11.tif
Click here to download high resolution image

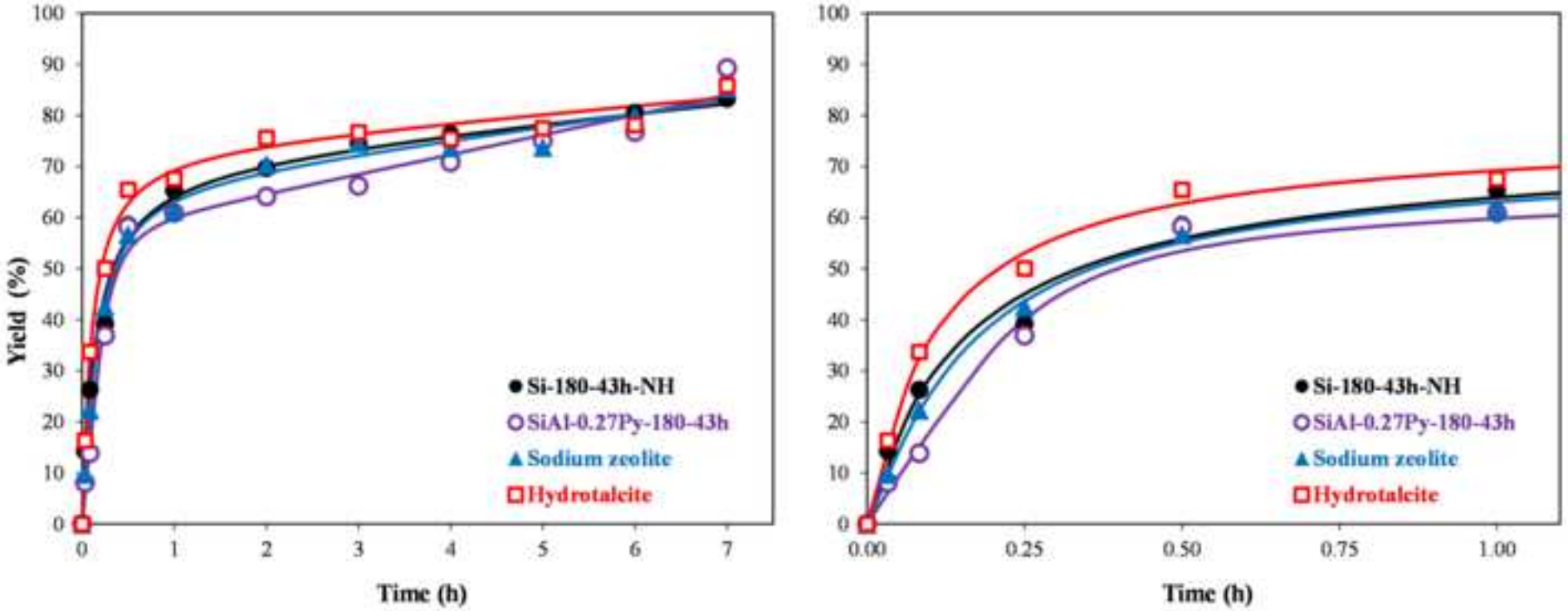

fig_12.tif
Click here to download high resolution image

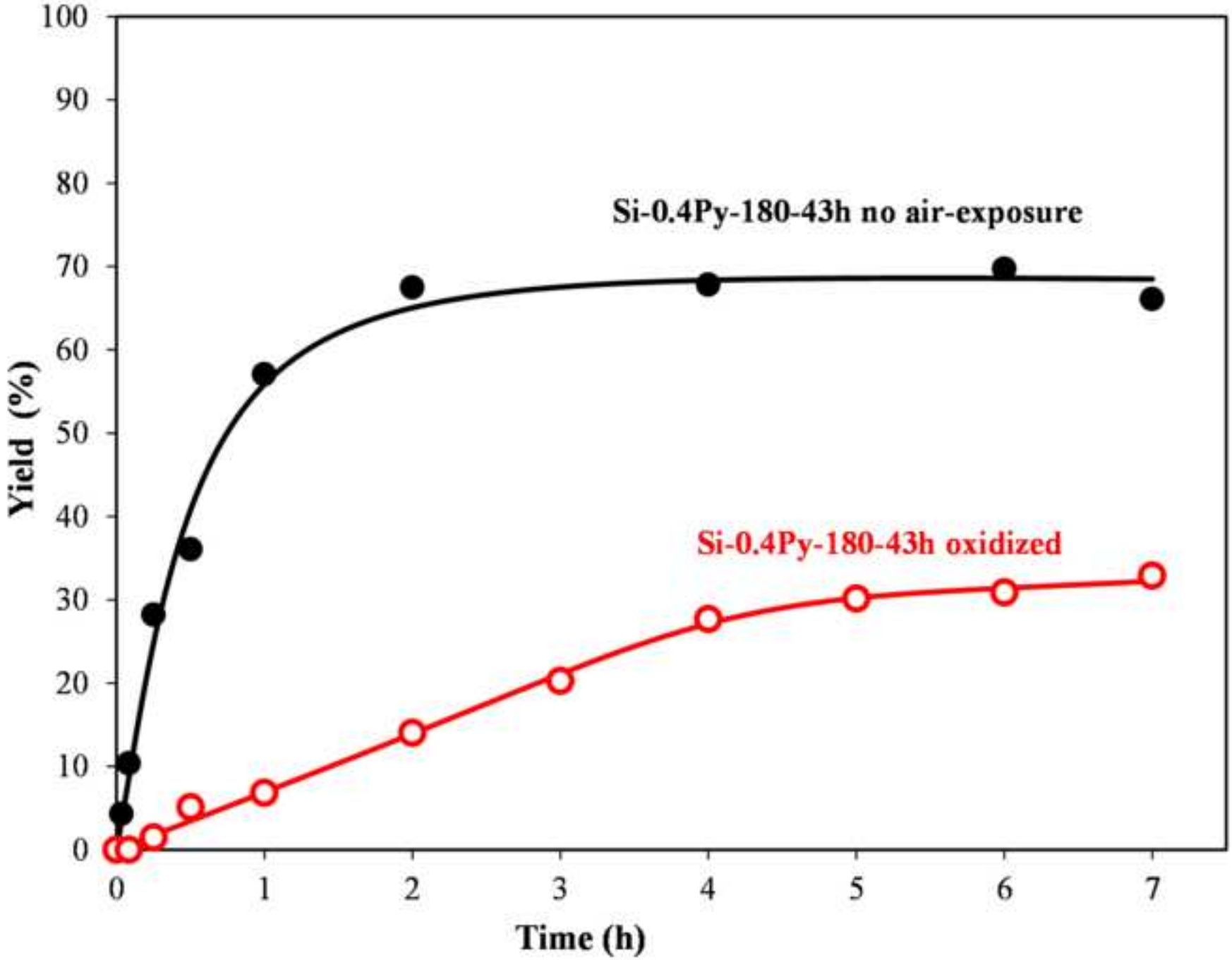

fig_s1.tif

Click here to download high resolution image

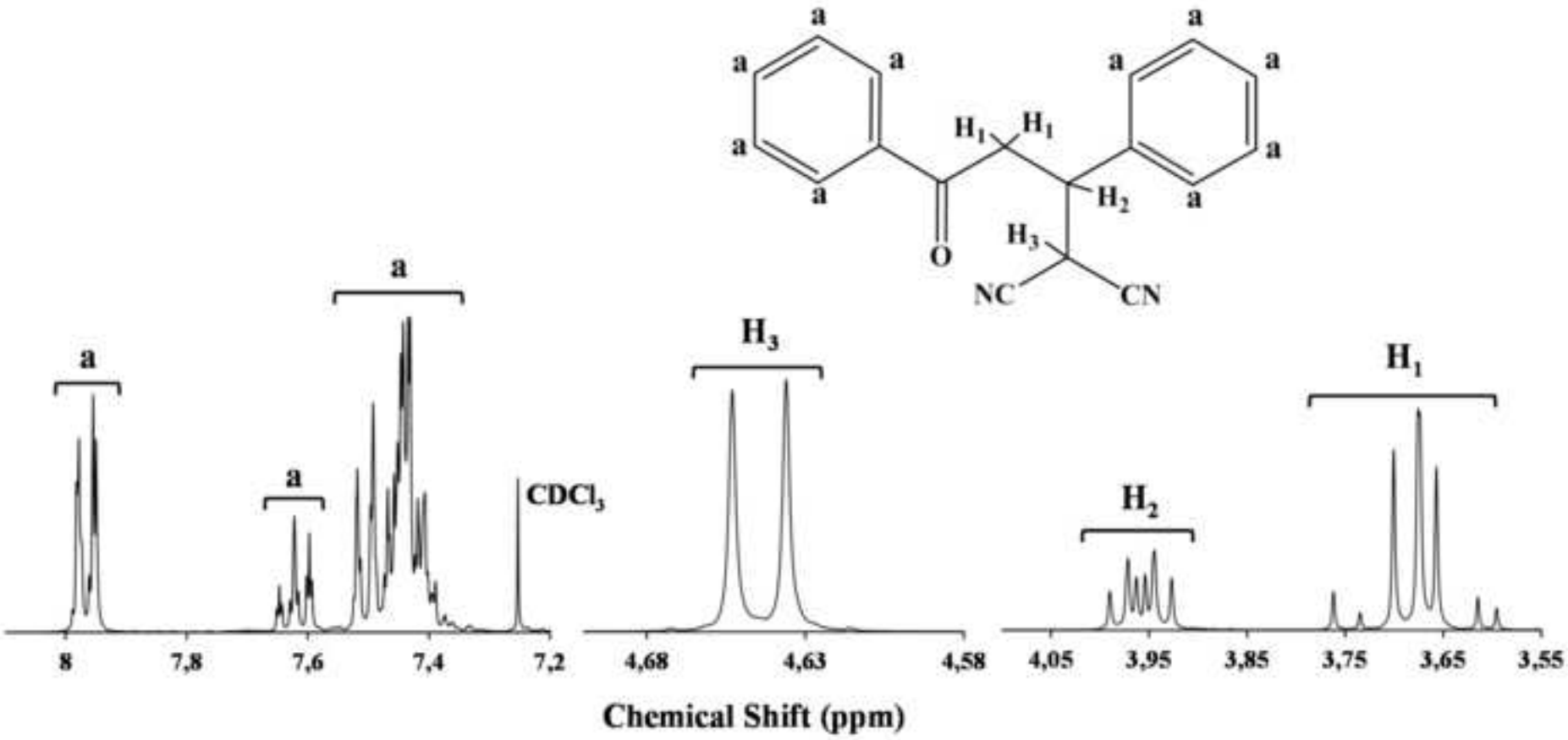

fig_s2.tif

Click here to download high resolution image

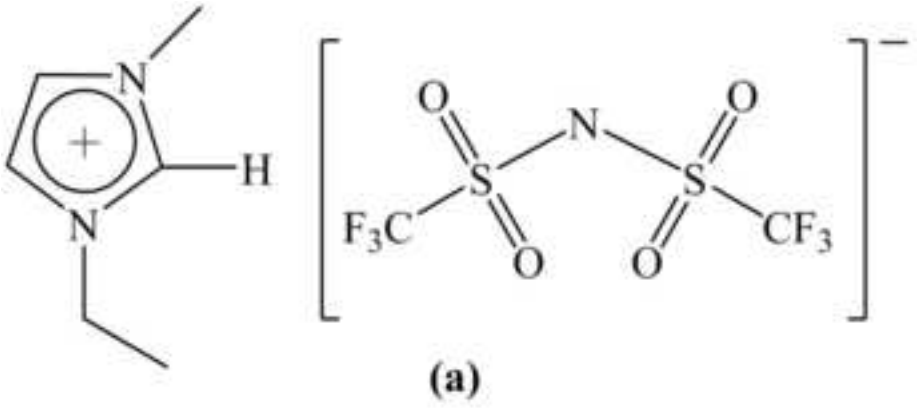

(a)

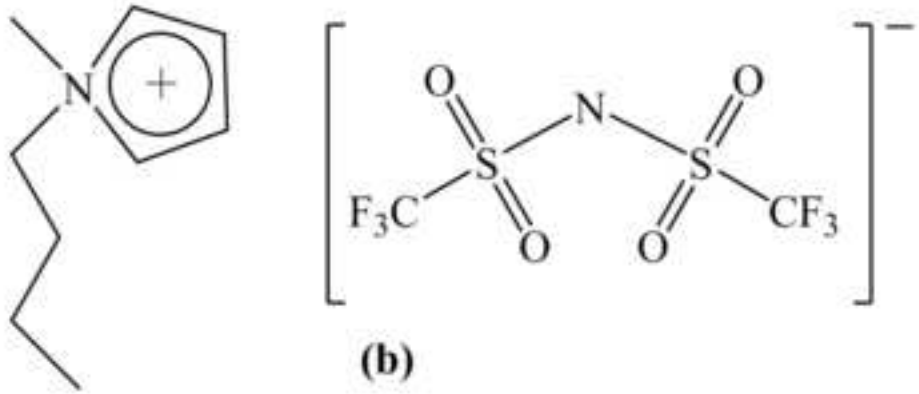

(b)

fig_s3.tif

Click here to download high resolution image

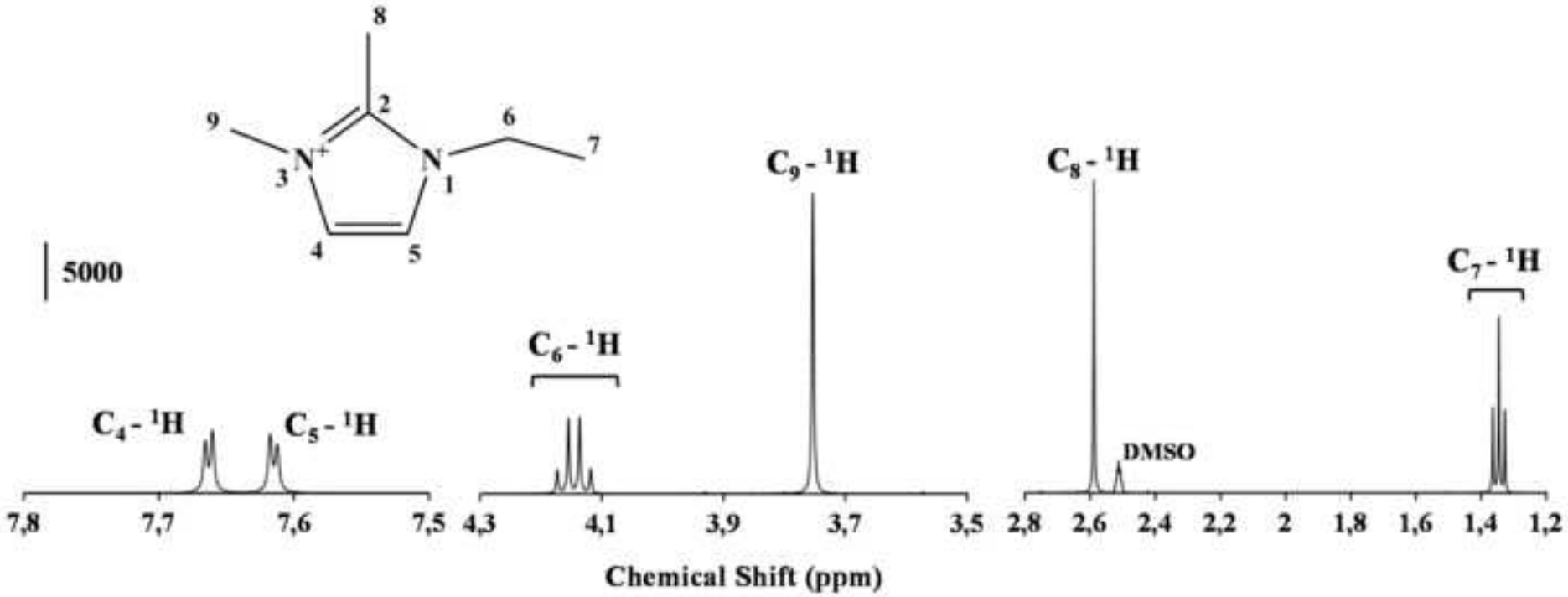

fig_s4.tif
Click here to download high resolution image

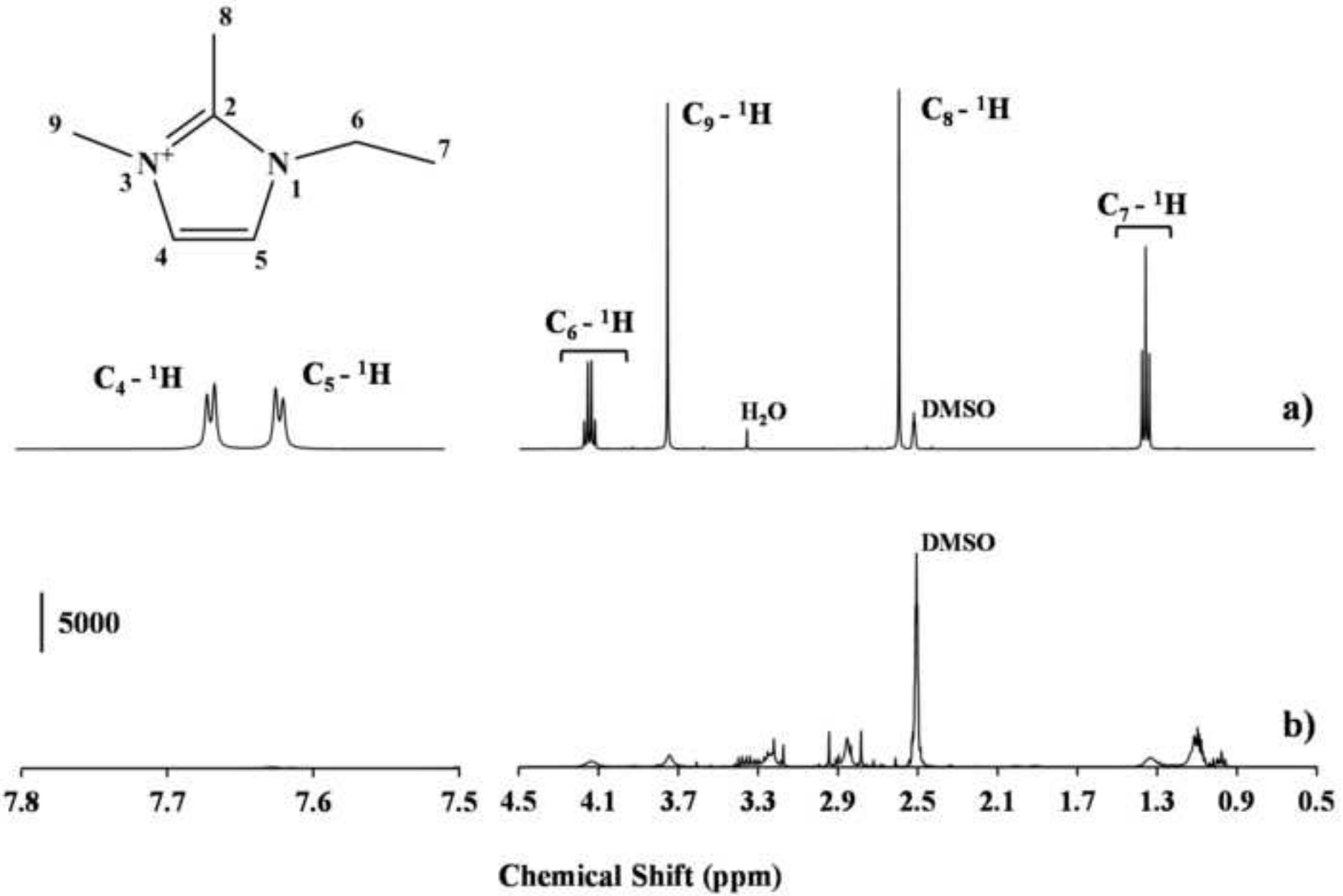

fig_s5.tif

Click here to download high resolution image

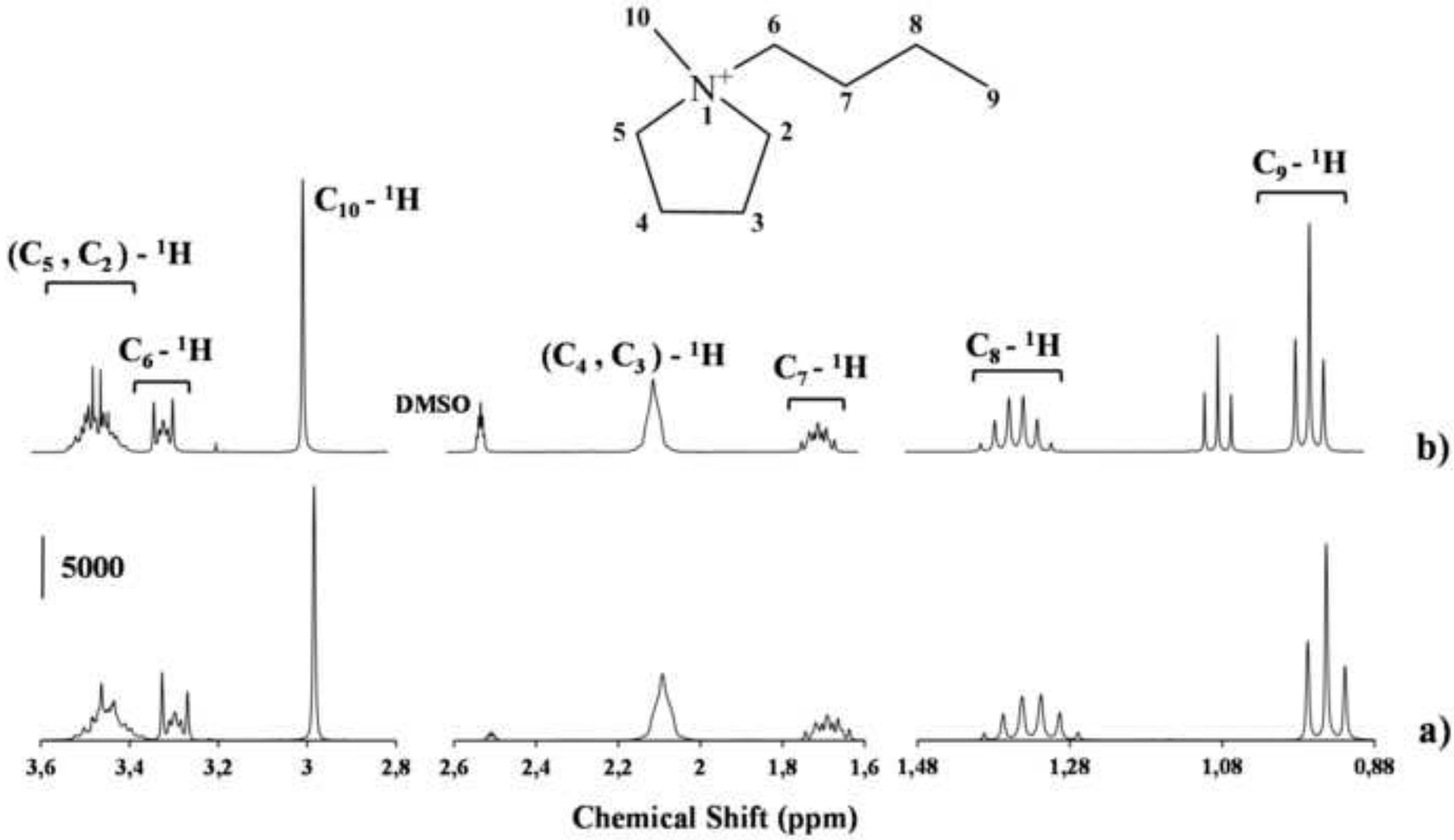

fig_s6.tif
Click here to download high resolution image

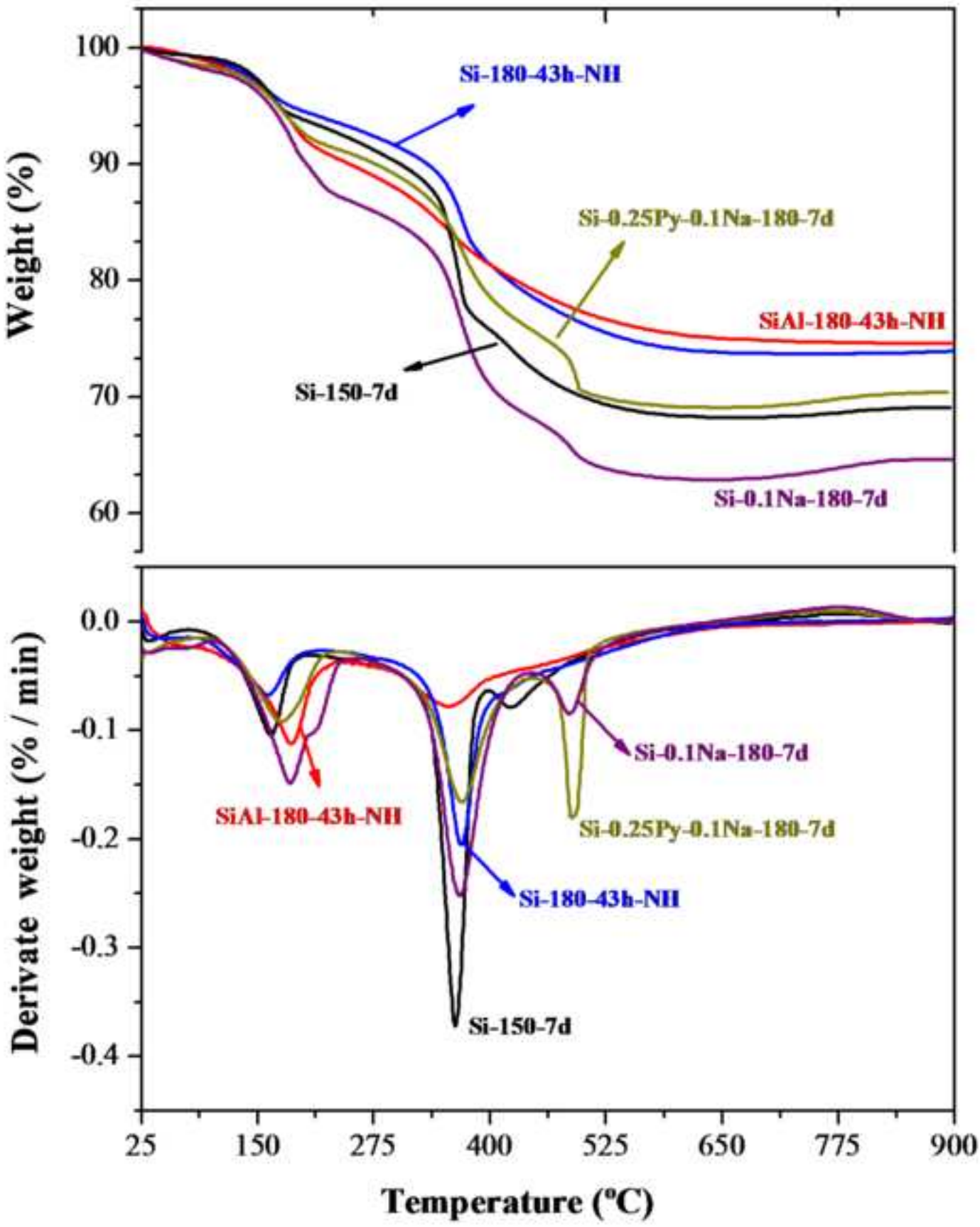

fig_s7.tif
Click here to download high resolution image

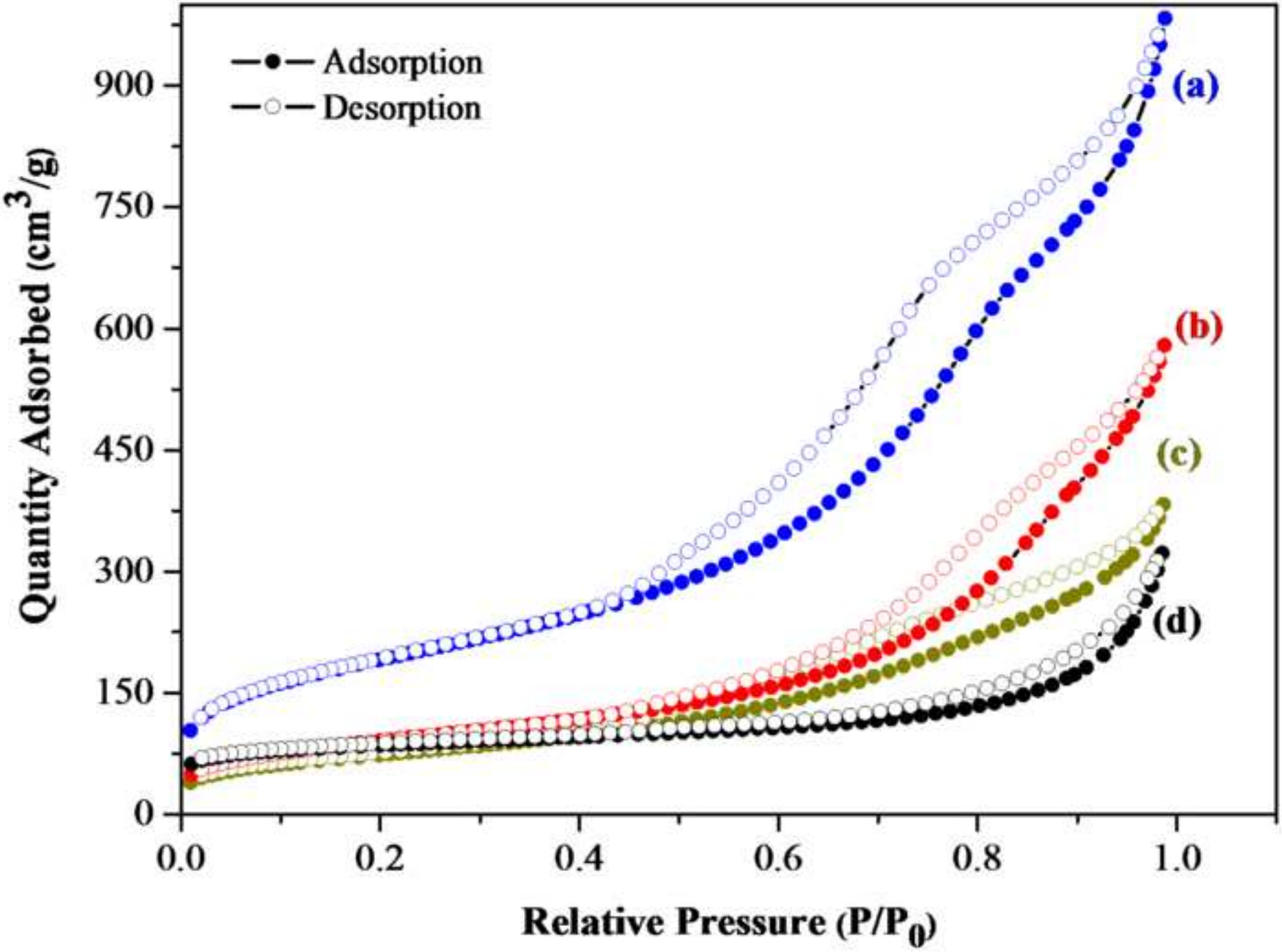

fig_s8.tif
Click here to download high resolution image

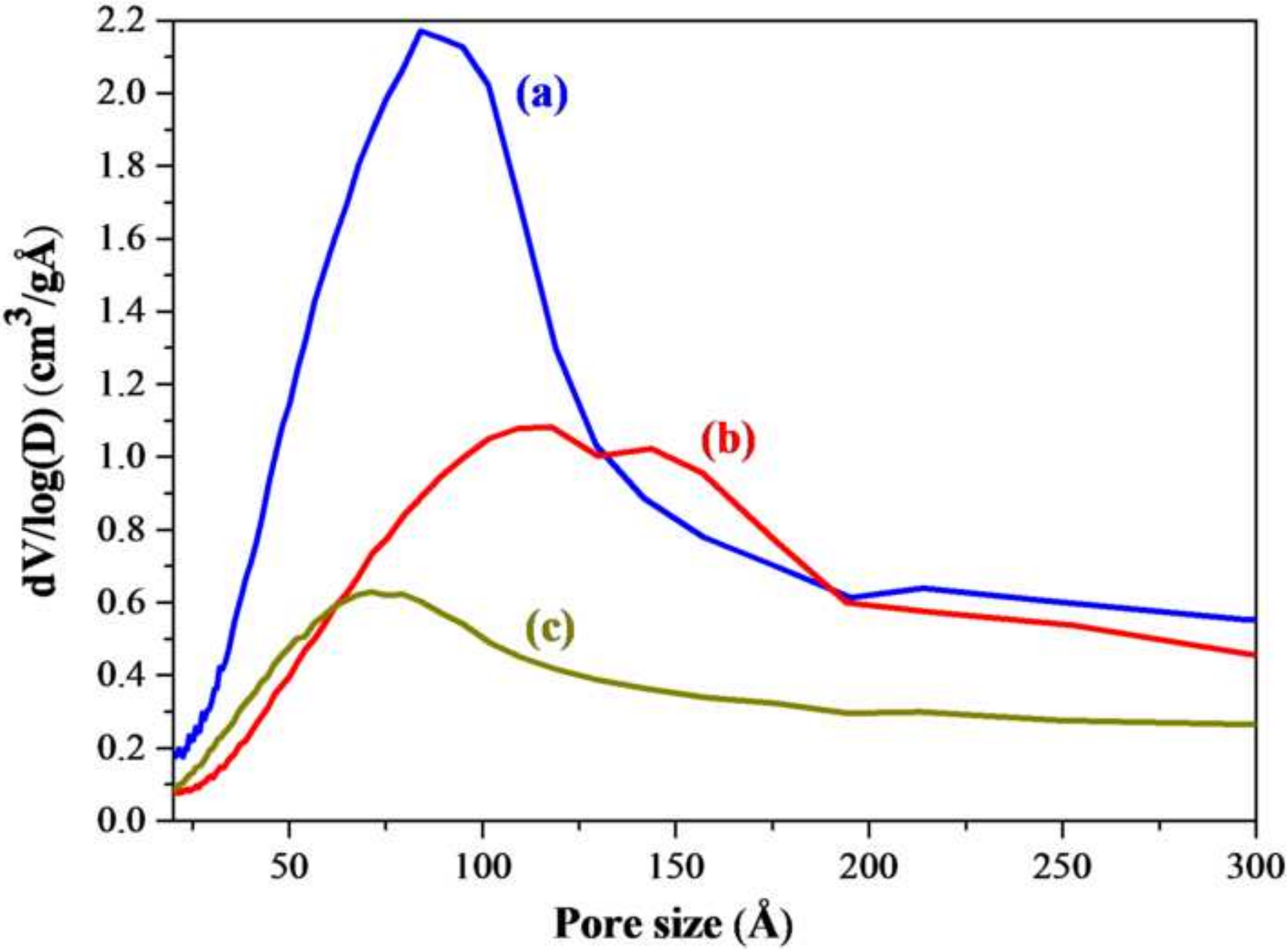

fig_s9.tif
Click here to download high resolution image

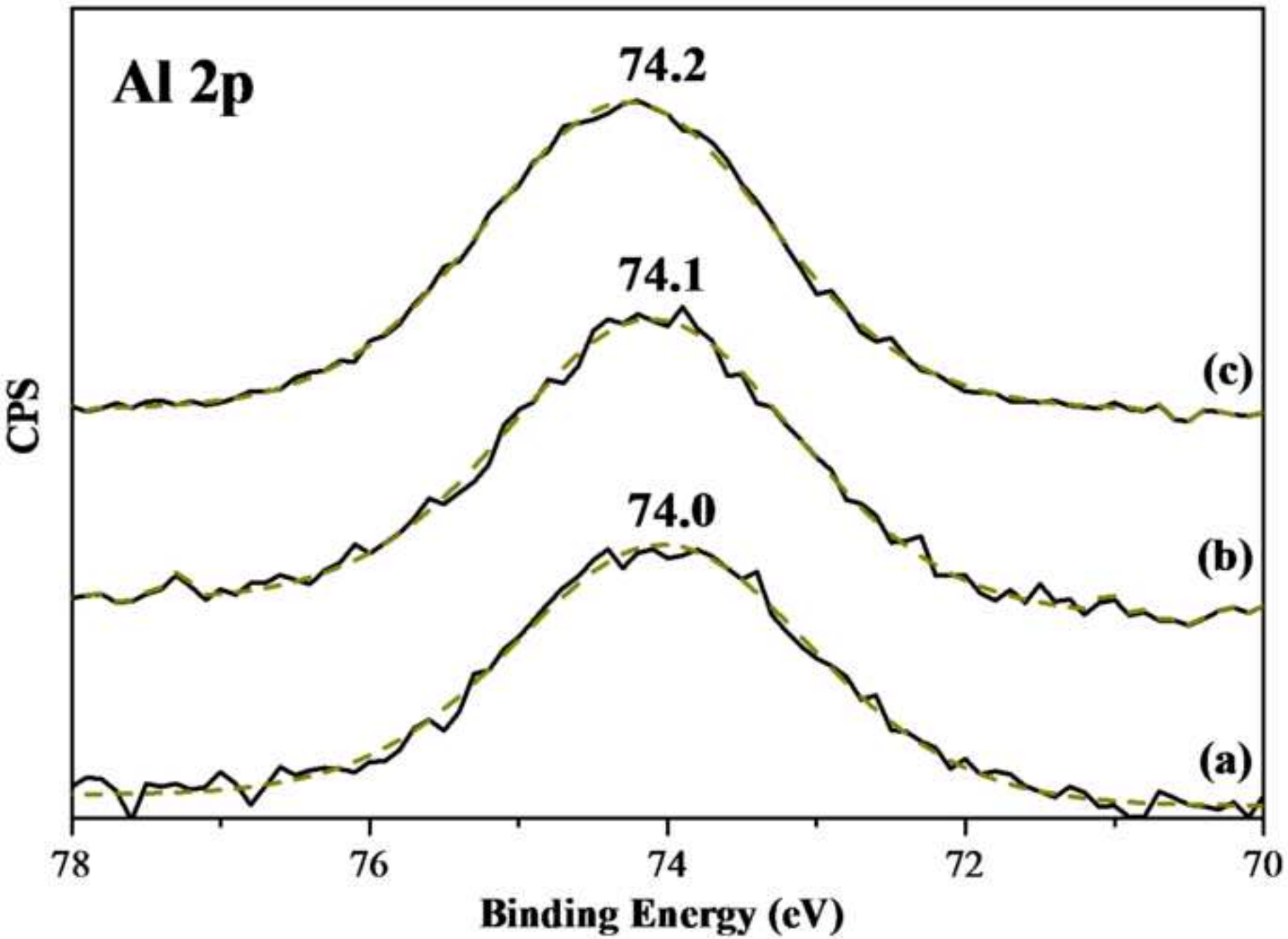

fig_s10.tif

Click here to download high resolution image

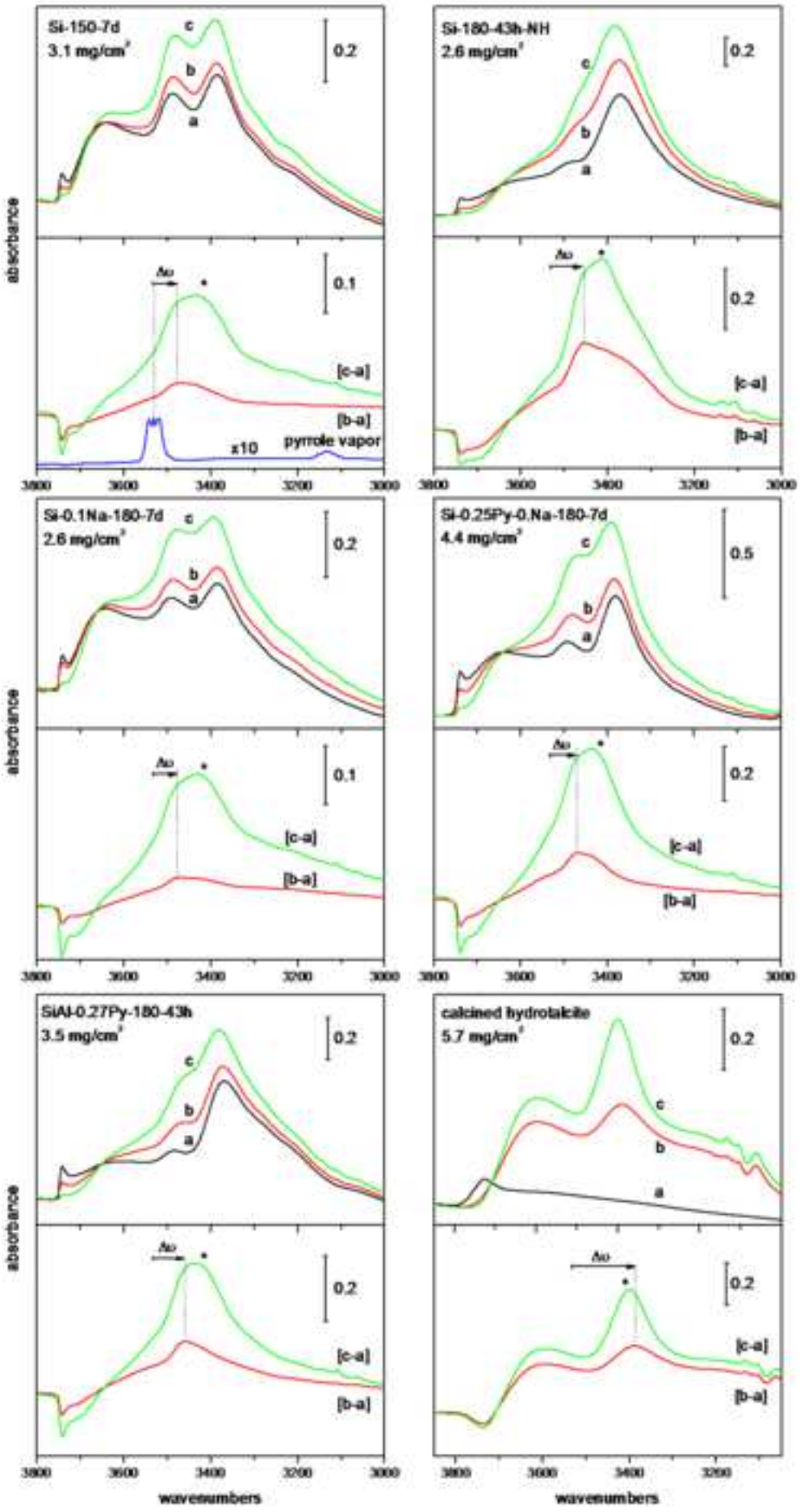

scheme_1.tif

Click here to download high resolution image

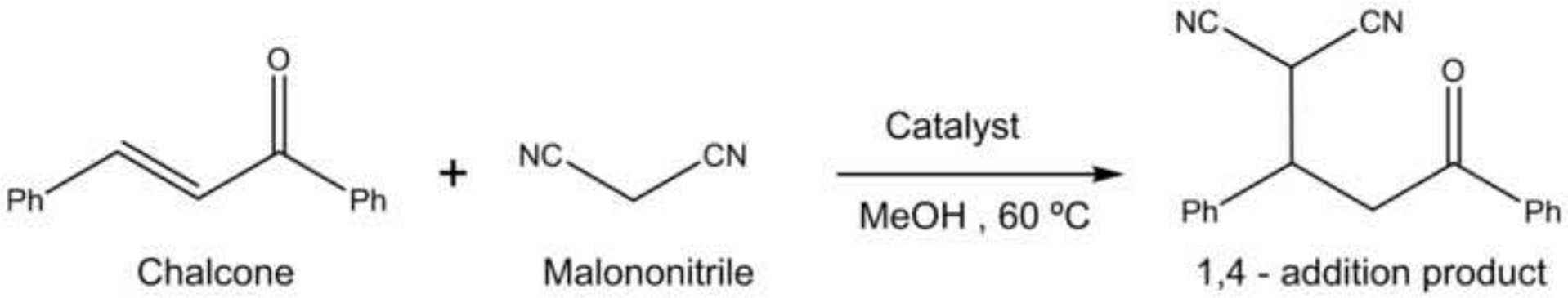

scheme_2.tif
Click here to download high resolution image

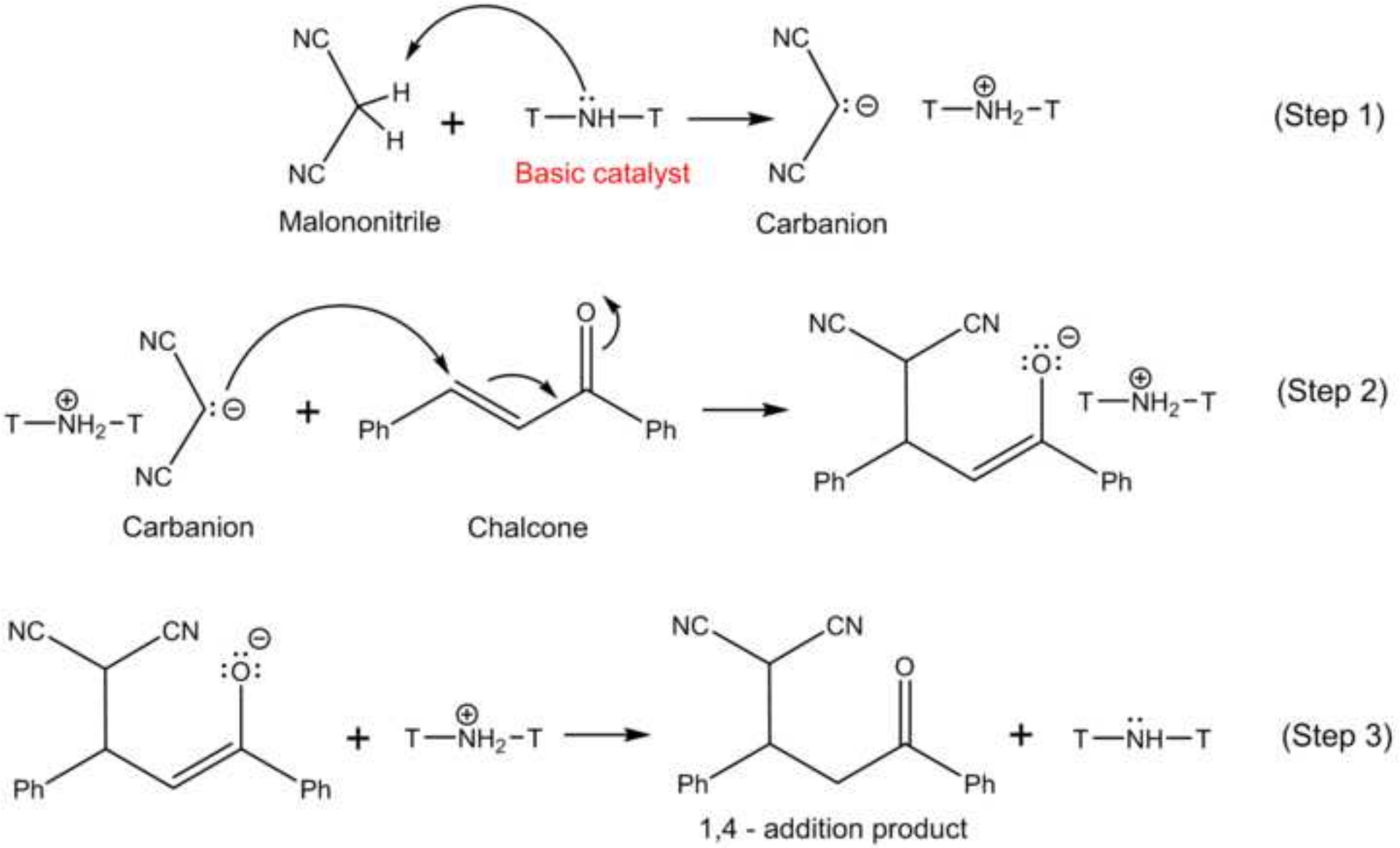

Mol Files

Click here to download Mol Files: 2-(3-oxo-1,3-diphenylpropyl)malononitrile.mol

Mol Files

Click here to download Mol Files: 109-77-3_malononitrile.mol

Mol Files

Click here to download Mol Files: 123-75-1_pyrrolidine.mol

Mol Files

Click here to download Mol Files: 614-47-1_chalcone.mol

Mol Files

Click here to download Mol Files: 174899-82-2_C2C1imTF2N.mol

Mol Files

Click here to download Mol Files: 223437-11-4_C4C1pyrrTf2N.mol